2016

ASSEMBLY AND DEGRADATION OF A TRIMERIC MEMBRANE PROTEIN ACRB

Qian Chai
University of Kentucky, qch223@gmail.com
Digital Object Identifier: http://dx.doi.org/10.13023/ETD.2016.283

STUDENT AGREEMENT:

I represent that my thesis or dissertation and abstract are my original work. Proper attribution has been given to all outside sources. I understand that I am solely responsible for obtaining any needed copyright permissions. I have obtained needed written permission statement(s) from the owner(s) of each third-party copyrighted matter to be included in my work, allowing electronic distribution (if such use is not permitted by the fair use doctrine) which will be submitted to UKnowledge as Additional File.

I hereby grant to The University of Kentucky and its agents the irrevocable, non-exclusive, and royalty-free license to archive and make accessible my work in whole or in part in all forms of media, now or hereafter known. I agree that the document mentioned above may be made available immediately for worldwide access unless an embargo applies.

I retain all other ownership rights to the copyright of my work. I also retain the right to use in future works (such as articles or books) all or part of my work. I understand that I am free to register the copyright to my work.

REVIEW, APPROVAL AND ACCEPTANCE

The document mentioned above has been reviewed and accepted by the student's advisor, on behalf of the advisory committee, and by the Director of Graduate Studies (DGS), on behalf of the program; we verify that this is the final, approved version of the student's thesis including all changes required by the advisory committee. The undersigned agree to abide by the statements above.

Qian Chai, Student

Dr. Yinan Wei, Major Professor

Dr. Dong-Sheng Yang, Director of Graduate Studies

ASSEMBLY AND DEGRADATION OF A TRIMERIC MEMBRANE PROTEIN ACRB

DISSERTATION

A dissertation submitted in partial fulfillment of the requirements for the degree of Doctor of Philosophy in the College of Arts and Sciences at the University of Kentucky

By

Qian Chai

Lexington, Kentucky

Director: Dr. Yinan Wei, Professor of Chemistry

Lexington, Kentucky

2016

ABSTRACT OF DISSERTATION

ASSEMBLY AND DEGRADATION OF A TRIMERIC MEMBRANE PROTEIN ACRB

Multidrug efflux pumps are membrane proteins that actively transport foreign objects out of cells. The active efflux of these pumps is a critical self-defense mechanism that enables the survival of bacteria under hostile environments. Efflux pump AcrB is a member of the Resistance-Nodulation-Division (RND) super family. In *E. coli*, it associates with periplasmic protein AcrA and outer membrane channel TolC to extrude a variety of noxious compounds out of cell from both the cytoplasm and the periplasm. My dissertation research focused on two aspects of this multidrug efflux pump: the oligomerization process during the biogenesis of AcrB and its degradation.

Oligomerization is an important aspect of the structure and function for many proteins and has been the subject of many studies. However, most of such studies focused on soluble proteins. The oligomerization process of membrane proteins, including AcrB, is rarely explored. In chapter 2, the co-assembly of AcrB variants co-expressed in the same cell was used as a tool to investigate the assembly of AcrB trimers during its bio-production. By monitoring the portion of pure trimers containing only one type of subunit and hybrid trimers containing a mixture of the

two kinds of subunits, it was found that the oligomerization of membrane proteins is not a random process as the formation of pure trimer is favored.

In chapter 3, the GALLEX system was used to monitor AcrB oligomerization in cells under the native condition. Previously GALLEX has only been used to monitor the oligomerization of small transmembrane proteins. By constructing a series of fusion proteins with different linker length between LexA and AcrB, and optimizing inducer concentration, we finally developed a system that could be used to differentiate AcrB trimers of different oligomerization affinities.

While chapters 2 and 3 focus on the trimerization of AcrB, a critical step of its biogenesis, chapters 4 and 5 focus on its life time and degradation. In chapter 4, the life time of AcrB was measured by incorporating non-natural amino acid azidohomoalanine (AHA) into protein translation. Using this method, it was determined that that the half-life of both AcrA and AcrB in *E. coli* were six days. The surprisingly long lifetime of these detoxification proteins might represent a strategy by the bacteria to conserve energy and maximize their competition niche for survival in a hostile environment.

In chapter 5, the degradation process of ssra tagged AcrB was investigated. *In-vivo* degradation test showed that properly inserted AcrB can be digested after addition of ssra-tag to its C-terminus. It was found that cytoplasmic unfoldase-protease complex ClpXP and chaperone SspB are involved in the degradation. *In vitro* assay is still being optimized to quantitatively analyze the activity of ClpXP in the degradation of AcrB.

Keywords: multidrug efflux pump, AcrB, oligomerization, assembly, degradation

Qian Chai

June. 6th , 2016

ASSEMBLY AND DEGRADATION OF A TRIMERIC MEMBRANE PROTEIN ACRB

By

Qian Chai

Yinan Wei, Ph.D.

Director of Thesis

Dong-sheng Yang, Ph. D.

Director of Graduate Studies

June 6th, 2016

ACKNOWLEDGEMENTS

First of all, I would like to give my most honest and sincerest appreciation to my advisor, Dr. Yinan Wei. As a patient instructor, she is always available to discuss research problems with students. As a wise mentor, she sets a great example for us about how to resolve problem independently, face challenge directly and think positively. As a warm-hearted friend, she genuinely cares everyone around her and is always ready to help people out. I want to thank her from bottom of my heart for all the support and guidance she has given to me over these years during the pursuit of my doctorate and the profound influence she has had on my life.

I would like to express my sincere thanks to my committee members, Dr. Allan Butterfield, Dr. DongshengYang from chemistry department, Dr. Luke Moe from department of plant and soil sciences, and my outside examiner Dr. Harry LeVine from department of molecular and cellular biochemistry. They have graciously sacrificed their time and attention to attend my committee meetings, proof-read my dissertation. Their advices have always reminded me thinking critically about my research.

I sincerely enjoyed the company of all my group members. Our postdoc Dr. Wei Lu and Dr. Jun Fang have taught me basic biochemistry techniques and given me valuable suggestions about my research. Discussions with our previous graduate students Dr. Linliang Yu, Dr. Meng Zhong, Dr. Cui Ye, Shen Geng and Brent Ferrel have always inspired deeper thinking. Our present group members Xinyi Zhang, Zhaoshuai Wang and Thilini Abeywansha have provided me a lot of help

and brought me tons of fun in every day lab work. All these people have made our lab a great environment to learn and make progress as a researcher.

I want to thank Dr. Rebecca Dutch and her student Stacy Webb from department of molecular and cellular biochemistry for offering me help in pulse-chase experiment, Dr. Robert Sauer from Massachusetts Institute of Technology and Dr. Dirk Schneider from University of Mainz (Germany) for providing me plasmids.

I also want to thank ladies and gentlemen from main office and IBU office, who have offered me numerous help. Their kindness has created such a warm and friendly climate in chemistry department.

I need to thank National Science Foundation for the funding support which makes my research continue.

Last but not least, I would like to extend my deepest gratitude to my parents, my husband and my daughter. Without their unconditional love, trust, support and encouragement, I will not have the chance to come to Lexington and finish my graduate study at UK. My family is the most precious treasure in my life.

TABLE OF CONTENTS

LIST OF TABLES

LIST OF FIGURES

LIST OF ABBREVIATIONS

AAA+: ATPases associated with diverse cellular activities

ABC: ATP-binding cassette

AHA: azidohomoalanine

Amp: ampicillin

ATP: adenodine triphosphate

BCIP: 5-bromo-4-chloro-3’-indoyl phosphate p-toluidine

Cam: chloramphenicol

CAT: chloramphenicol acetyltransferase

CD: circular dichroism

CPS: carbamoyl phosphate synthetase

Cryo-EM: cryo-electron microscopy

Cys: cysteine

DBD: DNA binding domain

DDM: n-dodecyl β-D-Maltopyranoside

DegU-P: phosphorylated DegU

DPC: decylphosphocholine

EtBr: ethidium bromide

FRET: Förster Resonane Energy Transfer

GpA: glycophorin A

HiaBD1: Hia binding domain 1

IMMP: intramembrane metalloprotease

IMP: inosine monophosphate

IPTG: isopropyl β-D-1-thiogalactopyranoside

Kan: kanamycin

LB: lysogeny broth

L/F-trasnferase: leucyl/phenylalanyl-tRNA protein transferase

MATE: multidrug and toxic compound extrusion

MBP: maltose binding protein

MDR: multidrug resistance

Met: methionine

MetAPs: methionine aminopeptidase

MFP: membrane fusion protein

MFS: major facilitator superfamily

MIC: minimum inhibitory concentration

MSDs: membrane-spanning domains

NaPi: sodium phosphate

NBDs: nucleotide-binding domains

NBT: nitro blue tetrazolium choloride

Ni-NTA: nickel-nitriloacetic acid

OD: optical density

ONP: o-nitrophenol

ONPG: o-nitrophenyl-beta-D-galactoside

PCR: phlymerase chain reaction

PMFS: phenylmethysulfonyl fluoride

PVDF: polyvinylidene difluoride

RND: resistance-nodulation-division

SDS-PAGE: sodium dodecyl sulfate-polyacrylamide gel electrophoresis

SMR: small multidrug resistance

TBTA: Tris(benzyltriazolylmethyl) amine

TCEP: tris (2-carboxyethyl) phosphine

TM: transmembrane

UMP: uridine monophosphate

Chapter I Introduction

1.1 Protein Oligomerization

1.1.1 Advantages of Protein Oligomerization

Bioinformatics studies have revealed that more than 35% of proteins exist and function as oligomers instead of monomers.[1] Oligomeric proteins have multiple peptide chains which can be the same (for homo-oligomerization) or different (for hetero-oligomerization).[2] Oligomerization has brought in many advantageous features for organisms in many different aspects.[3] First of all, oligomeric proteins are more stable than monomer proteins.[4] The stability advantage relies on the fact that oligomeric proteins have reduced surface area, which provides proteins more protection, and makes them more resistant to degradation and denaturation compared with monomeric proteins.[5-7] Such stability has been exploited by thermophilic organisms. To improve thermo-stability of protein, an increase in oligomerization state has been observed among proteins from thermophilic organisms.[8] Another example is the hexameric insulin that exists in crystalline granule and resists protease digestion. As soon as the oligomer dissociates in blood, monomer insulin is rapidly degraded.[9]

More significantly, there are many functional advantages for oligomeric proteins. First, oligomerization provides protein a possibility to adopt a variety of symmetrical structures, including rings, cages, or funnels, and therefore are suitable for specific morphological functions. One example is the *E. coli* Wza protein, an outer membrane protein that is responsible for transporting lipid-linked polysaccharides across the periplasm and outer membrane (Figure

1.1).[10] Oligomerization of eight monomers leads to the formation of a large tunnel with a central cavity of 15,000 Å^3, which is necessary for exporting polysaccharides across the outer membrane.

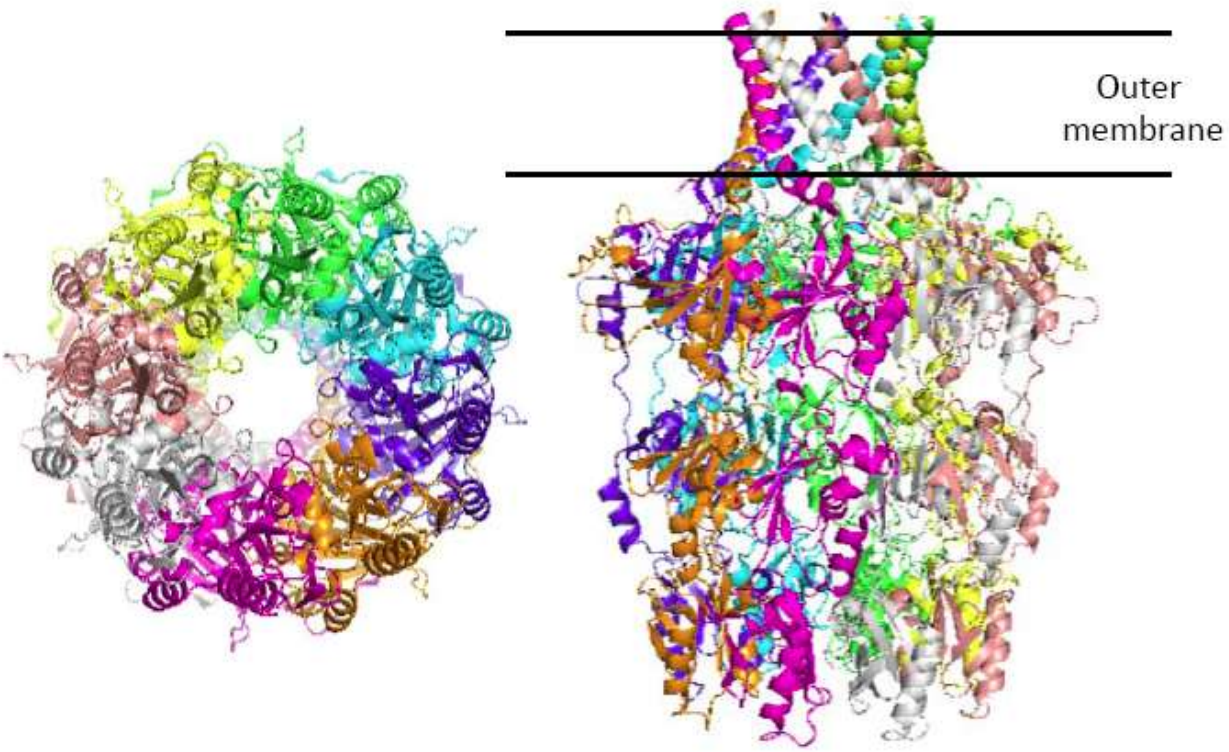

Figure 1.1 Crystal structure of Wza protein of *E. coli*. Each monomer is labeled in different color. Left image is the view of central cavity from periplasm. Right image is the side view of the octamer protein. Created from 2J58.pdb.[10]

Second, the equilibrium between association and dissociation can regulate activity of proteins.[11-13] In many enzymes, residues from more than one subunit form active sites, which are located on the interface. Oligomerization stimulates activity, and dissociation results in activity decreases.[14] Glutamine synthetase of bacteria is an enzyme involved in nitrogen metabolism. It catalyzes the condensation of glutamate and ammonia to form glutamine.[15] Bacterial glutamine synthetase is functional in its dodecamer form, which is superimposed by two face-to-face hexameric rings.

Oligomerization brings residues from adjacent monomers together to compose the active site, which binds adenosine triphosphate (ATP) and glutamate at opposite ends. For each enzyme there are a total of 12 active sites. Upon dissociation, activity of this enzyme drops.[16, 17]

Third, oligomeric proteins can provide multiple points of interaction to increase the binding strength between the ligand and the protein, while monomeric proteins usually have one binding site. Hia is an autotransporter protein expressed in many Gram-negative pathogenic bacteria such as *Haemophilius influenza*, which plays important roles in the pathogenesis of both systemic diseases such as meningitis and sepsis, and localized respiratory tract diseases including otitis media and bronchitis.[18] it has been confirmed that colonization of these pathogens is promoted by adhension proteins such as Hia. Hia is a highly stable trimer partially embedded in the outer membrane and its adhensive activity comes from its binding domains, HiaBD1 and HiaBD2 (Figure 1.2).[19] HiaBD1 is composed of three acidic binding pockets, each provided by one monomer. These binding pockets provide multiple interactions with receptor molecules simultaneously and thus strengthen the binding of Hia to specific receptor. It was reported in 2006 that the trimeric structure increases the adhesive affinity of Hia for host respiratory epithelial cells through multivalent binding and leads to infection.[19]

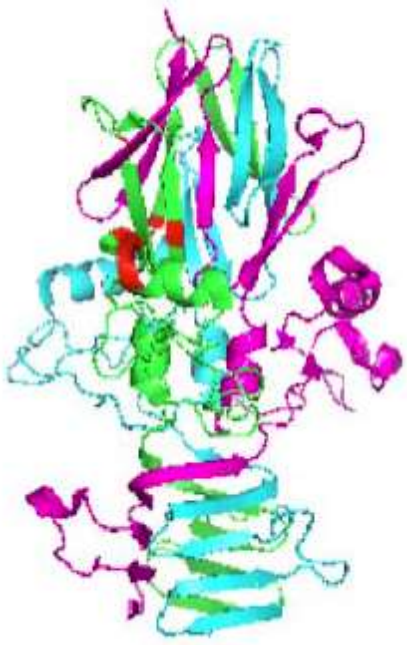

Figure 1.2 Trimeric structure of the HiaBD1. Residues composed of acidic binding pocket in one monomer are color-labeled in red. This image is created from 1s7m.pdb.

Except for multivalent binding, another important aspect of oligomers cooperativity is allosteric regulation.[20, 21] Allosteric regulation is commonly observed in oligomeric enzymes, in which binding of a ligand to the non-active site of enzyme, usually in one subunit, changes the conformation of the protein, and subsequently affects the binding affinity of the ligand to another subunit in the same oligomer.[22] A classic example of allosteric regulation is the Bohr Effect of the tetrameric hemoglobin, in which the affinity of one subunit for oxygen is decreased when another subunit binds carbon dioxide. [23]

Allosteric regulators can modify activity of enzymes by changing the oligomerization state of proteins.[24, 25] Carbamoyl phosphate synthetase (CPS) in bacteria catalyzes the synthesis of

carbamoyl phosphate from glutamine or ammonia and bicarbonate with hydrolysis of ATP.[26] The basic building block of this enzyme is a (αβ) monomer. It has two oligomerization states, one is $(\alpha\beta)_2$ dimer, which is inactive. The other is its active form, $(\alpha\beta)_4$ tetramer. The oligomerization state of CPS can be regulated by allosteric ligands, which are metabolites ornithine, inosine monophosphate (IMP), and uridine monophosphate (UMP). Ornithine and IMP are activators, since binding of these effectors to the allosteric domain promote transition from dimer to tetramer. UMP is an inhibitor which stabilizes the dimer of CPS and inhibits formation of active tetramer.[27]

1.1.2 Experimental Techniques in the Study of Protein Oligomerization

As discussed above, oligomerization is an important aspect in the study of protein structure and function. Many approaches have been developed to investigate the kinetics and thermodynamics of protein oligomerization.[28-31] However, compared with soluble protein, thermodynamic analysis of membrane protein has been hampered by various experimental difficulties.[32] Since membrane proteins reside in lipid bilayer membrane rather than the aqueous cytoplasm, features of detergent micelles or lipid bilayers must be considered when studying membrane proteins. Currently, several techniques have been developed to study the oligomerization of membrane proteins, including sedimentation equilibrium analytical ultracentrifugation, Förster Resonance Energy Transfer (FRET), disulfide cross-linking, and *in vivo* systems such as TOXCAT and GALLEX.

Sedimentation equilibrium analytical ultracentrifugation is one of the most popular techniques used in the determination of the stoichiometry and stability of membrane protein complexes.[33] It can be used to determine the oligomerization state of a protein, and measure the association constant in a monomer-oligomer equilibration.[34] In this method, samples are subjected to ultracentrifugation at a high speed to induce protein sedimentation. During ultracentrifugation, a protein concentration gradient is formed in the sample. In the meantime, diffusion acts as an opposite force to disrupt this concentration gradient. Eventually, a balance between sedimentation and diffusion is achieved and while the sample is still spinning, absorbance is measured to obtain the concentration distribution in the equilibrium system. Concentration is a function of position (or radius) within the ultracentrifugation cell. By plotting the absorbance value at a specific wavelength vs. radius, information like molecular mass and thermodynamic

constant can be obtained after mathematical analysis. For membrane protein, the research subject is always protein-detergent complexes instead of only protein and this problem can be circumvented by choosing a detergent whose density matches that of the solvent, so that detergent in the system will not affect test result.

FRET has been exploited for measuring the thermodynamics of transmembrane helix dimerization.[35-37] FRET is a useful tool in studying protein-protein interaction, protein-DNA interaction, and protein conformational changes.[38-40] The basic mechanism is energy transfer between two chromophores, for which the absorption spectrum of the acceptor must overlap the fluorescence emission spectrum of the donor (Figure 1.3A). When placed in close proximity (typically 10-100 Å), energy transfer will take place between donor and acceptor through dipole-dipole coupling (Figure 1.3B).[41] By linking donor and acceptor chromophores to different bio-molecules respectively, and measuring the FRET efficiency, association between target bio-molecules can be detected.

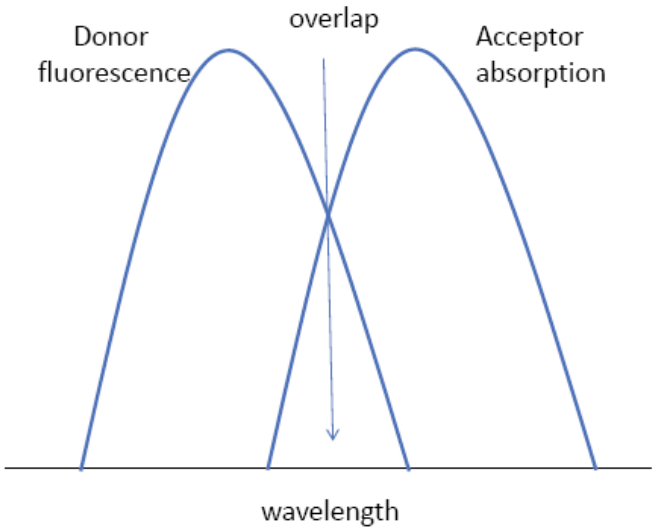

A.

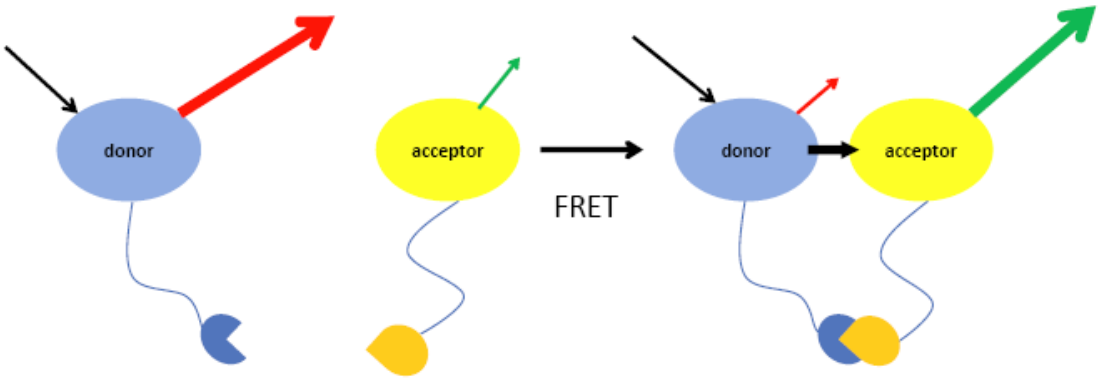

B.

Figure 1.3 Schematic mechanism of FRET. A. In a donor-acceptor pair, the fluorescence emission spectrum of donor must partly overlap with the absorption spectrum of acceptor. B. When donor and acceptor are in proximity, energy transfer will occur. In this process, fluorescence emission of donor decreases while emission of acceptor increases.

In 1994, the Engelman group utilized FRET to study glycophorin A helical transmembrane (GpA TM) domain dimerization in phospholipid bilayer.[42] Two populations of GpA TM peptides were separately labeled with donor chromophore 2, 6-dansyl chloride or acceptor chromophore dabsyl chloride. And when association between GpA TM occurs, quenching of 2,6-dansyl chloride by

dabsyl chloride was detected. By fitting the detected energy transfer to specific donor-acceptor ratio, GpA TM was found to form a dimer in lipid bilayer.

Subunit interaction can also be detected by cross-linking, exploiting the ability of two cysteines (Cys) residues which are in proximity in space to form disulfide bonds.[43] Disulfide cross-linking has been widely used in studies of protein folding, structure and stability.[44, 45] In 2003, thiol-disulfide exchange reaction was used to quantitatively explore the thermodynamics of membrane protein for the first time.[46] DeGrado and co-workers reported their application of disulfide cross-linking in measuring the thermodynamics of membrane protein association in detergent micelles. Their research subject was the transmembrane helix domain of M2 protein from the influenza A virus, which has been previously shown to self-associate into tetramer, while maintaining its drug-binding affinity in the meantime.[47] Residue 19 in the transmembrane fragment is a cysteine, which can form disulfide-bonds with Cys19 from another segment when subunit association occurs. Under reversible redox conditions created by using a buffer containing reduced (GSH) and oxidized (GSSG) glutathione at the proper ratio, monomer-tetramer equilibrium was achieved and quantified. Based on those data and further thermodynamic analysis, association constants for the tetramerization equilibrium in decylphosphocholine (DPC) detergent micelles were obtained. Five months after this paper was published, the same research group reported that they had expanded this model system to phospholipid bilayer which better mimicked the natural membrane as compared to detergent micelles.[48] As of today the cross-linking method has been applied to study membrane protein oligomerization in several other systems including dimerization of outer membrane phospholipase A and subunits interaction of glycoprotein Ib on platelets.[49, 50]

While these three techniques have been used to study the oligomerization of membrane proteins *in vitro*, either in detergent micelles or lipid bilayers, two genetic screen systems, TOXCAT and GALLEX, have been developed for *in vivo* studies.[51, 52] In those assay systems, the target transmembrane domain is linked with a specific DNA binding domain of a regulator protein, which can recognize and bind to specific DNA sequences and regulate the expression of a downstream reporter product upon dimerization.

TOXCAT was developed by Russ and Engelman in 1999. In their study, the N-terminal DNA binding domain of ToxR, which is a dimerization-dependent transcriptional activator, and a transmembrane domain of protein GpA were linked together (Figure 1.4).[51, 53] The C-terminal part of this protein was fused with the maltose binding protein, which functions as a monomeric periplasmic anchor. ToxR dimer can bind and activate a reporter gene encoding chloramphenicol acetyltransferase (CAT). By detecting the expression level of CAT, information about the strength of GpA TM association can be obtained. For TM mutants whose dimerization ability are compromised, expression level of CAT decrease significantly, which differentiate them from native TMs. Thus, residues that play important roles in oligomerization can be identified. In addition, another application of this strategy is to screen random peptide sequences libraries for novel oligomerization motifs.[54] The advantage of this system is the association of peptide domains can be detected in natural cell membrane instead of membrane-mimic environment.

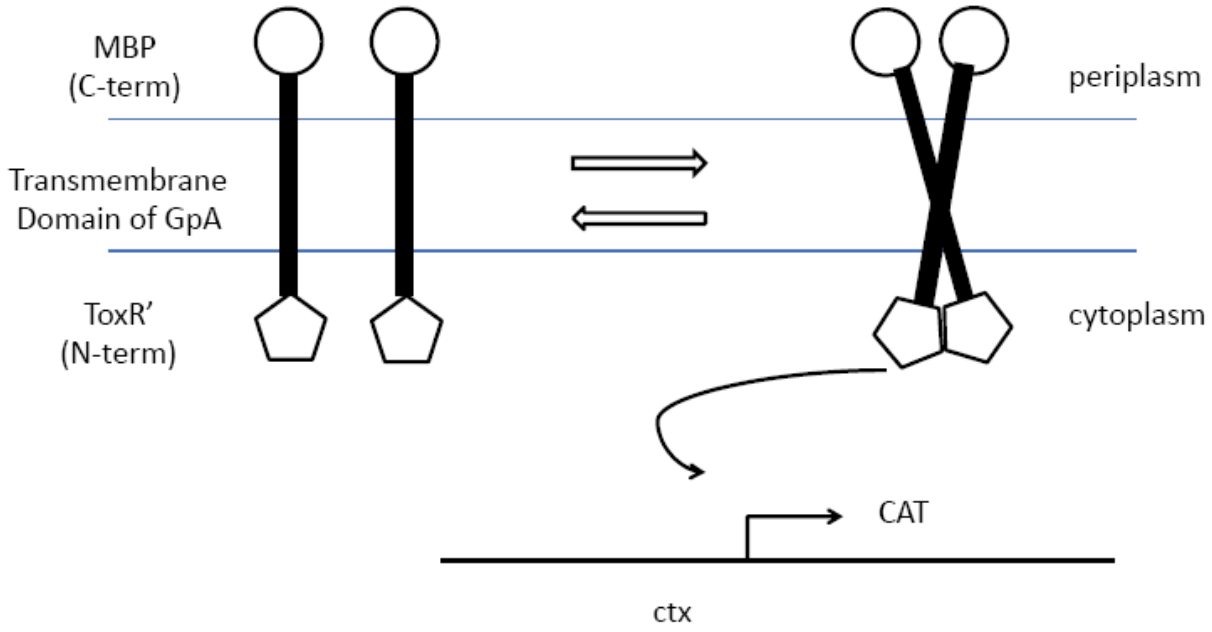

Figure 1.4 Schematic diagram of mechanism for the TOXCAT assay system. The cytoplasmic domain of ToxR (labeled as ToxR') is fused to the N-terminal of the target TM. Maltose binding protein (MBP) is fused to the C-terminal of the TM. Oligomerization of TM mediates dimerization of ToxR, which activate expression of CAT at the ctx promoter.

1.2 Proteolysis in Prokaryotes

1.2.1 The Proteolytic Machinery in Bacteria

A series of chaperone-protease complexes play important roles in general proteolysis and regulated processive proteolysis.[55] These complexes include ClpAP, ClpXP, ClpCP, in which ClpA, ClpX, ClpC are chaperones.[56, 57] These chaperones are AAA+ (abbreviation for ATPases associated with diverse cellular activities) ATPase which can unfold substrate and translocate it to the corresponding protease, such as ClpP.[58] ClpA is distinguished from ClpX based on their respective substrate specificity.[59] ClpC is a subfamily of ClpA-like proteins.[60] Those ATPases assemble into hexamers, while ClpP composes of two heptamer rings stacking together. The hexameric ring of ATPase is located on top of the proteolytic chamber entrance of ClpP. With 14 proteolytic active sites inside the chamber, the space can accommodate unfolded proteins as big as 50 kDa (Figure 1.5).[61]

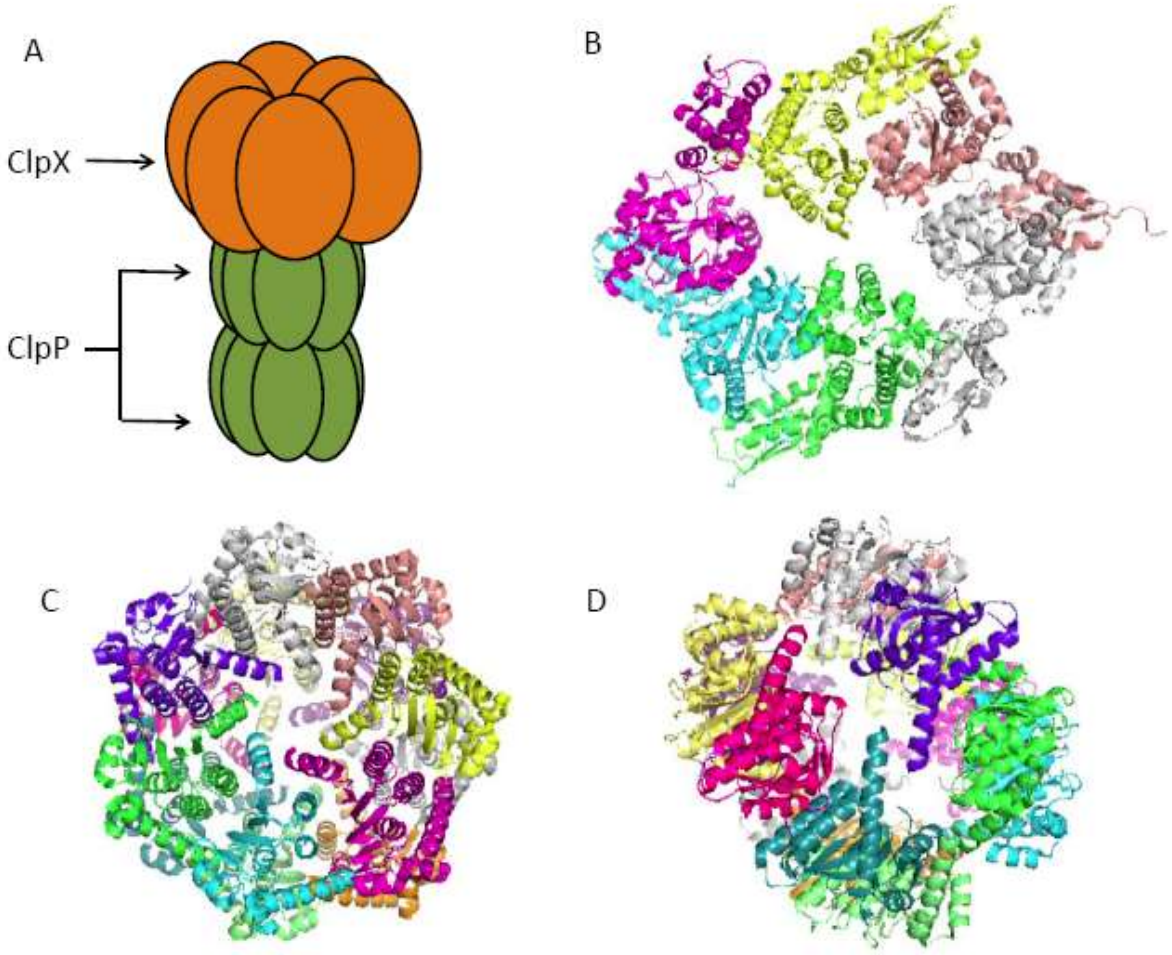

Figure 1.5 Structure of ClpX and ClpP. A. ClpX-ClpP complex. B. Crystal structure of hexameric ring of ClpX. This image is created from 3hte.pdb. C. Crystal structure of two superimposed heptameric rings of ClpP (top view), this image is created from 2ce3.pdb. D. Crystal structure of two superimposed heptameric rings of ClpP (side view), this image is created from 2ce3.pdb.

Lon is an important protease with functions of protein quality control and cellular physiology regulation in prokaryotes and eukaryotes, in which the ATPase domain and proteolytic domain are fused in the same polypeptide chain. It believed that the degradation process is carried on as

follows. Substrates are firstly recognized by the N-terminal domain, and then unfolded by the central ATPase domain. After being transported to the C-terminal proteolytic domain by the ATPase domain, unfolded substrates are finally digested. Although the crystal structure of the full length Lon protein from bacteria hasn't been obtained, crystal structures of truncated Lon and Lon protein from Archaea reveal that Lon protein functions in the form of a hexameric ring.[62, 63]

FtsH is an ATP-dependent Zn metalloprotease, which is active in the hexamer state.[64] Each subunit is anchored to the inner membrane by two trans-membrane sequences, while most part of this protease exists in cytoplasm.[65] Both soluble and membrane proteins can be digested by FtsH, with assistance of specific functional partner proteins.[66, 67] The proteolysis process of membrane proteins can either start from the N-terminus or the C-terminus of the substrates.[68] It was found by Ogura's research group that the bulky uncharged residue Phe228, which is located around the central pore of the hexameric ring, is essential for the proteolysis activity.[69]

One example of an ATP-independent protease is the periplasmic protease DegP. Located in the periplasm, DegP cannot utilize ATP, which only exists in the cytoplasmic compartment, as the energy source. It can degrade damaged or denatured proteins in periplasm produced in response to environmental stress such as heat shock. The protease activity of DegP is exhibited when the temperature is elevated, while at lower temperature DegP is switched to chaperone activity, and the proteolytic domain is inactive. The crystal structure presented by Krojer et al. in 2002 has shown that DegP is a hexamer formed by two trimeric rings with staggered association.[70] However, many functional features of DegP cannot be explained by this crystal model. In 2008,

Krojer et al. reported two different oligomeric states of DegP, 12-mer and 24-mer, by X-ray crystallography and cryo-electron microscopy (cryo-EM).[71] It is proposed that the formation of the large oligomer cage is induced by the presence of substrates.

1.2.2 Protein Degradation in Bacteria

Protein level in cells is not simply controlled by transcription or translation. Another important factor to maintain homeostasis of protein is protein degradation. Different types of abnormal proteins, like misfolded or denatured proteins, are removed by general proteolysis, which is an important way to assure protein quality in cells. One example of protein quality control is the ssrA-tagging system, which is utilized by organisms to dispose of peptides resulting from stalled biogenesis.[72] SsrA tag is a short peptide composed of 11 amino acids, AANDENYALAA.[73] SsrA RNA comes from 10S RNA fraction in *E. coli*. On one hand, it functions as tRNA, since alanine is added to it by alanyl-tRNA synthetase. On the other, when mistakes happen during protein translation, it can function as mRNA and the ssrA tag can be attached to the C-terminus of the incomplete peptide.[74] The addition of the ssrA tag leads to complete degradation of labeled peptides by specific ATPase-protease complex.

However, purpose of most proteolysis, which is regulated proteolysis, is not just to get rid of non-functional proteins. It is involved in various cellular processes, like cell growth, differentiation, signal transduction, stress response, pathogenesis, biofilm formation and protein secretion etc.[75-78] Initiation of proteolysis can be triggered by diverse factors from either the environment or inside the cell. In the proteolysis of CtsR in *B. subtilis*, heat shock stimulates degradation.[79] Under normal culture conditions without heat shock, stabilized CtsR inhibits expression of heat shock genes. When there is a heat shock stimulus, adaptor protein McsB will bind to CtsR, which leads to conformational change of CtsR.[80] Subsequently, CtsR is inactivated and then digested by ClpCP ATPase/protease complex.[81]

One type of intrinsic recognition signal of proteolysis resides at the N-terminus of protein substrates, which is described as the N-end rule pathway.[82, 83] In 1991, Tobias and colleagues demonstrated that some proteolysis processes in bacteria follow N-end rule pathway.[84, 85] They found that when the N-end residue of a specific protein from bacteria is arginine, lysine, leucine, phenylalanine, tyrosine or tryptophan, the degradation rate of this protein is greatly accelerated (half-life ~mins), compared with corresponding protein with other residues at the N-terminus (half-life ~hours). These amino acids are named destabilizing residues. Among them, leucine, phenylalanine, tyrosine and tryptophan are primary destabilizing residues, while arginine and lysine are secondary destabilizing residues. While primary destabilizing residues directly mediate protein degradation, secondary destabilizing residues recruit a leucyl/phenylalanyl-tRNA protein transferase (L/F-transferase or Aat) to add primary destabilizing residues leucine or phenylalanine to the N-terminus.[86] In 2007, the Erbse group has found that ClpS is the adaptor, which binds to the N-terminal destabilizing residues of proteolysis substrates, and then transports the substrates to the ATPase/protease complex ClpAP for degradation.[87] Methionine, which is a stabilizing residue, is the N-terminal residue for newly-synthesized proteins. Although it can be removed during co-translational modification by methionine aminopeptidases (MetAPs) if the second residue has a small side chain, like glycine, cysteine, alanine or serine, the resulted N-terminal residue is still a stabilizing residue.[88] This constrains the substrates scope of N-end pathway proteolysis and ensures that the pathway is a regulated process. The N-end rule proteolysis can be tightly controlled by the removal of stabilizing residues or addition of destabilizing residues at the N-terminus.

In response to diverse stimuli, both degradation signals in substrate proteins can be triggered, or adaptor proteins will interact with substrate proteins.[89-91] These changes can initiate regulated proteolysis, which either completely breaks down proteins (processive proteolysis) or modify proteins by partial degradation (non-processive proteolysis).[92] One example is the activation of flagellar gene expression by regulated processive proteolysis of phosphorylated DegU (DegU-P).[93] Bacteria utilize flagella, which whip like appendages, to move through liquids or over solid surfaces towards nutrients. Flagella-enabled motility plays an important role in pathogenesis of bacteria.[94] In *Bacillus subtilis*, expression of flagellar filament protein, flagellin, is activated by proteins SwrA, SwrB and sigma factor sigma D. When sigma D directly interacts with antisigma factor FlgM in the absence of SwrA and SwrB, expression of flagellin is inhibited. DegU is a two-component system response regulator transcription factor. It was found that phosphorylated DegU can activate expression of FlgM, and subsequently inhibit formation of flagella indirectly.[95] Ogura's research group has demonstrated that DegU-P can be degraded by ClpCP complex.[96] Upon proteolysis, FlgM expression is inhibited and flagellin expression is activated by sigma D regulation.

Regulated proteolysis is not only used for completely destroying protein, but also utilized by cells to partially digest target protein and turn it into an active regulatory factor at specific time and location upon certain signals. PodJ is a scaffolding protein which involved in polar organelle development in alphaproteobacteria *C. crescentus*.[97] It has two isomers, $PodJ_L$ is the complete version and $PodJ_S$ is the truncated, non-processive proteolysis product, which is anchored to the membrane. PodJ is a large protein composed of 974 amino acids.[98, 99] The structure of PodJ can be divided into three parts, the cytoplasmic N-terminus, a single transmembrane domain, and

finally a periplasmic C-terminus portion. At least three proteases are involved in the cascade proteolysis process of PodJ. First, the periplasmic aspartic protease PerP cleaves the periplasmic domain of PodJ, leaving the transmembrane domain and cytoplasmic domain.[100, 101] Immediately, intramembrane metalloprotease (IMMP) MmpA degraded the transmembrane portion, which relieved the cytoplasmic domain $PodJ_S$.[102] $PodJ_S$ is required for recruiting polar factors that are important for pole development after cell division. After cell differentiation, $PodJ_S$ is digested by another protease, which hasn't been identified so far.[103]

1.3 Multidrug Resistance (MDR) of Bacteria

Multidrug resistance is defined as antimicrobial resistance or insensitivity shown by microorganisms to antimicrobial medicines.[104-106] Microorganisms like bacteria, virus, fungi and parasites all can develop resistance to administrated medicines. Among them, multidrug resistance of bacteria is most threatening to global public health.[107, 108] MDR-associated worldwide health problem includes, but not limited to spreading and persistence of infections, especially hospital-acquired infections, increased mortality rates due to infections out of control, and rising medical research cost, which is aimed to develop novel antimicrobial agents with diverse targeting mechanisms.[109-111]

Alexander Fleming has said that there is probably no chemotherapeutic drug to which in suitable circumstances the bacteria cannot react by in some way acquiring 'fastness' resistance.[112] MDR are developed by bacteria through various mechanisms, which can be divided into intrinsic mechanisms and acquired ones. Intrinsic mechanisms are usually conferred by genes naturally existing in microorganisms, while acquired mechanisms include MDR-related gene mutations and transfer of resistance genes carried by mobile genetic materials.[113]

Antibiotics can be either degraded or chemically modified by certain enzymes, and consequently lose their activity.[114] The genes expressing those enzymes can be obtained by plasmid transformation, while in some other cases, these genes naturally locate in chromosome of organisms. Moore et al. found in 2005 by that in *Bacteroides fragilis*, tetracycline antibiotics can be hydroxylated by yhe enzyme, flavin-dependent monooxygenase. After hydroxylation, the

resulting product is not stable at physiological pH and antibiotic activity of the compounds is lost.[115]

When drug targets are modified via genetic mutation, the efficiency of antibiotics greatly decreases.[116] One example of MDR resulted from substrate alteration is vancomycin resistance in Gram-positive cocci.[117] Vancomycin acts by binding to the D-Ala-D-Ala C-terminus of the pentapeptide building block of peptidoglycan, which forms the cell wall of Gram-positive bacteria.[118] Gene mutation or mobile gene transfer produces an enzyme which synthesizes D-Ala-D-lactate instead of D-Ala-D-Ala. Vancomycin has low affinity to the altered substrate, and thus the replacement of the terminal Ala by a lactate results in vancomycin resistance in the microorganism.[119]

Drug efflux pumps have also played an important role in the development of MDR.[120, 121] Drug efflux pumps in bacteria can be classified according to their energy source or substrate specificity. Some of these pumps have high specificity of substrate exportation, and only chemicals with certain structural features can be pumped out of cells, while others are more promiscuous in terms of efflux substrates. Some efflux proteins need to form complexes with other proteins to generate a complete transportation system, and can expel a wide range of structurally unrelated compounds.[122, 123] It has been reported that the overexpression of the multidrug pump system AcrAB-TolC is strongly correlated with fluoroquinolone, ciprofloxacin, tetracycline resistance in many different MDR strains.[124]

1.4 Multidrug Efflux Pumps of Bacteria

Multidrug efflux pumps are membrane protein complexes that actively transport foreign objects out of cells. The active efflux of these pumps is a critical self-defense mechanism that enables the survival of bacteria under hostile environments.[125, 126] The currently identified drug efflux pumps can be categorized into five major families, based on their number of transmembrane domains, type of substrates, and energy sources (Figure 1.6). They are the resistance-nodulation-division (RND) family, the major facilitator superfamily (MFS), the ATP-binding cassette (ABC) superfamily, the small multidrug resistance (SMR) family and the multidrug and toxic compound extrusion (MATE) family.[127, 128] Among them, ABC super family is the only primary transporter, which efflux compounds out of cell upon ATP hydrolysis. Proteins from other families are secondary porter, whose transportation process is coupled with the electrochemical gradient of H^+ or Na^+ across the membrane.[129]

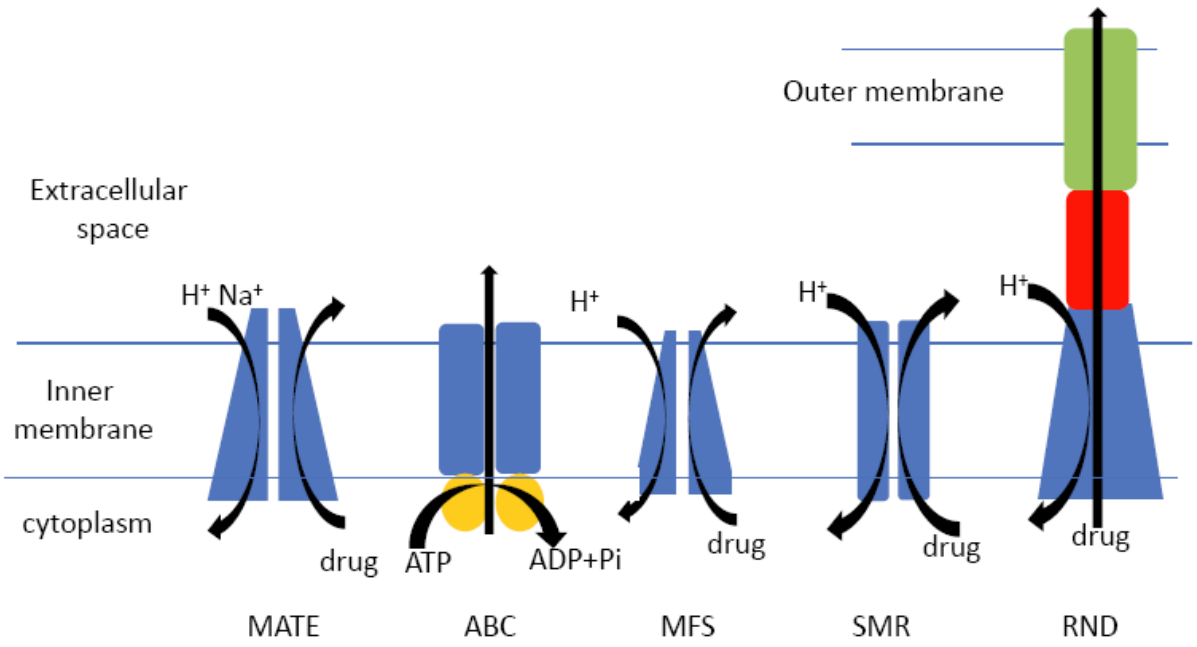

Figure 1.6 Five major families of multidrug resistant pumps.

RND family transporters play important roles in MDR resistance of bacteria. Overexpression of RND pumps has been associated with development of MDR resistance in different strains.[130] Deletion of RND transporters makes those strains susceptible to therapeutic antibiotics.[131] The transporters of this family have large periplasmic domains, and always associate with a periplasmic fusion protein and an outer membrane protein to form a complete efflux channel spanning the two layer membrane of Gram-negative bacteria to pump a variety of compounds out of cells, including many antibiotics and chemotherapeutic agents.[132] The inner membrane protein is a drug/proton antiporter, which is responsible of capturing substrate and providing energy for the whole pump system. The most intensively studied examples of this class are the AcrAB-TolC tripartite complex in *E. coli*. and MexAB-OprM in *Pseudomonas aeruginosa*.[133, 134] Besides antibiotics, RND efflux pump is also capable of transporting host derived chemicals such as bile salts and fatty acids. This efflux allows bacteria to survive in the hostile host environment.[135]

MFS is the largest secondary transporter family, containing more than 10,000 proteins with sequenced genes. These proteins can be categorized into 76 classes, which can be found in all kindoms of life.[136, 137] Each type of MFS transporter can only efflux compounds with certain structural features. The wide range of their substrates include carbohydrates, lipids, amino acids and nucleosides, as well as other molecules.[138] From the numerous members of MFS family, few proteins have been intensively investigated, such as *E. coli* lactose permease LacY, whereas most of MFS proteins have unknown function.[139] Various MFS transporters are involved in different physiology processes. Some sugar porters in MFS family participate in cellular uptake of glucose

and polysaccharides, which is important in sustaining metabolism and energy homeostasis in organisms.[140] Structural elucidation of MFS proteins hasn't matched with the identification of new proteins. Up to date, only 7 from 6 subfamilies have reported crystal structures. Most of the proteins have 12 transmembrane helices, and both the N- and C-terminus face the cytoplasm.[141]

ABC superfamily proteins transport molecules driven by the energy released from ATP hydrolysis. As a general structural feature, all ABC transporters are composed of 4 domains or subunits. Two of them are hydrophobic membrane-spanning domains (MSDs), which are believed to directly constitute the translocation channel across the membrane, whereas the other two are hydrophilic nucleotide-binding domains (NBDs) which catalyze the hydrolysis of ATP at the cytoplasmic surface and provide energy for substrates transportation.[142, 143] Some ABC proteins function as efflux pumps, which export proteins related to pathogenesis, or other compounds like peptide antibiotics and drug. Other ABC proteins serve as bacterial uptake system with the assistance of a high-affinity solute binding protein, which is located in the periplasm in Gram-negative bacteria or tethered to the cell surface in Gram-positive bacteria.[144, 145]

The SMR transporter family has been only found in bacteria. By utilizing the proton motive force across the membrane, a wide variety of molecules such as cationic detergents, dyes and antibiotics are extruded out of cell, which confers resistance against those toxic compounds of bacteria. As implied by the name, SMR proteins are relative small, and composed of about 100-140 residues with 4 transmembrane (TM) α-helices spanning the cytoplasmic membrane.[146, 147] EmrE is the most studied SMR family member, whose crystal structure indicates that it functions

as an asymmetrical homodimer (Figure 1.7)[148]. TM helix 1 (TM 1) and TM helix 3 (TM3) of each monomer constitute the substrate binding pocket within the membrane, whereas the interaction between TM 4's of different monomers are associated with the dimer formation. Glu14 is the key residue, which is conserved in most SMR proteins.[149] It plays major role in recognizing cationic substrates, and also in facilitating entrance of protons during efflux.

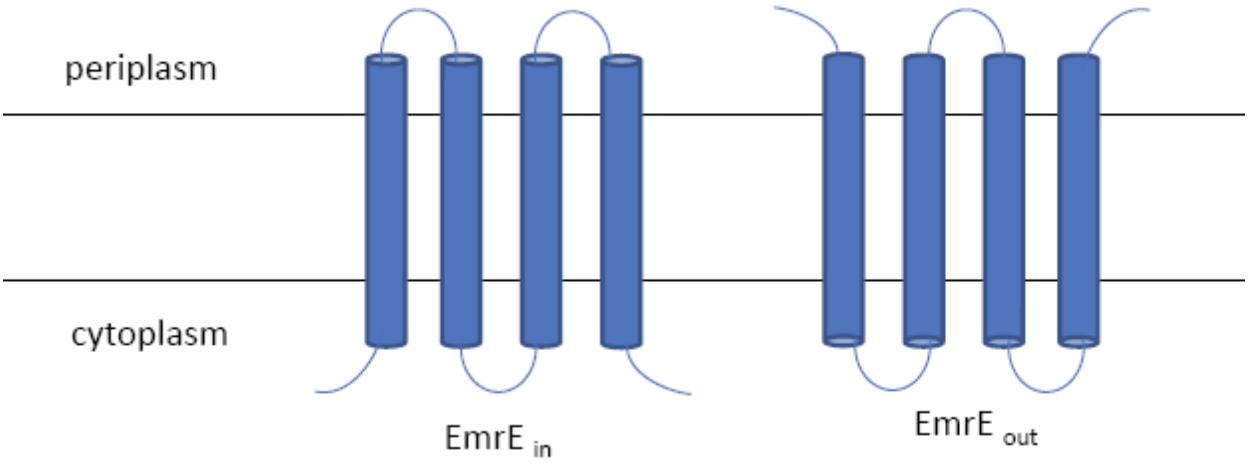

Figure 1.7 Asymmetrical homodimer of EmrE.

Proteins from multidrug and toxic compound extrusion (MATE) family can be found not only in prokaryotes, but also in eukaryotes, like yeasts, fungi, plants and mammals. The presence of a MATE transporter in bacteria was reported to correlate with resistance to tigecycline, which is a new glycylcycline-class antibiotic.[150] The substrate transportation mechanism of MATE protein is thought to be coupled with the antiport of Na^+ across the membrane. The first MATE-type transporter is NorM, which was identified and reported by Morita et al. in 1998.[151] Although more MATE proteins have been characterized, there is no apparent conserved peptide sequence

for the majority of MATE transporters. They have about 40% similarity, which suggests an overall conserved structure and function. Most of them are around 400-500 amino acids long, and have 12 transmembrane helices.[152] In 2010, He et al. published a crystal structure of NorM from *Vibrio cholerea*, showing that the protein has an outward-facing conformation, and a cation-binding site was identified in proximity to transportation relevant residues. The proposed transportation mechanism is the binding of cation from extracellular environment induces the outward-facing conformation changing to inward-facing conformation. Substrate binding causes the conformation changing back to outward-facing, allowing substrates exportation (Figure 1.8).[153]

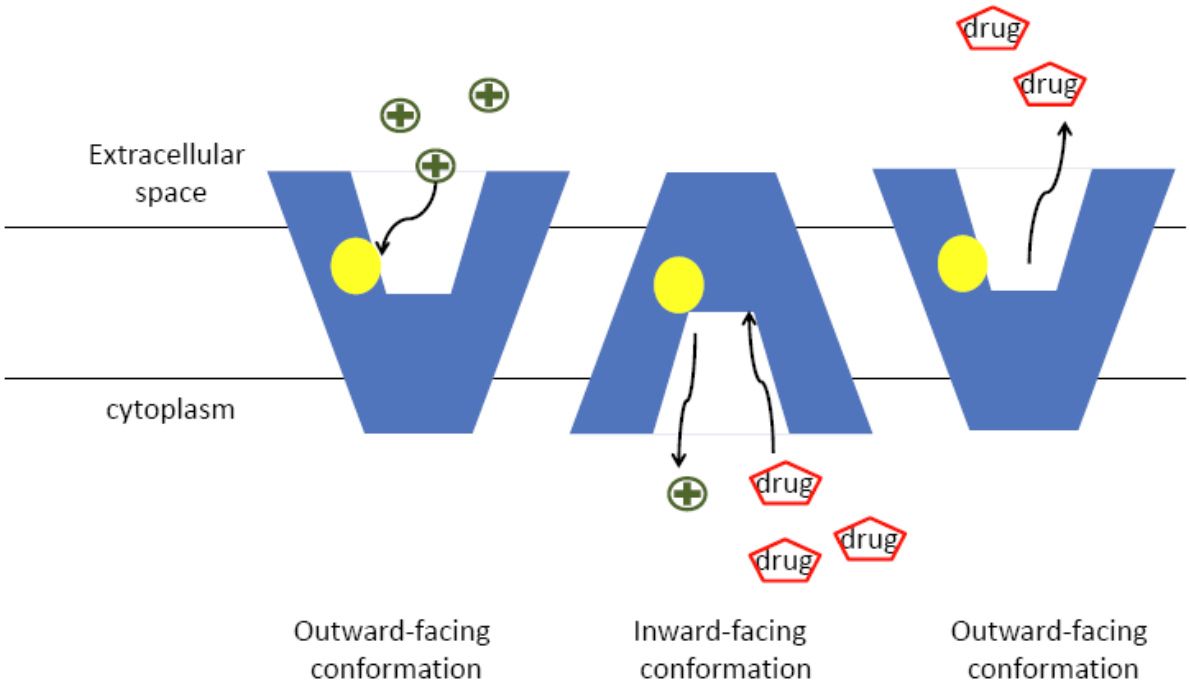

Figure 1.8 Proposed drug transportation mechanism of NorM protein. Cation (green) binding induces outward-facing conformation changing to inward-facing conformation. Cation is

released in cytoplasm and drug compounds from the cytoplasm bind to the transport protein, which changes conformation to outward-facing. And the bound drug molecules are released into the extracellular space.

1.5 Introduction of AcrB

Escherichia coli thrive in the intestinal tract, where there are high concentrations of bile salts. Bile salts are toxic to cells at high concentration.[154] Enteric flora *E. coli* can survive at a bile salt concentration as high as 20 mM. It is initially thought that the outer-membrane of Gram-negative bacteria could prevent the influx of the destructive compounds.[155] In 1997 Nikaido and coworkers discovered that the active efflux transporter AcrB, which is located in the inner membrane of *E. coli*, plays an important role in the resistance.[156] In addition to bile salts, AcrB transports a broad range of compounds, including cationic dyes like crystal violet, ethidium bromide, rhodamine 6G, antibiotics like novobiocin, tetracyclines, penicillins, and detergents like Triton X-100 and sodium dodecylsulfate (Figure 1.9).[157] Active efflux by AcrB and its homologues is critical for multidrug resistance in Gram-negative bacteria.[158]

Efflux pump AcrB is a member of the Resistance-Nodulation-Division (RND) super family.[159] In *E. coli*, it associates with periplasmic protein AcrA, which belongs to the Membrane Fusion Protein family (MFP), and outer membrane channel TolC to form a tripartite complex that spans the inner membrane, periplasmic space, and outer membrane of an *E. coli* cell (Figure 1.10). This tripartite complex extrudes a variety of noxious compounds out of cell from both the cytoplasm and the periplasm. In this complex, AcrB is the component that binds substrate first and transports substrates through a 'channel-tunnel' formed by docking with TolC out into external environment.[160] AcrA is a periplasmic protein which nearly spans the entire periplasm and presumably assists the tight interaction between AcrB and TolC.

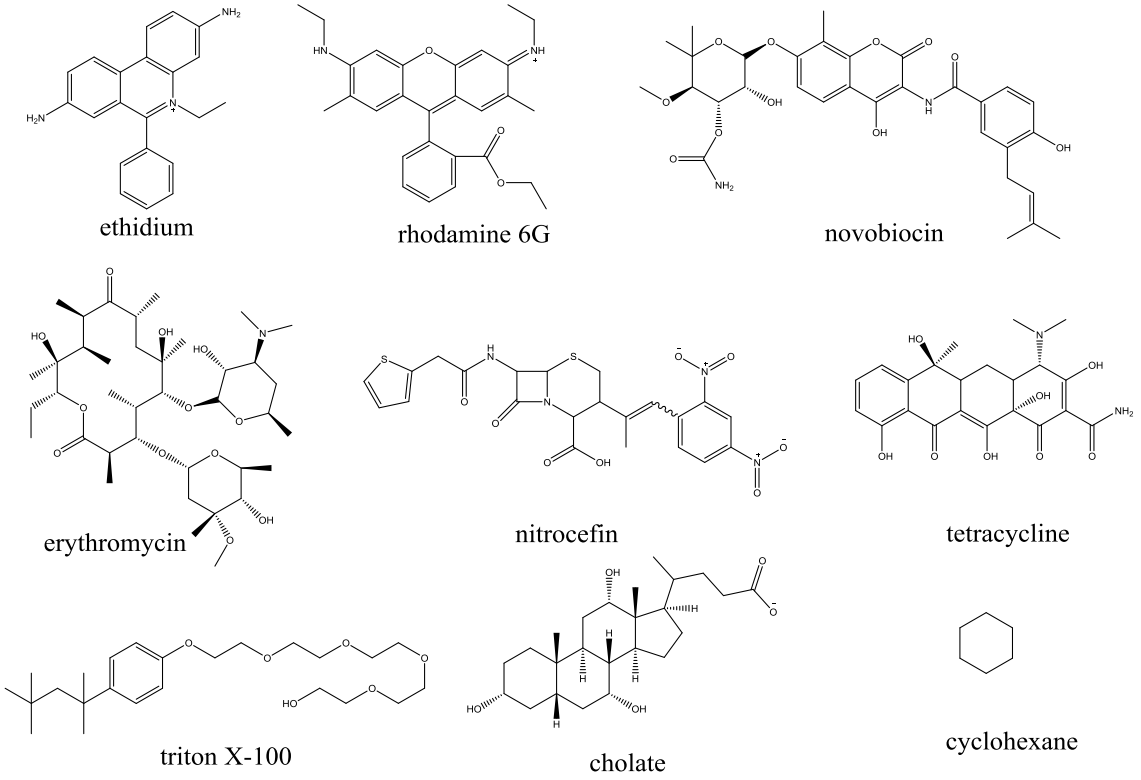

Figure 1.9 Selected substrates of the AcrA-AcrB-TolC efflux system.

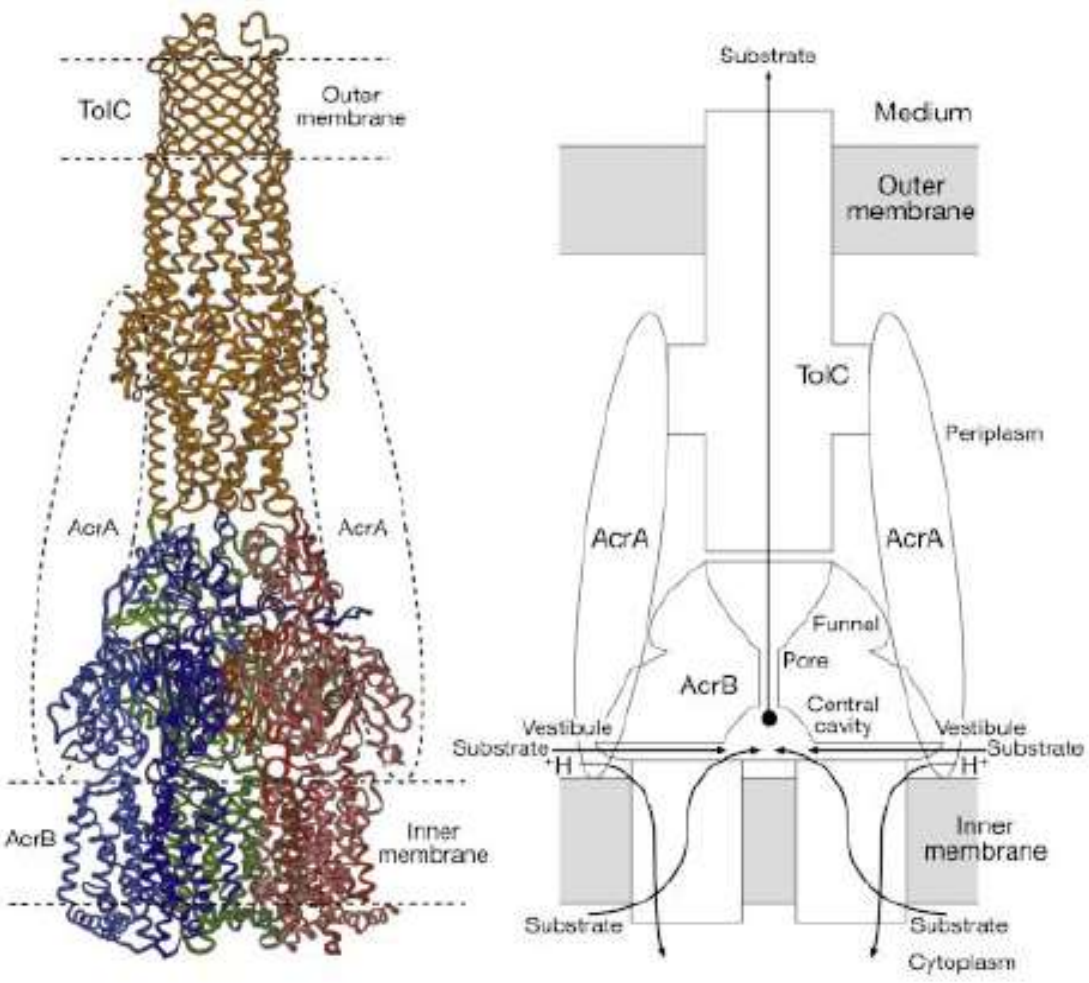

Figure 1.10 Docking structural model and drug efflux mechanism of AcrA-AcrB-TolC tripartite complex. AcrA is represented by dotted ovals in the left model. Reprinted by permission from Macmillan Publishers Ltd: Nature (Murakami, S., Nakashima, R., Yamashita, E., and Yamaguchi, A. Crystal structure of bacterial multidrug efflux transporter AcrB, 419, 587-593) ©2002.

AcrB functions as a trimer, containing three identical subunits of 1049 residues. Murakami et al. determined the first crystal structure of AcrB in 2002 at 3.5 Å resolution.[160] The entire architecture can be divided into 3 parts. The bottom part is a transmembrane domain containing

twelve transmembrane alpha-helices from each protomer. Transmembrane domains from three protomers form a central channel spanning the entire inner membrane and link to the pore structure in the periplasm (Figure 1.10). The section immediately above the transmembrane domain and located in periplasm is the pore domain. Each protomer is composed of four subdomains, each of which is a complex of beta-strands and alpha-helices. In the middle of the trimer, each protomer contributes an alpha-helix, forming the pore structure as mentioned above (Figure 1.11). Between the pore domains of neighboring subunits, there is a tunnel called the vestibule which connects the bottom of the pore to the periplasm. It has been proposed to be a pathway for substrates in the periplasm to enter the pore. The TolC docking domain is above the pore domain and presumably connects TolC with AcrB. Each docking domain has two mixed-beta-sheet subdomains. And the docking domains from all three protomers together form a funnel-like structure. The diameter of the top of the funnel is very close to that of the bottom of TolC. Each docking domain possesses a hairpin structure which inserts into the neighboring protomer and this hairpin structure is critical to the interaction between adjacent protomers (Figure 1.12).

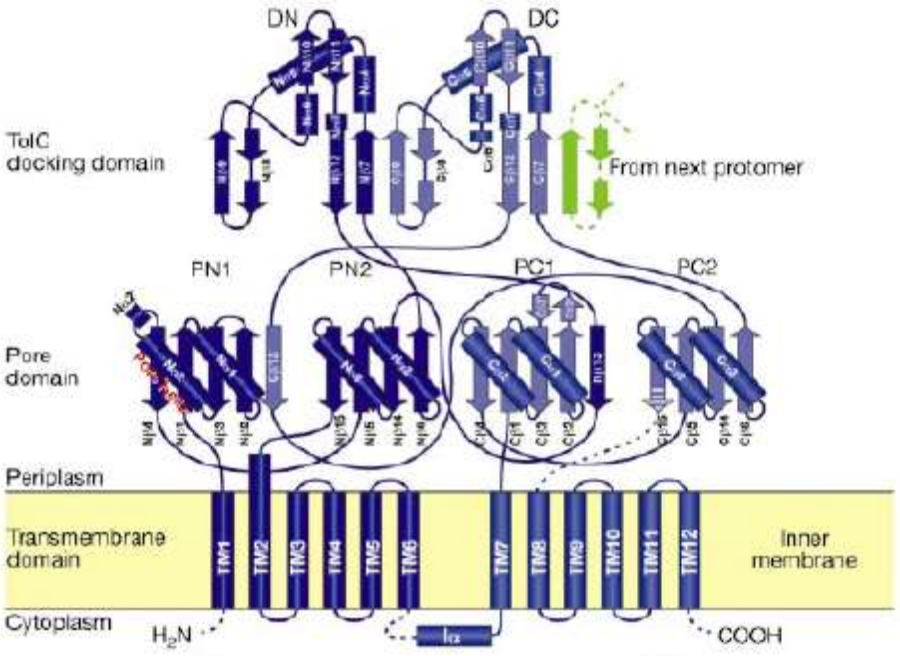

Figure 1.11 Topology diagram of an AcrB protomer showing the secondary structure elements. Cylinders and arrows are alpha-helices and beta-strands, respectively. Definition of different domains and position of the inner membrane were shown. Reprinted by permission from Macmillan Publishers Ltd: Nature (Murakami, S., Nakashima, R., Yamashita, E., and Yamaguchi, A. Crystal structure of bacterial multidrug efflux transporter AcrB, 419, 587-593) ©2002.

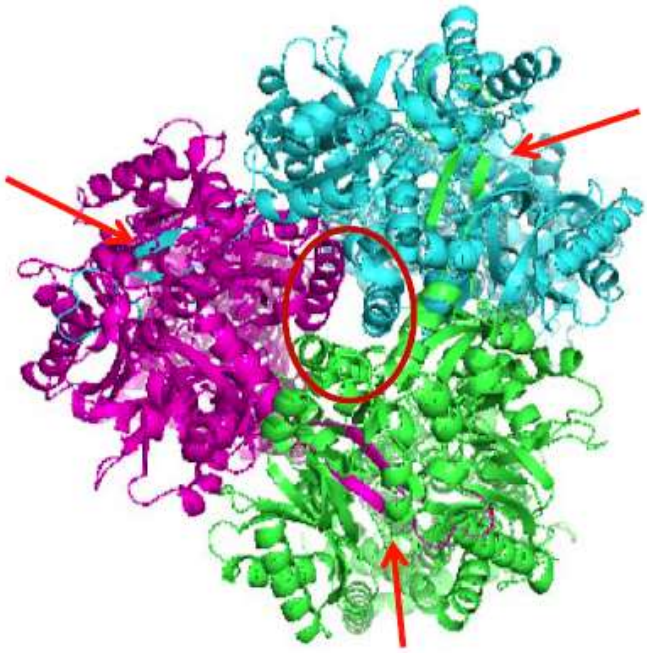

Figure 1.12 Top view of an AcrB trimer in ribbon representation. Each protomer is individually colored. The red arrows show the hairpins critical for trimerization. The red circle depicted the pore structure formed by three alpha-helices, each contributed by one protomer. This image is created from 2GIF.pdb.

In 2006, Murakami et al. determined the crystal structure of AcrB bound with substrates, which has provided researchers a foundation to speculate the transport mechanism of AcrB.[161] Conformations of the three protomers in an AcrB trimer are distinctively different. Only one protomer binds substrate, even when the concentration of drug reaches saturation in the co-crystallization system. And there are also conformational differences between the other two protomers. Researchers have proposed a three-step rotary mechanism for AcrB, in which each protomer is in a different state at any time of transportation: access, binding, and extrusion (Figure 1.13).[130, 161, 162] During the transportation process, each protomer cycles through the

access, binding, and extrusion states sequentially, and then goes back to the access state. In the access state, the vestibule is open and the substrate has access to it. In the binding state, the binding pocket in the protomer expands so that it has enough space to accommodate a substrate. Finally protomer bound with a substrate rotates into the extrusion state, when vestibule is closed and the exit pass is open. The substrate is released into the funnel structure of TolC docking domain of AcrB.

The structure and function of AcrB has been the subject of many studies. While the efflux mechanism, interaction with AcrA/TolC, and substrate binding and translocation pathway of AcrB have been thoroughly investigated, little is known about its oligomerization process. AcrB is an obligate trimer, existing and functioning exclusively as a trimer.[161] The trimerization process of AcrB is an indispensable component for the understanding of AcrB facilitated drug resistance, and yet little work has been done to elucidate this process.

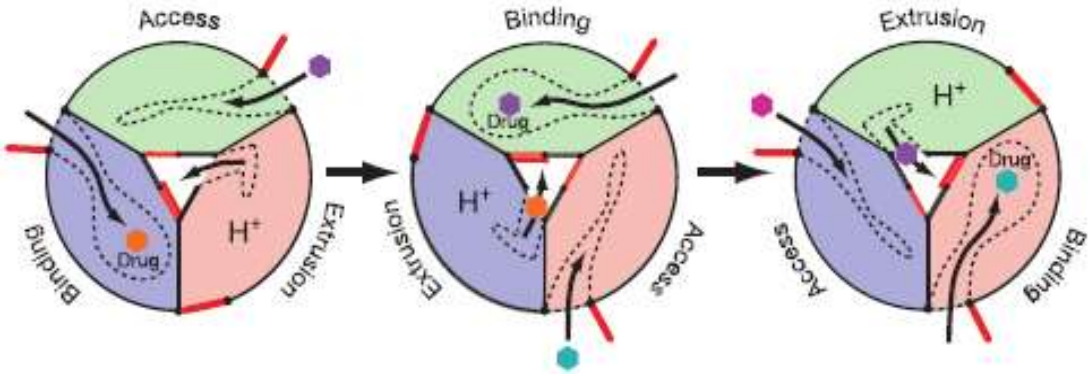

Figure 1.13 Schematic diagram of the proposed three-step rotatary drug efflux mechanism of AcrB (top view). Entrance and exit of each protomer are depicted as red lines. Dotted lines represent the drug binding pocket and the translocation pathway. Small hexagons represent substrates. Reprinted by permission from Macmillan Publishers Ltd: Nature (Murakami, S.,

Nakashima, R., Yamashita, E., Matsumoto, T. and Yamaguchi, A. Crystal structure of a multidrug transporter reveal a functionally rotating mechanism, 443, 173-179) ©2006.

Chapter II Assembly of AcrB Trimer in Cell Membrane

2.1 Introduction

Biotinylation is a reaction to attach biotin covalently to proteins. It is a widely used protein labeling method for the purpose of protein detection, immobilization and purification.[163] In nature, biotinylation occurs as a type of post-translational modification, which is catalyzed by biotin ligase, also known as Biotin Holoenzyme Synthetase (BHS). During this process, biotin is attached to a natural substrate through the formation of an amide linkage between biotin carboxyl group and the epsilon-amino group of a specific lysine residue (Figure 2.1).[164] In 1999, a 15-residue peptide was reported by Schatz group as a minimal substrate for BHS with comparable biotinylation kinetics as natural substrate. The sequence of this 15-mer is GLNDIFEAQKIEWHE, and is named the avitag. The avitag can be fused at either N-terminus or C-terminus of the target protein. [165] With advantages of small size and high efficiency of biotinylation, the avitag becomes a widely used protein tag which can serve a variety of purposes, such as protein purification, detection and immobilization. In this study, I fused the avitag at the C-terminus of AcrB as a specific marker in the study of monomer co-assembly in the cell membrane.

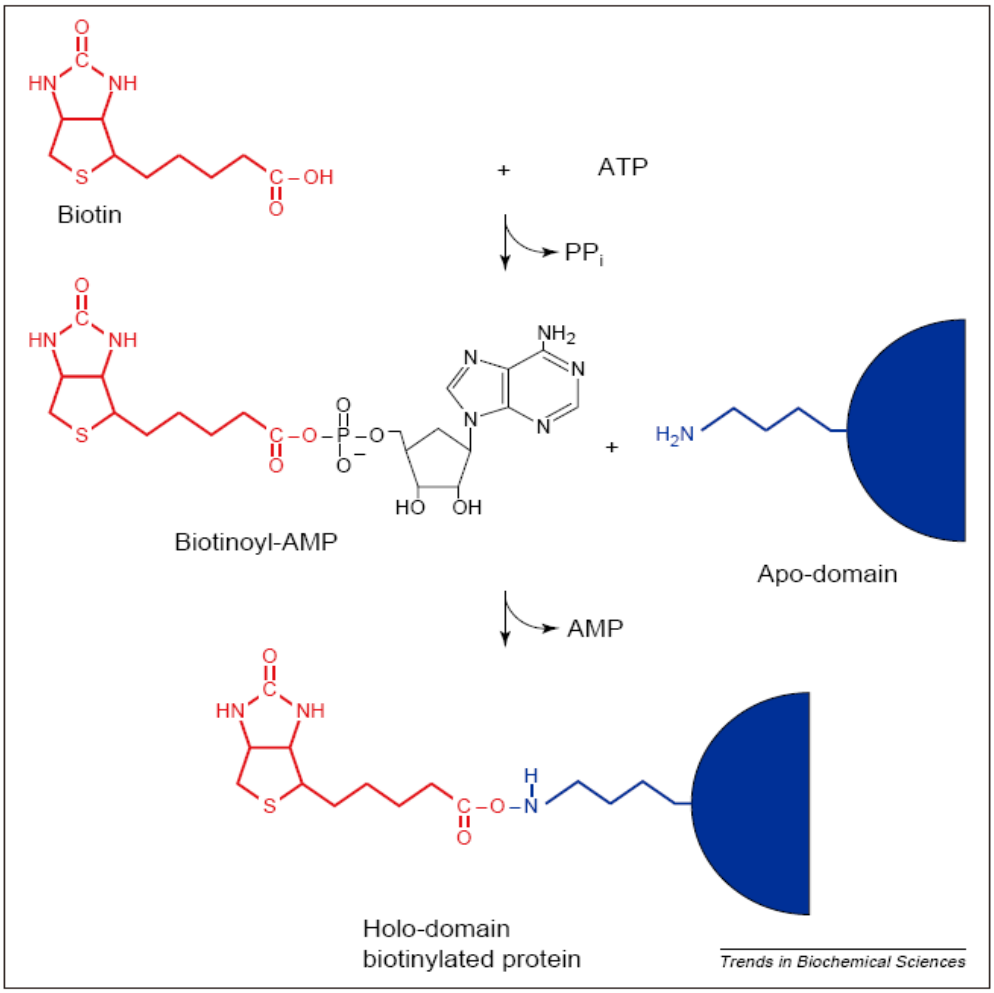

Figure 2.1 The biotin protein ligase (BPL) reaction. Reprinted from Trends in Biochemical Sciences, 24, Chapman-Smith, A. and Cronan Jr., J. E., The enzymatic biotinylation of proteins: a post-translational modification of exceptional specificity, 359-363, Copyright (1999), with permission from Elsevier.

As discussed in the previous chapter, oligomerization is a dominant phenomenon in protein structure due to its several functional advantages over monomers.[3] For example, oligomers can adopt a variety of symmetrical structures to provide specific morphological functions.[166] Cooperativity of oligomeric proteins, including allosteric regulation and multivalent binding, as

well as equilibration between monomer and oligomer serves as a mechanism for activity regulation.[167, 168] Although bioinformatics studies reveal that around 35% of proteins exist and function as oligomers instead of monomers, the process by which monomers assembling into oligomers in the cell is poorly understood.[1, 169] By studying the oligomerization of inner membrane protein AcrB, our group has previous found that individual subunits of AcrB folded before oligomerization, and monomer folding and trimerization were two sequential steps.[170] In the following study, another aspect of the oligomerization of AcrB homo-trimer has been investigated. This research answers the questions, how do monomeric subunits of AcrB form trimers, and whether the assembling is a completely random process or does it follow any other rules. To answer these questions, AcrB constructs with different tags were designed and expressed in the same cell, and then their co-assembling behavior was studied.

2.2 Materials and Methods

2.2.1 Materials

Protein molecular weight marker (Spectra Multicolor High Range Protein Ladder) for SDS-PAGE was from Thermo (Rockford, IL). The custom polyclonal rabbit anti-AcrB antibody was obtained from GenScript (Piscataway, NJ).[170] All enzymes for nucleic acid manipulation were from New England Biolabs (Ipswich, MA) and all the chemicals from BioWorld (Dublin, OH). The parent wild-type (BW25113) and AcrB deficient *ΔacrB* strains were obtained from the Yale Coli genetic stock center. The *ΔacrB* strain lacks the chromosomal *acrB* gene and is kanamycin resistant.

2.2.2 Cloning, expression and purification of AcrB and its mutants

The gene encoding AcrB was amplified through Polymerase Chain Reaction (PCR) from template *E. coli* genomic DNA. After PCR, amplified AcrB genes were inserted into pBAD33 between digestion sites XbaI and HindIII, or into pAC5 between SacI and HindIII, respectively.

Protein coding sequences in all plasmids used in this study were confirmed by DNA sequencing. Plasmid pBAD33-$AcrB_{histag}$ and pAC5-$AcrB_{avitag}$ were then transformed respectively into an *E. coli* strain deficient in gene *acrB* (BW25113*ΔacrB*) for protein expression. Bacteria containing plasmid pBAD33-$AcrB_{histag}$ were cultured at 37 ℃ in Lysogeny Broth (LB) media with 50 μg/mL kanamycin and 25 μg/mL chloramphenicol, while bacteria containing plasmid pAC5-$AcrB_{avitag}$ with 50 μg/mL kanamycin and 100 μg/mL ampicillin. Co-transformed bacteria containing both plasmid pBAD33-$AcrB_{histag}$ and pAC5-$AcrB_{avitag}$ were cultured at 37 ℃ in LB media with 50 μg/mL kanamycin, 25 μg/mL chloramphenicol and 100 μg/mL ampicillin. The

same ampicillin and kanamycin concentrations were used throughout the study, unless otherwise noted. After overnight culture, cells were harvested by centrifugation at 7,000×g for 10 min at 4 ℃. Bacterial cells were used immediately for purification.

$AcrB_{histag}$ was purified using metal affinity chromatography as described.[171] Briefly, the cell pellet was resuspended in a lysis buffer (30 mM sodium phosphate buffer solution (NaPi), 0.5 M NaCl, 10% glycerol, 1mM phenylmethylsulfonyl fluoride (PMSF), pH 7.5) and then sonicated using a Fisher Scientific Sonicator Dismembrator (MODEL 150E) on ice for 20 min with 5 sec on/off intervals and 75% amplitude to break the cells. After centrifuged at 15,000×g for 20 min at 4 ℃, the supernatant containing soluble proteins were discarded, while the precipitant which contains the membrane was re-suspended in an extraction buffer (30 mM NaPi, 0.5 M NaCl, 10% glycerol, 1% Triton X-100, pH 7.5) and then shaken on ice for 2 h. The extraction mixture was then centrifuged at 15,000×g for 20 min at 4 ℃. AcrB was recovered in the supernatant. Imidazole was added in the supernatant (pH~7.5) to a final concentration of 10 mM and the supernatant was incubated with nickel-nitriloacetic acid (Ni-NTA) resin at 4 ℃ for 45 min. After incubation, the supernatant-resin mixture was loaded to a column, washed using a buffer containing the indicated concentration of imidazole (30 mM NaPi, 0.5 M NaCl, 10% glycerol, 1% triton, 10-100 mM imidazole, pH 7.5) and eluted using an elution buffer (30 mM NaPi, 0.5 M NaCl, 10% glycerol, 0.03% n-Dodecyl β-D-Maltopyranoside (DDM), 200 mM imidazole, pH 7.5). Purified protein was analyzed in sodium dodecyl sulfate-polyacrylamide gel electrophoresis (SDS-PAGE) and visualized using Coomassie Blue staining.

2.2.3 Drug susceptibility assay

AcrB activity was measured using a drug susceptibility assay.[172] *E. coli* strain BW25113*ΔacrB* was used as the host cell. BW25113*ΔacrB* strains transformed with plasmid pQE70-AcrB or the empty vector pQE70 were used as positive and negative controls, respectively. Freshly transformed cells were plated on LB agarose plates containing the corresponding antibiotics. A single colony was used to inoculate a LB media. The exponential-phase cultures of different strains were diluted to an OD_{600nm} unit of 0.1 using LB broth. 5 μL of this culture was used to inoculate 2 mL of LB media containing the indicated concentration of erythromycin or novobiocin. The cultures were incubated with shaking at 37 ℃ overnight. The next morning, OD_{600nm} of each sample was measured. The lowest concentration of drug that completely inhibited the growth of bacteria was recorded as the minimum inhibitory concentration (MIC). Each experiment was repeated at least three times.

2.2.4 Analysis of expression levels of AcrB by immunoblotting

Freshly transformed colonies of BW25113*ΔacrB* containing plasmid pBAD33-$AcrB_{histag}$ or pAC5-$AcrB_{avitag}$ were used to inoculate LB medium containing proper antibiotics. After culturing at 37 ℃ overnight, cells were harvested by centrifugation at 7,000 ×g for 10 min at 4 ℃, and then resuspended in a lysis buffer (30 mM NaPi, 0.5 M NaCl, 10% glycerol, 1mM PMSF, pH 7.5) to an OD_{600nm} of 15. Equal volumes of the re-suspended solution were withdrawn and sonicate on ice for 20 min with 5 sec on/off intervals and 75% amplitude to lyse the cells. After centrifugation at 15,000 ×g for 20 min at 4 ℃, the supernatant containing soluble proteins were discarded. The cell paste containing membrane vesicles was re-suspended in an extraction buffer (30 mM NaPi, 0.5 M NaCl, 10% glycerol, 1% Triton X-100, pH 7.5) and then was shaken on ice

for 2 h. The extraction mixture was then centrifuged at 15,000×g for 20 min at 4 ℃. AcrB was extracted into the supernatant. SDS-Loading buffer was then added into the samples. The samples were resolved using SDS-PAGE and transferred to a polyvinylidene difluoride (PVDF) membrane for Western blot analysis using a polyclonal rabbit anti-AcrB primary antibody and an alkaline phosphatase-conjugated anti-rabbit secondary antibody. Protein-antibody conjugates were visualized using substrates *Nitro blue tetrazolium chloride* (NBT) and 5-bromo-4-chloro-3'-indoyl phosphate p-toluidine (BCIP).

2.2.5 Determination of the biotinylation level of AcrB

A standard sample, $AcrB_{histag\text{-}avitag}$, was first purified as described above. This AcrB construct contains both histag and avitag, in which a stretch of 30 residues containing LEHHHHHHSGGGSGGGLNDIFEAQKIEWHE was added to the C-terminal of AcrB. The corresponding plasmid, pBAD-$AcrB_{histag\text{-}avitag}$, was transformed into BW25113*ΔacrB* for protein expression. The presence of the avitag did not interfere with the purification of the protein through the histag. The biotinylation level of purified $AcrB_{histag\text{-}avitag}$ was determined using a commercial biotinylation quantification kit (Pierce Biotin Quantitation Kit).[173, 174]

Next, we used a mixture of purified $AcrB_{histag\text{-}avitag}$ and $AcrB_{histag}$ to create a calibration plot. For this plot, a series of standard solutions were made, each contained the same amount of AcrB, but with an increasing ratio of $AcrB_{histag\text{-}avitag}$ to $AcrB_{histag}$ (Figure 2.2). The samples were subjected to anti-AcrB Western blotting and anti-Biotin Western blotting. All samples have bands of the same intensity in anti-AcrB Western Blotting, while in anti-biotin Western blotting an increase of band intensity was observed due to the increase of $AcrB_{histag\text{-}avitag}$ portion.

Figure 2.2 Schematic diagram of the biotinylation level measurement. A series of standard solutions with increasing percentage of $AcrB_{histag\text{-}avitag}$ were prepared. In anti-biotin Western blot, standard solution with higher $AcrB_{histag\text{-}avitag}$% showed more intense band. By comparing band intensity of protein sample with the ladder, its $AcrB_{avitag}$% can be estimated. Blue represents AcrB without biotinylation ($AcrB_{histag}$), and yellow represents AcrB with biotinylation ($AcrB_{histag\text{-}avitag}$ in standards and $AcrB_{avitag}$ in the unknown sample).

To determine the level of biotinylation in co-expressing strains, detergent was used to extract AcrB from co-transformation strain. Before loading AcrB sample on gel, AcrB concentration was adjusted to the same level as the concentration in standard samples. In anti-biotin Western blot, band intensity comparison revealed the percentage of $AcrB_{avitag}$ in crude membrane extraction. Biotinylation level of purified AcrB was determined similarly.

2.3 Results and Discussions

2.3.1 Drug tolerance of strains BW25113*ΔacrB* containing plasmid pBAD-AcrB$_{histag}$ or pAC5-AcrB$_{avitag}$

To examine if the introduction of the fusion tags at the C-terminus affects the structure and function of AcrB, we tested the drug susceptibility of an *acrB* gene knockout strain containing these plasmids. In addition to the two strains containing these plasmids, strain *BW25113ΔacrB* with no plasmid and with plasmid encoding wild-type AcrB (pET22b-AcrB) were used as negative and positive controls, respectively. MIC data were summarized in Table 2.1.

Table 2.1 MIC of BW25113*ΔacrB* transformed with different plasmids (μg/ml).

	Ery	Nov	R6G	TPP
No plasmid	2	5	5	5
pET22b-AcrB	80	320	640	640
pBAD-AcrB$_{histag}$	80	320	640	640
pAC5-AcrB$_{avitag}$	80	320	640	640

It can be seen that strain *BW25113ΔacrB*-pBAD33-AcrB$_{histag}$ and *BW25113ΔacrB*-pAC5-AcrB$_{avitag}$ both had the same MIC as the positive control, indicating that these two AcrB constructs were fully active.

2.3.2 Expression level of AcrB in two plasmids

The relative expression level of AcrB$_{histag}$ and AcrB$_{avitag}$ was determined through anti-AcrB Western blot analysis (Figure 2.2). Under the same experimental condition, the band intensity of

$AcrB_{histag}$ was twice the intensity of $AcrB_{avitag}$. Therefore, the relative expression level of AcrB from pBAD33-$AcrB_{histag}$ is twice the expression level from pAC5-$AcrB_{avitag}$.

Figure 2.3 Anti-AcrB Western blot image shows relative expression level for two plasmids, pBAD33-AcrBhistag (left lane), pAC5-AcrBavitag (right lane).

If the assembly of AcrB subunits follows a total random pattern, the abundance of hybrid trimers and pure trimers should follow the statistical analysis as shown in Figure 2.4.

		r = 1	3	4	8	16
$\frac{r}{r+1}\times\frac{r}{r+1}\times\frac{r}{r+1}=\frac{r^3}{(r+1)^3}$		$\frac{1}{8}$	$\frac{27}{64}$	$\frac{64}{125}$	$\frac{512}{729}$	$\frac{4096}{4913}$
$\frac{r}{r+1}\times\frac{r}{r+1}\times\frac{1}{r+1}\times 3=\frac{3r^2}{(r+1)^3}$		$\frac{3}{8}$	$\frac{27}{64}$	$\frac{48}{125}$	$\frac{192}{729}$	$\frac{768}{4913}$
$\frac{r}{r+1}\times\frac{1}{r+1}\times\frac{1}{r+1}\times 3=\frac{3r}{(r+1)^3}$		$\frac{3}{8}$	$\frac{9}{64}$	$\frac{12}{125}$	$\frac{24}{729}$	$\frac{48}{4913}$
$\frac{1}{r+1}\times\frac{1}{r+1}\times\frac{1}{r+1}=\frac{1}{(r+1)^3}$		$\frac{1}{8}$	$\frac{1}{64}$	$\frac{1}{125}$	$\frac{1}{729}$	$\frac{1}{4913}$

Figure 2.4 Statistical analysis of the expected distribution of co-assembling of co-expressed AcrB subunits based on the random mixing mechanism. "r" is the relative expression level of AcrB from one gene source (e.g., the genomic DNA or plasmid #1, white circles) over the other gene source (e.g., plasmid #2, gray circles) in the experimental system. If trimerization in the cell

membrane is completely random, then $r^3/(r+1)^3$ of all trimers will contain three white subunits, and $1/(r+1)^3$ of all trimers will contain three gray subunits. The other trimers will contain either two gray subunits $[3r/(r+1)^3]$ or two white subunits $[3r2/(r+1)^3]$. The corresponding fractions for each species are calculated for cases when r equals to 1, 3, 4, 8, or 16.

According to the analysis shown in Figure 2.4, white circles are $AcrB_{histag}$, grey circles are $AcrB_{avitag}$, and the r value is 2. The relative abundance of pure trimers $(AcrB_{histag})_3$, $(AcrB_{avitag})_3$, and hybrid trimers $(AcrB_{histag})_2(AcrB_{avitag})_1$ and $(AcrB_{histag})_1(AcrB_{avitag})_2$ are 8, 1 and 12, 6, respectively. If there are 27 trimers overall, 8 of them are pure $AcrB_{histag}$ trimer, 12 of them contain 2 $AcrB_{histag}$ subunits each trimer, and 6 of them have 1 $AcrB_{histag}$ subunit each trimer, only 1 is a pure $AcrB_{histag}$ trimer (Figure 2.4). Thus, through examining the relative abundance of pure and mix trimer, we would be able to test if the random assembly model is correct.

Proteins extracted from a strain co-expressing $AcrB_{avitag}$ and $AcrB_{histag}$ were subjected to metal affinity purification. Before purification, the overall level of biotinylation depends on the intrinsic expression level of each type of subunits. Since the expression level of $AcrB_{histag}$ was twice of the expression level of $AcrB_{avitag}$, the expected percentage of the biotinylated AcrB was ~33%. When the AcrB sample was subjected to purification using metal affinity chromatography, only trimers containing at least one $AcrB_{histag}$ subunit would bind to the column and be purified. Therefore, $(AcrB_{avitag})_3$ would be lost. However, since it only accounted for 1/27 of the overall number of trimers, the final biotinylation level of the purified sample would not be affected too much and drop slightly to ~31% (Figure 2.5). Based on this analysis, if the assembly of trimers is

completely random, we expect the level of biotinylation of the sample to remain roughly the same before and after purification.

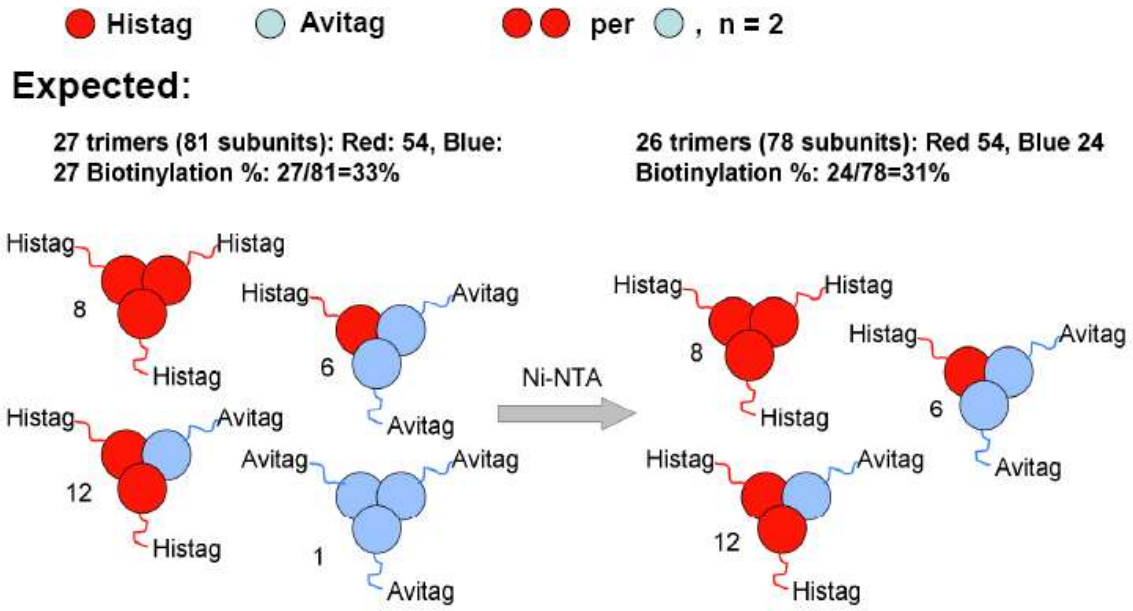

Figure 2.5 Schematic illustration of the co-expression of $AcrB_{histag}$ and $AcrB_{avitag}$. The relative expression level of $AcrB_{histag}$ to $AcrB_{avitag}$ is 2 to 1. Assuming subunits randomly co-assemble into trimers, among 27 trimers, statistically there will be 8, 12, 6, and 1 trimers that contain 3, 2, 1, or 0 $AcrB_{histag}$. The overall biotinylation level is 33%. Once purified using metal affinity chromatography, only trimers containing at least one $AcrB_{histag}$ would be retained. Therefore, 31% of subunits should be biotinylated in purified samples.

2.3.3 Identification of proper washing and elution condition for $AcrB_{histag}$ and $AcrB_{avitag}$

AcrB has a low level of intrinsic affinity to Ni-NTA resin. To find the proper imidazole concentration that selectively elute $AcrB_{avitag}$ or $AcrB_{histag}$, I performed step-wise elution using 20 bed volume (BV) of 10 mM, 10 BV of 50 mM, 2 BV of 100 mM and 6 BV of 500 mM

imidazole in PBS buffer (30 mM phosphate buffer, 200 mM NaCl, pH 7.5). The eluent was collected in 1 mL (2 bed volume) fractions. The first fraction at 10 mM, the first and last fractions at 50 mM, as well as fractions at 100 and 500 mM imidazole were analyzed using SDS-PAGE (Figure 2.5).

Figure 2.6 showed the representative washing-elution patterns of $AcrB_{histag}$ and $AcrB_{histag\text{-}avitag}$. Two conclusions can be drawn based on these results. First, the presence of the avitag sequence at the C-terminal of the histag did not affect the binding and purification of the protein using metal affinity chromatography. Second, PBS buffer containing 10 and 50 mM imidazole did not wash off a significant amount of $AcrB_{histag}$. Buffer containing 100 mM imidazole eluted a significant amount of AcrB, while the majority of AcrB were eluted at 500 mM imidazole. Purified $AcrB_{histag}$ and $AcrB_{histag\text{-}avitag}$ were adjusted to the same concentration, and then mixed at different ratio to establish a series of standard solutions and used in the determination of biotinylation level.

A.

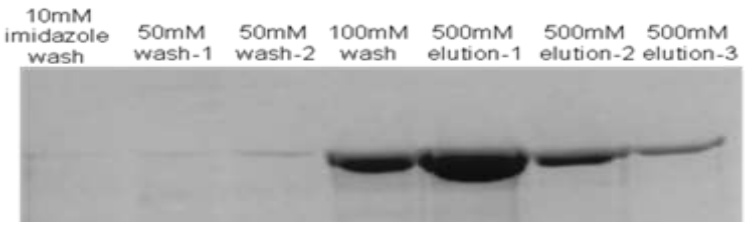

B.

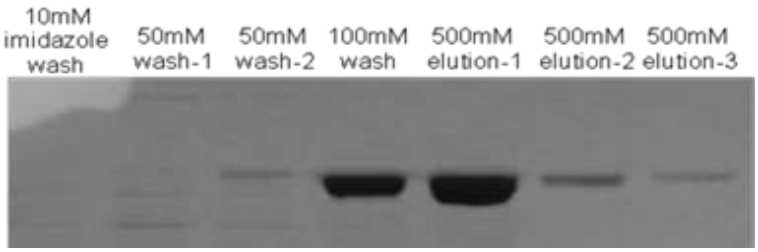

Figure 2.6 A. Gradient washing and elution of $AcrB_{histag}$. B. Gradient washing and elution of $AcrB_{histag\text{-}avitag}$.

2.3.4 Elution patterns of AcrB from co-expression

As discussed above, the biotinylation level of purified AcrB from BW25113*ΔacrB* containing both plasmids pBAD-$AcrB_{histag}$ and pAC5-$AcrB_{avitag}$ could be used to verify the random assembly model. We loaded membrane vesicles extracted from *BW25113ΔacrB* co-expressing $AcrB_{histag}$ and $AcrB_{avitag}$ to the column and eluted following the steps of 10 bed volumes of 10 mM, 10 bed volumes of 50 mM, 2 bed volumes of 100 mM, 2 bed volumes of 200 mM, and finally 2 bed volume of 500 mM imidazole. Eluent was collected in 1 mL (2 bed volume) fractions. The first fraction at 10 mM, the first and last fractions at 50 mM, as well as fractions at 100, 200, and 500 mM imidazole were analyzed using SDS-PAGE (Figure 2.7A). The major elution fraction occurred at 50 mM-1, while the relative intensity of this band was weaker than the corresponding band in $AcrB_{avitag}$ purified alone. In addition, proteins could be detected in all elution fractions, while the 200 mM fraction was slightly stronger than the 100 mM fraction.

We also tested the co-purification of these two proteins by mixing membrane vesicles extracted from *BW25113ΔacrB* expressing either $AcrB_{histag}$ or $AcrB_{avitag}$, which was immediately subjected to metal affinity purification (Figure 2.7B). In this case while both fusion proteins existed in the solution, we believe they did not exchange subunits in the time scale (~1 h) of purification. Consistent with our expectation, there was no detectable difference in the result of purification when the mixture was equilibrated for 2 h before purification. The mixture was purified and eluted under the same condition as described above. The elution pattern was drastically different

from that of the co-expressed sample. The predominant band appeared at 200 mM imidazole, similar as $AcrB_{histag}$ purified alone. In addition, weak bands could be observed in 50 mM elution fractions, which were likely $AcrB_{avitag}$. The band intensity of the first fraction of 50 mM elution (50 mM-1) was weaker than the corresponding band in $AcrB_{avitag}$ purified alone, which could be a result of competitive binding between $AcrB_{histag}$ and $AcrB_{avitag}$ to the resin.

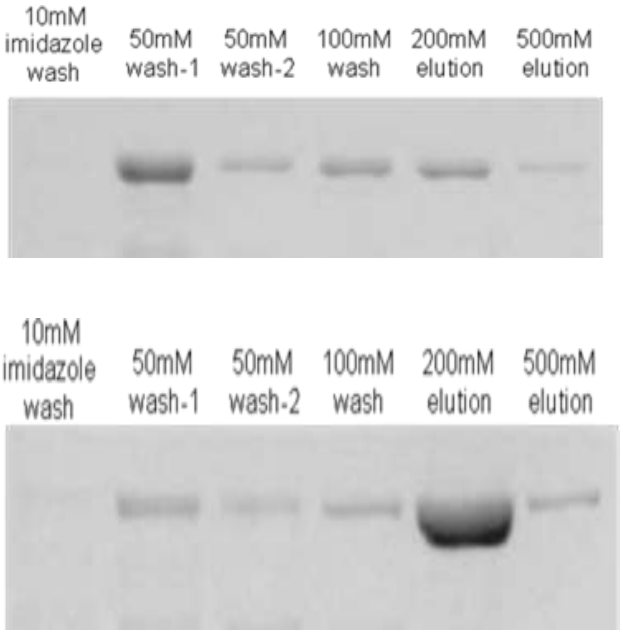

Figure 2.7 A. Gradient elution of co-expressed $AcrB_{histag}$ and $AcrB_{avitag}$. B. Gradient elution of co-purified $AcrB_{histag}$ and $AcrB_{avitag}$ individually expressed and mixed after extraction.

2.3.5 $AcrB_{avitag}$ in co-expressed samples was retained longer on Ni-NTA resin than $AcrB_{avitag}$ in mixed samples

Different elution patterns indicated that AcrB trimer composition of co-expressed sample was different from that of the simply mixed sample. The relative amounts of $AcrB_{avitag}$ and $AcrB_{histag}$ in each elution fraction were determined using anti-biotin Western blot. As described previously, concentrations of purified $AcrB_{histag}$ and $AcrB_{histag\text{-}avitag}$ were adjusted to be the same using SDS-

PAGE. By mixing two types of protein with different volume ratio, a series of standard solutions were made, in which $AcrB_{avitag}$% increased gradually (at the same time, $AcrB_{histag}$% decreased). In anti-biotin Western blot membrane, the series of standard samples generated a band pattern in which band intensity is getting higher when moving from low $AcrB_{avitag}$% to high.

To determine the relative $AcrB_{avitag}$% in each elusion fraction, the AcrB concentration of the samples were adjusted to be the same as the standards. From anti-biotin Western blotting, $AcrB_{avitag}$% can be estimated by comparing band intensity of samples to the standards. Figure 2.7A showed that in aliquots samples from co-transformed strain, $AcrB_{avitag}$ existed at similar levels in all samples (from low imidazole concentration washing to high imidazole concentration elution). Since the bands intensity decreased gradually from washing sample to elution (Figure 2.7B), it means $AcrB_{avitag}$% decreased from 50 mM imidazole wash (similar intensity as 70% ladder) to 200 mM imidazole elution (less intense than 30% ladder).

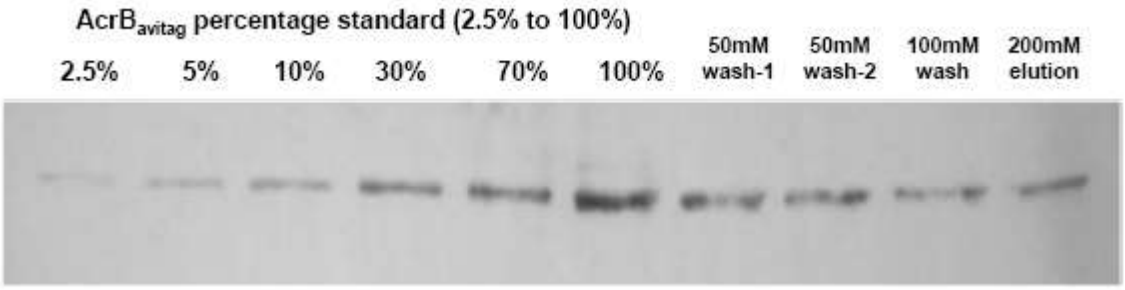

A.

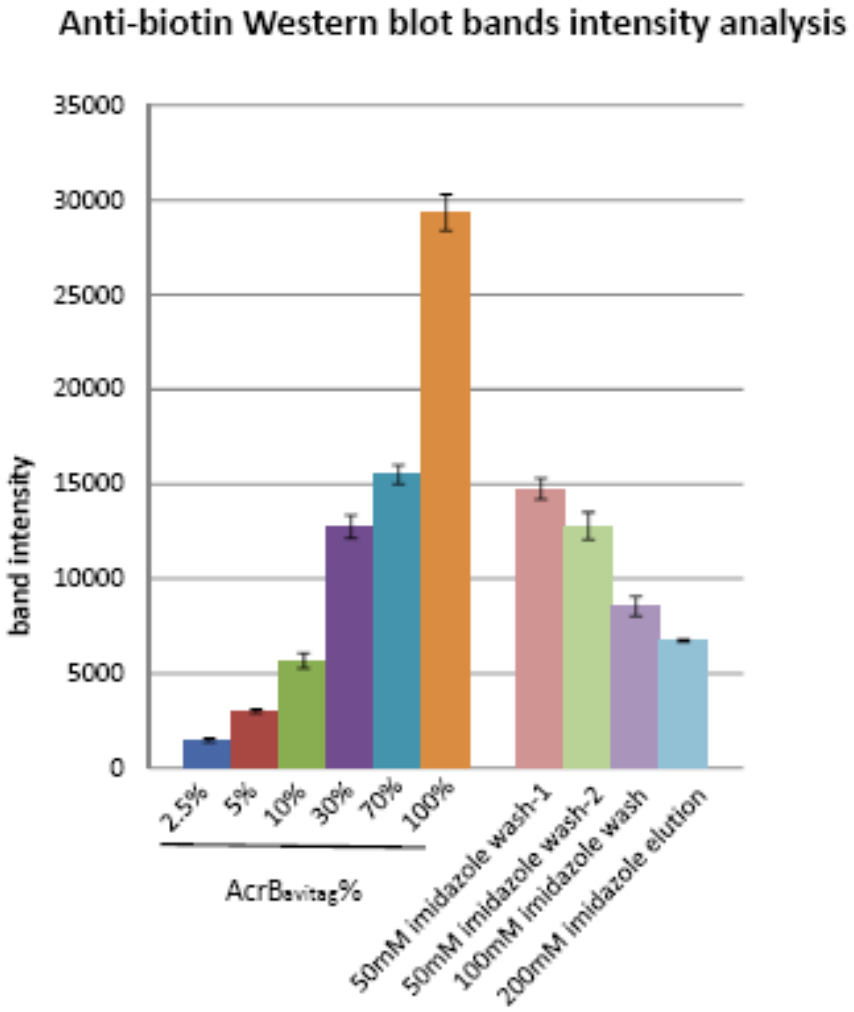

B.

Figure 2.8 A. Anti-biotin Western blot for determining AcrB$_{avitag}$% in purified AcrB from co-expression. B. Anti-biotin Western blot bands intensity analysis by software imageJ.

For the control sample, in which individually expressed $AcrB_{histag}$ and $AcrB_{avitag}$ was mixed before purification as described above, the pattern of biotinylation was completely different. As shown in Figure 2.9, no biotinylation was detected for samples eluted at 200 mM and 500 mM imidazole, indicating that $AcrB_{avitag}$% in elution aliquots were too low to be detected by anti-biotin immunoassay. For the sample eluted at 50 mM imidazole, $AcrB_{avitag}$% was close to 100%. The concentration of $AcrB_{avitag}$ decreased dramatically in the sample eluted at 100 mM imidazole.

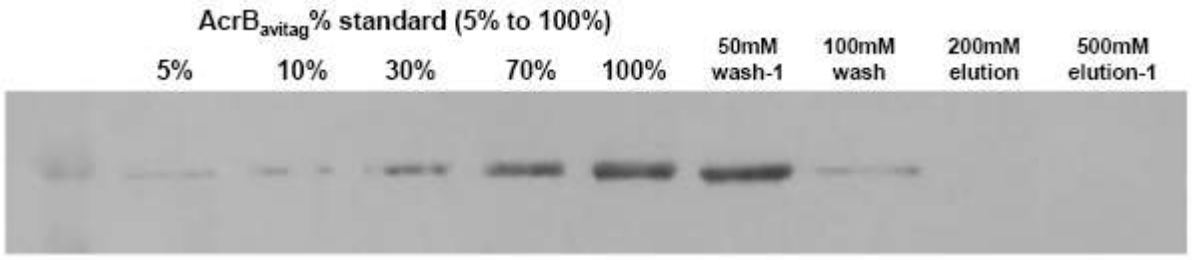

Figure 2.9 Anti-biotin Western blot for determining $AcrB_{avitag}$% in purified AcrB from a mixture of individually expressed $AcrB_{histag}$ and $AcrB_{avitag}$.

In the co-purification case, membrane extractions containing individually expressed $AcrB_{histag}$ or $AcrB_{avitag}$ were mixed right before purification. Since no time was allowed for subunit exchange, there should just be pure $AcrB_{histag}$ trimers and $AcrB_{avitag}$ trimers. The anti-biotin Western blot result (Figure 2.8) showed that the binding between pure $AcrB_{avitag}$ trimer and Ni-beads was weak and the majority of proteins could be effectively eluted using a buffer containing 50 mM imidazole. The small amount of leftover $AcrB_{avitag}$ could be completely eluted by the buffer containing 100 mM imidazole. The difference between the biotinylation patterns as shown in Figure 2.7A and 2.8 indicated that $AcrB_{avitag}$ associate with $AcrB_{histag}$ to form hetero-trimer during co-expression. These hybrid trimers had different $AcrB_{avitag}$/$AcrB_{histag}$ ratios, and thus had

different affinities with Ni-NTA. In summary, co-assembly process of AcrB did occur in cells with two AcrB gene sources based on data obtained so far.

In the above analysis, we assumed that all $AcrB_{avitag}$ subunits were biotinylated for the simplification of discussion. However, the reference point for comparison in this study was the relative levels of biotinylation of the sample in crude membrane extracts, as well as in sequential washing/ elution fractions during metal affinity purification. Therefore, the absolute level of biotinylation of $AcrB_{avitag}$ would not affect the interpretation of the experimental result.

2.3.6 Assembly of AcrB trimer is not completely random

By comparing anti-biotin Western blot band patterns of co-transformed strain with that of extraction mixture, we can conclude that co-assembly of $AcrB_{avitag}$ and $AcrB_{histag}$ happened during co-expression. But whether the co-assembly process follows the random assembly model remains unclear. Previous data and analysis have shown that the relative expression level from pBAD33-$AcrB_{histag}$ and pAC5-$AcrB_{avitag}$ was around 2:1. If AcrB from two gene sources were randomly co-assembled, only pure $AcrB_{avitag}$ trimer would be washed off Ni-NTA at imidazole concentration less than 100 mM, while hybrid trimers and pure his-trimers would remain bound until the imidazole concentration rose to 200 mM. According to the random co-assembly model, $AcrB_{avitag}$% in these elution aliquots should be around 31% (Figure 2.4) which was close to the $AcrB_{avitag}$% of crude membrane extraction before Ni-NTA purification (33%).

To test this assumption, $AcrB_{avitag}$% in crude membrane extraction of co-expressed sample was determined (Figure 2.10). Through comparing $AcrB_{avitag}$% in detergent extracts with the

standards, $AcrB_{avitag}$% was estimated to be 30%. This result was consistent with the observation that the expression level ratio of $AcrB_{histag}$ to $AcrB_{avitag}$ was approximately 2 to1.

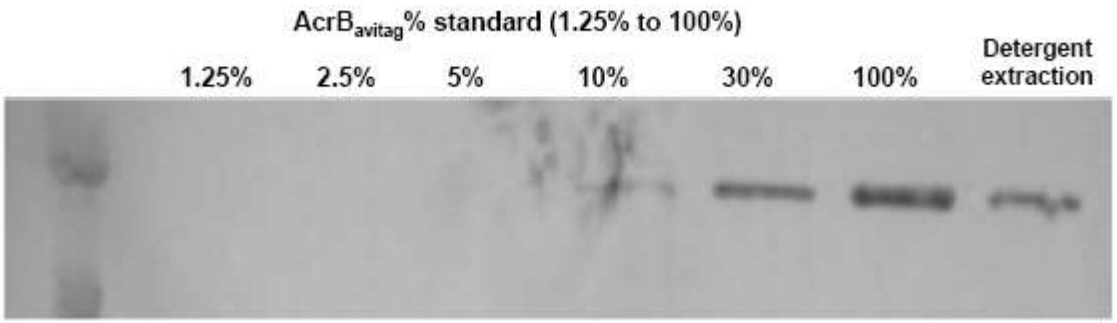

Figure 2.10 Anti-biotin Western blot image for determining $AcrB_{avitag}$% in detergent extraction of co-expressed sample before purification.

Similarly, the percentage of $AcrB_{avitag}$ was determined for the elution fraction at 200 mM imidazole. As shown in Figure 2.11, $AcrB_{avitag}$% was around 5%-10%. This difference indicated that AcrB trimer assembly was not completely random.

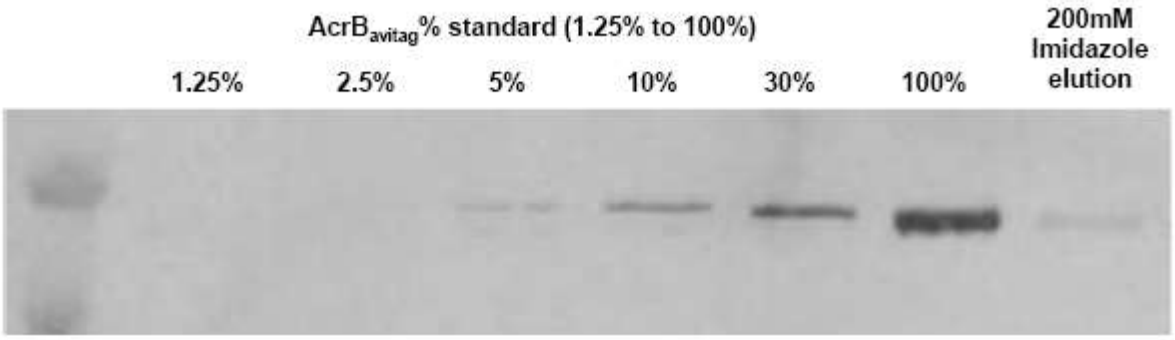

Figure 2.11 Anti-biotin Western blot image for determining $AcrB_{avitag}$% in the 200 mM imidazole elution fraction of co-expressed sample.

2.4 Conclusions

As a summary, based on the above results as well as several other experiments performed by other members of our group, we conclude: 1) co-assembly of AcrB from different gene sources occurs, but not in a random fashion, and 2) the formation of pure trimer is favored. How could the formation of pure trimer be initially favored? One possible explanation for this preference is the "clustering effect" (Figure 2.12). Ribosomes are known to form polysomes where multiple ribosomes translate a single mRNA simultaneously, resembling a chain of pearls when visualized under an electron microscope (EM).[175] When two AcrB variants are expressed together in the same cell (Figure 2.12, red and blue), the structure of polysome determines that subunits of the same type would present at high concentration at the site of production. The elevated concentration of a specific type of subunit favors the formation of pure trimers. Hybrid trimer forms when two polysomes translating different types of subunits happen to locate close to each other, or when monomers diffuse away from its site of production. In addition, AcrB trimers associate/dissociate and equilibrate between pure and hybrid trimers in the cell membrane. The clustering of nascent monomers could also explain the lack of free monomers in the cell membrane—for obligate oligomers such as AcrB, monomers or assembling intermediate multimers are rarely observed. Due to the clustering of ribosomes in a polysome, multiple copies of monomers are made close to each other both in time and space, which greatly promoted the efficiency of oligomerization. Therefore, the majority of nascent monomers could have assembled into trimers before leaving their birthplace.

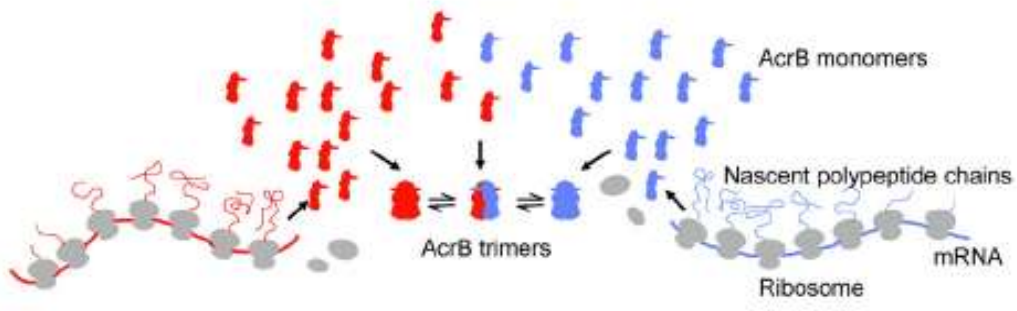

Figure 2.12 Hypothesis of the clustering effect during the production of AcrB trimers.

Chapter III Measurement of Membrane Protein AcrB Trimerization in Cells by the GALLEX System

3.1 Introduction

GALLEX is a genetic screening system which has been used to study protein oligomerization *in vivo*.[51, 176] In the GALLEX assay system, the target transmembrane domain is linked with a specific DNA binding domain of a regulator protein LexA, which can recognize and bind to specific DNA sequences and regulate the expression of a downstream reporter product upon dimerization.[177] LexA acts as a transcription suppressor that negatively regulates the transcription of many different genes in *Escherichia coli* in its dimer form.[178-179] Structure of LexA contains a C-terminal dimerization domain and an N-terminal DNA binding domain (LexA DBD) which does not contribute to dimerization (Figure 3.1).[180-182] As early as 1995, the Schnarr group fused the LexA DBD to the protein Fos to investigate the homo-dimerization capability of Fos variants.[183] Dimerized LexA DBD can recognize an op+/op+ operator sequence which controls the transcription of chromosomal *lacZ* gene in an engineered strain. When homo-association of target protein occurs, LexA DBDs are pulled together and dimerize.[52] Then dimerized LexA DBDs bind to op+/op+ operator and repress transcription of *lacZ*. Subsequently, activity of beta-galactosidase decreases.[184] In this system, protein homo-oligomerization can be measured by testing the activity of beta-galactosidase.

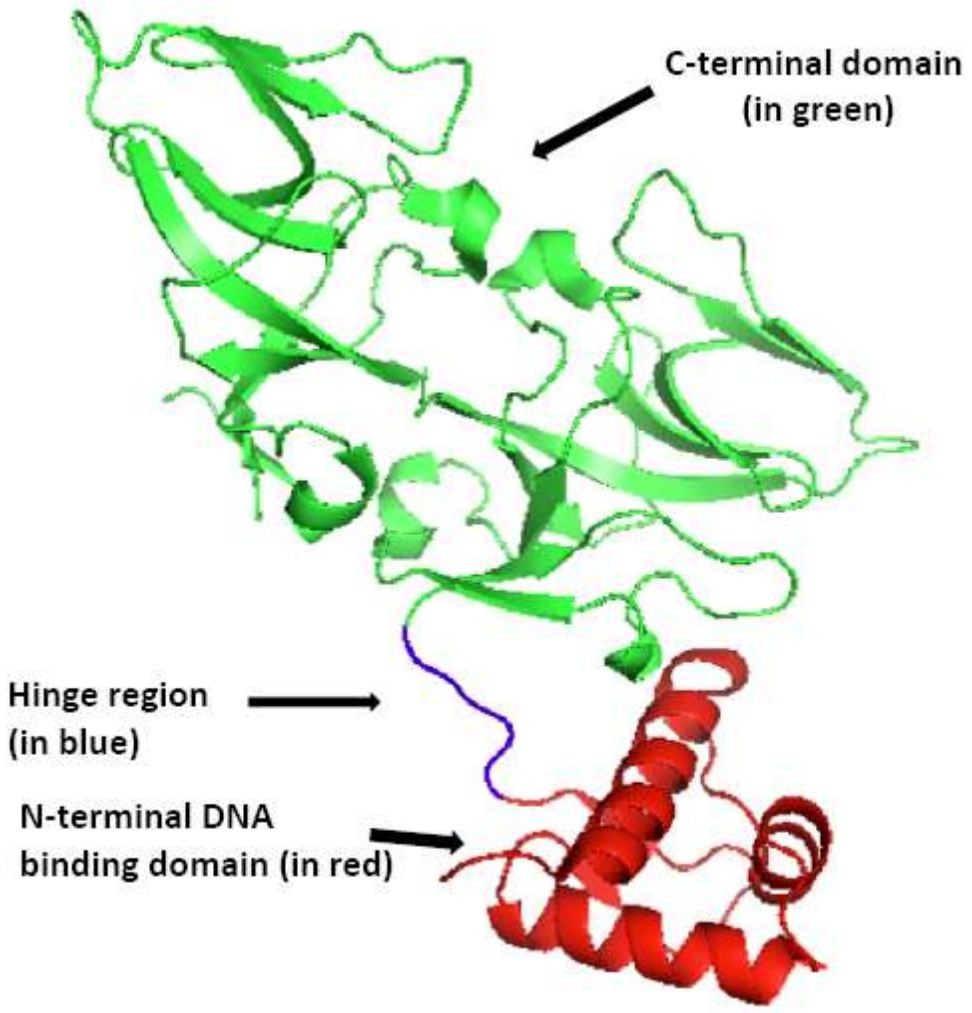

Figure 3.1 Structure of LexA. N-terminal DNA binding domain is colored in red. C-terminal domain is colored in green. Short hinge region linking N-terminal and C-terminal domains is colored in blue (Created from 1JHF.pdb). [185]

To further expand the LexA system to study hetero-oligomerization of proteins, the same group has developed a more advanced system in which two LexA derivatives with different DNA binding specificities are employed.[186] Wild-type LexA recognizes the original sequence (op+), while the recognition sequence of LexA408 variant is an altered operator (op408). Then a

reporter strain (SU202) is constructed in which the chromosomal *lacZ* gene is under the control of an op+/op408 hybrid operator. Hetero-oligomerization of proteins fused to wild-type LexA and LexA408 can be then detected by monitoring the repression of *lacZ* gene (Figure 3.2).

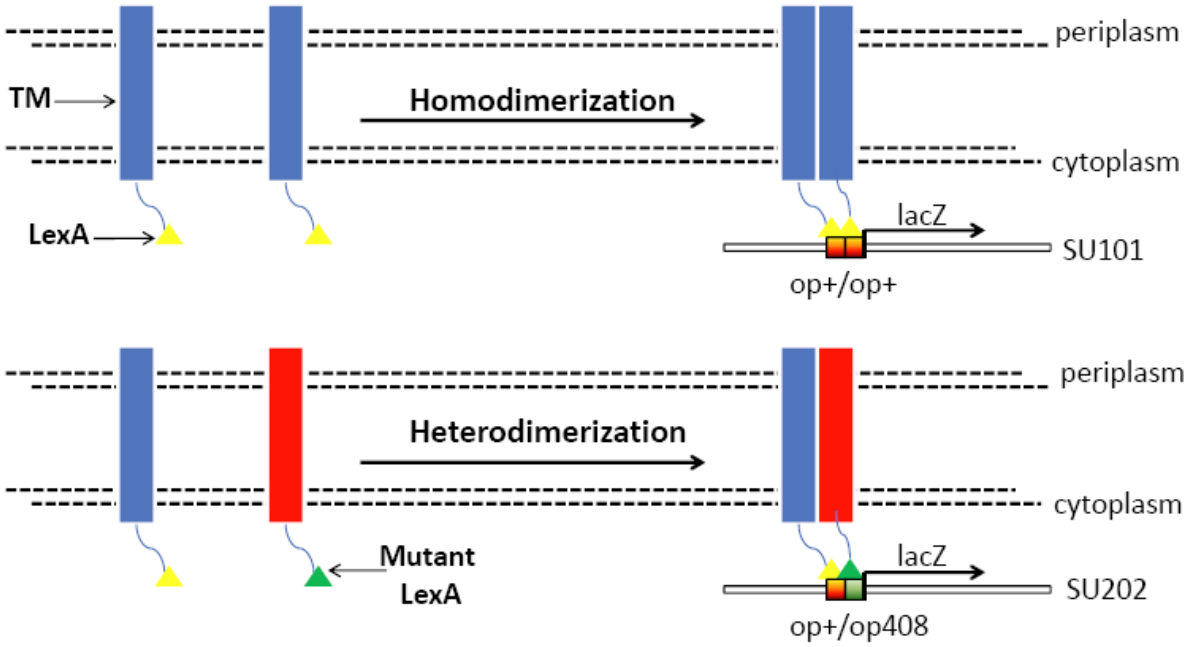

Figure 3.2 Schematic diagram of transcriptional repression of *lacZ* gene by LexA dimer. In homodimerization assay, expression of the *lacZ* gene in strain SU101 is driven by a promoter under the control of an operator (op+/op+). In heterodimerization assay, expression of the *lacZ* gene in strain SU202 is driven by a promoter that under the control of a mixed operator (op+/op408). When dimerized LexA bind to corresponding operator, transcription of the *lacZ* gene is repressed, resulting in activity decrease of beta-galactosidase.

In 2002, this LexA assay system was applied to explore interaction of transmembrane protein by the Engelman group and named the GALLEX system.[52] In their study, the glycophorin A transmembrane domain (GpA TX helix) was linked either with the wild-type or the mutant LexA DBD and transformed into strain SU101 or SU202 for homo-dimerization or hetero-dimerization

study respectively. The GALLEX system is widely used in many other protein interaction studies, like hetero-dimerization of alpha and beta subunits of integrins, transmembrane domain interaction of human ErbB, and the role of transmembrane helix-helix interaction in the assembly of the major histocompatibility complex.[187-189]

3.2 Materials and Methods

3.2.1 Materials

Plasmids pBLM-LexA-wt-GpA, pBLM-LexA-mut-GpA and strains SU101 are gifts from professor Dirk Schneider from University of Mainz (Germany).

3.2.2 Cloning and expression of LexA-AcrB fusion proteins

The gene encoding AcrB was amplified by PCR from the template plasmid pBAD33-AcrB. The digested fragment was inserted in frame into the expression vector pBLM between the restriction sites SacI and BamHI to create plasmid pBLM-LexA-AcrB. Then plasmid pBLM-LexA-AcrB was used as the template to construct plasmid pBLM-LexA-11aa linker-AcrB following the published protocol.[190] Similarly, plasmids pBLM-LexA-18aa linker-AcrB and pBLM-25aa linker-AcrB were constructed using the same method. Sequences of the linkers are listed in Table 3.1.

Table 3.1 Sequences of the linkers between LexA and AcrB.

Linker length	Linker sequence
11aa	ASGSS**GGGSGG**
18aa	ASG**GGGSGG**LSS**GGGSGG**
25aa	**GGGSGG**GASG**GGGSGG**LSS**GGGSGG**

3.2.3 Ethidium bromide (EtBr) accumulation assay

To examine if the introduction of LexA DBD at the N-terminus of AcrB affect the structure and function of AcrB, EtBr efflux activity of BW25113*ΔacrB* containing plasmid pBLM-lexA-linker-AcrB were tested. The EtBr accumulation assay was performed following a well-established protocol.[191] Briefly, the bacterial cells containing different AcrB mutants were cultured to an OD_{600} of 1. The cells were harvested and resuspended in buffer containing 10 mM sodium phosphate, 100 mM sodium chloride, 0.1% glycerol, pH 7.4 at a final OD_{600} of 0.2. Five μM EtBr was added to the diluted cells to monitor the fluorescence change at the room temperature using a Perkin Elmer LS-55 fluorescence spectrometer (Perkin Elmer, Waltham, MA). The excitation and emission wavelengths were set at 520 and 590 nm respectively.

3.2.4 McConkey agar test

Agar plates were prepared by adding 5 g of agar to 100 ml of DI water, following by autoclaving at 120 ^{o}C for 15 min. 15~20 ml hot agar with ampicillin (final concentration 100 mg/L) was placed in a sterile petri dish. The agar was allowed to cool and harden before SU101 strains transformed with different plasmids expressing fusion proteins were streaked on the surface of the agar. Then plates were incubated at 37 ^{o}C overnight.[192]

3.2.5 β-galactosidase activity assay

Activity of β-galactosidase was tested using the Miller Assay.[193] Briefly, 20 μl samples of culture were taken at certain OD_{600} and mixed into 80 μl permeabilization solution (100 mM Na_2HPO_4, 20 mM KCl, 2 mM $MgSO_4$, 0.9 mg/ml hexadecyltrimethylammonium bromide, 0.4 mg/ml sodium deoxycholate, 5.4 μl/ml β-mercaptoethanol). The permeabilization mixture was

kept for 30 min at 30 ^{o}C. Then 600 µl of 30 ^{o}C prewarmed substrate solution (60 mM Na_2HPO_4, 40 mM NaH_2PO_4, 1 mg/ml o-nitrophenyl-beta-D-galactoside, 2.7 µl/ml beta-mercaptoethanol) was added to initiate the reaction. After sufficient color developed, 700 µl stop solution (1 M Na_2CO_3) was added and the reaction time recorded. All samples were then centrifuged for 10 min at maximum speed. The supernant solution was transferred to a cuvette and the absorbance at 420 nm was measured. Enzyme activities were expressed by Miller unit, which was calculated using the following equation:

$$miller\ unit = 1000 \times \frac{Abs_{420}}{reaction\ time\ \times volume(0.02ml) \times Abs_{600}}$$

3.3 Results and Discussion

3.3.1 Design and construction of fusion proteins LexA-AcrB with various linkers

GALLEX has been widely used to detect dimerization of small membrane proteins (intact or segment). Due to the small size of those membrane proteins, fused LexA DNA binding domains are easily pulled together and dimerize, and then subsequently bind to promotor of *LacZ* which directly suppresses the production of beta-galactosidase. In this project, if LexA is directly linked to N-terminus of AcrB, it would be difficult for LexA monomers to encounter each other and dimerize, since AcrB is a large protein. I used the software Pymol to measure the distance between two AcrB monomers in a trimer, and found that the linear distance between the N-terminus of each AcrB pair is approximately 21 Å (Fig 3.3). The axial distance between two adjacent residues in alpha-helix is 1.5 Å, and 3.5 Å in beta-sheet. Assuming each residue in the linker fusing LexA and AcrB contributes 2 Å in length, at least 5 amino acids are needed to enable LexA dimerization. I constructed a series of fusion proteins with different linker length, 11aa, 18aa and 25aa using fast cloning method.[190] The template used is plasmid pBLM-LexA-AcrB, which is prepared by inserting AcrB into vector pBLM-LexA between digestion sites SacI and BamHI. There are five amino acids between LexA and AcrB, which is ASGSS due to the sequence of the digestion site. To make the 11aa linker, one unit of GGGSGG is added after ASGSS. For 18aa linker construct, two units of GGGSGG were added. For 25aa linker construct, there are three units of GGGSGG.

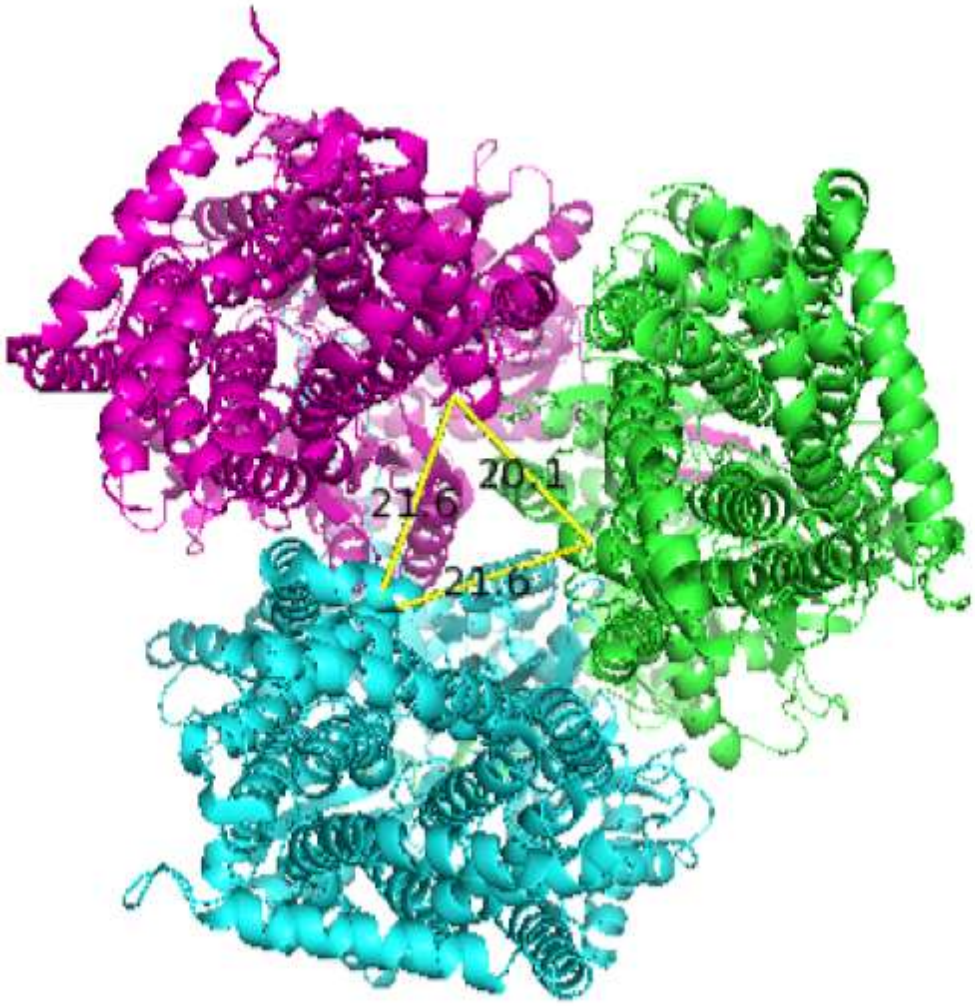

Figure 3.3 Linear distances between the N-terminus of neighboring AcrB monomers. Distance is measured by software Pymol. (created from 2GIF.pdb)[162]

3.3.2 Fusion of LexA DNA binding domain with various linkers to AcrB didn't affect the activity of the AcrAB-TolC system

Ethidium bromide (EtBr) is weakly fluorescent in aqueous buffer, but its fluorescence greatly increases upon intercalating into DNA.[194] As a substrate of AcrB, the entrance of EtBr into *E. coli* can be monitored through an increase of fluorescence emission, which gradually reaches a

plateau at saturation. In the presence of AcrAB-TolC, EtBr accumulates inside the cell very slowly and fluorescence intensity barely increases. Without the active efflux by AcrAB-TolC, it can enter the cell at a much faster rate, which results in a rapid elevation of fluorescence emission. To test the activity of fusion proteins LexA-AcrB with various linkers, EtBr accumulation assay was performed using intact BW25113 or BW25113*ΔacrB* cells transformed with plasmids encoding LexA-linker-AcrB constructs. From Figure 3.4, it can been seen that for all the linker constructs, the fluorescence intensity barely increase, which means that the fusion proteins LexA-linker-AcrB can be inserted into membrane and actively pump EtBr out of cells .

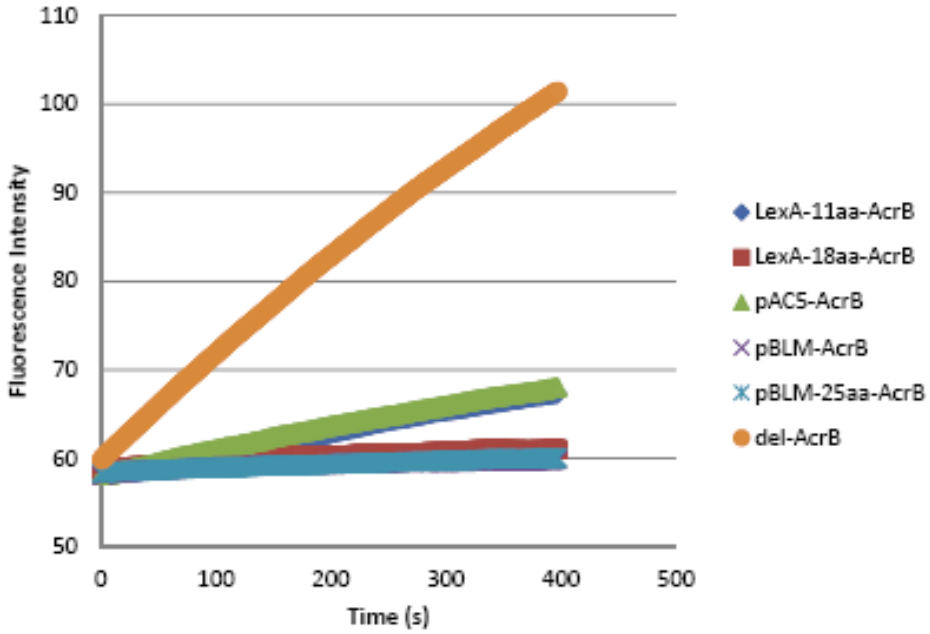

Figure 3.4 Real-time measurement of ethidium bromide accumulation for BW25113*ΔacrB* containing plasmids encoding different LexA-linker-AcrB constructs.

3.3.3 18aa is the proper linker length, which enables LexA dimerization

McConkey agar is a type of bacteria growth media which is used to differentiate strains by their ability to ferment lactose. One important component of McConkey agar is neutral red, which is a pH indicator. When pH of the medium is below 6.8, neutral red turns red. While the pH rises to above 8.0, the color changes to yellow. The product of lactose fermentation is acidic, which makes the medium around the colony red or pink. SU101 strains expressing different AcrB fusion proteins were streaked on McConkey agar plate and incubated at 37 ^{o}C overnight. It can be seen that medium around the strain expressing LexA-18aa-wt-AcrB is pale or yellow, while the medium around the strains expressing LexA-18aa-R780A-AcrB is red or pink as shown by Figure 3.5.

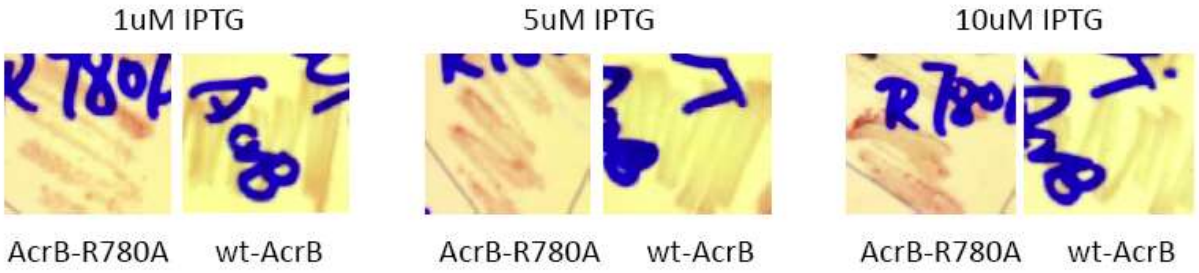

Figure 3.5 McConkey agar test result. When IPTG concentration is 1 μM, 5 μM, 10 μM, medium around strains expressing LexA-18aa-R780A-AcrB is red or pink, while strains expressing LexA-18aa-wt-AcrB is pale or yellow.

R780A is an AcrB mutant that has compromised trimer stability.[195] It was found by our previous group member Linliang that R780 is a key residue in AcrB, which greatly influences AcrB trimer association. This residue is located at the trimer interface (Fig 3.6A). When R780 was mutated to alanine, there is a significant decrease of trimer stability (Fig 3.6B).

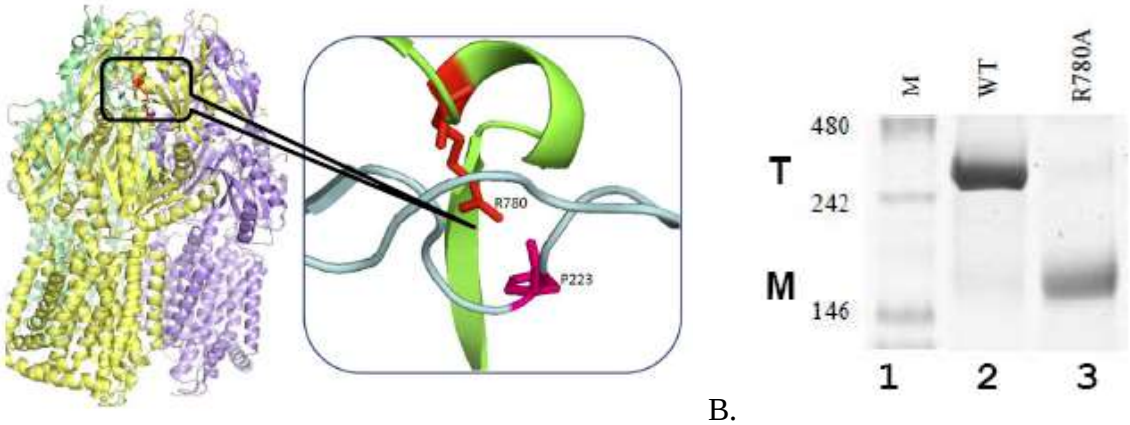

A. B.

Figure 3.6 AcrB mutant R780A. A. AcrB structure with side chains of R780 and P223 shown in red. The side chain of R780 is within H bond distance with the carbonyl oxygen of P223 (created from 2GIF.pdb). B. Blue native polyacrylamide gel electrophoresis for wild-type AcrB (lane 2) and mutant R780A-AcrB (lane 3, from left). From top to bottom, molecular weights of bands in lane 1 are marked on the left. Position of AcrB monomer (M) and trimer (T) are marked on the left. Note: Figure 3.6B was obtained by Linliang and is included here for the completeness of the discussion

For strains expressing fusion proteins with other linkers, like LexA-11aa-AcrB and LexA-25aa-AcrB, there is no difference between the wild-type AcrB and R780A mutant. This result indicates that the 18aa linker should have proper length to enable LexA DNA binding domains dimerization and then binding to the target *LacZ* promotor. It's possible that 11aa linker is too short for LexA to form dimers, while 25aa linker might be too long, which reduce the possibility of dimerization.

3.3.4 Strain with plasmid expressing LexA-18aa-wt-AcrB is non-lactose fermenting, while strain with plasmid expressing LexA-18aa-R780A-AcrB is lactose fermenting

The McConkey agar medium around colony containing plasmid pBLM-LexA-18aa-wt-AcrB is pale, while that of pBLM-LexA-18aa-R780A-AcrB is red or pink. The observation is consistent with our previous knowledge that wild-type AcrB exists as well-associated trimer, but R780A-AcrB cannot form a stable trimer.

3.3.5 SU101 strain with plasmid expressing LexA-18aa-wt-AcrB has lower β-galactosidase activity than that containing R780A mutant

The function of β-galactosidase in the cell is to hydrolyze lactose to glucose and galactose which can be utilized as carbon source by bacteria (Fig 3.7A). Besides the natural substrate lactose, synthetic compounds which have similar structures to lactose can also be cleaved by β-galactosidase. One example of lactose analogue is called o-nitrophenyl-β-D-galactoside (ONPG). Hydrolysis of ONPG yields one molecule of galactose and one molecule of o-nitrophenol (ONP), which has a yellow color (Fig 3.7B). When ONPG is in excess in the lydrolysis reaction, amount of produced o-nitrophenol is proportional to β-galactosidase activity. In *E. coli* strain SU101, the *lacZ* gene is under the control of the wild-type LexA DNA binding domain recognition sequence. When LexA DNA binding domains dimerize and bind to the promoter of the *lacZ* gene, production of β-galactosidase is suppressed. In the presence of ONPG, less yellow color is produced.

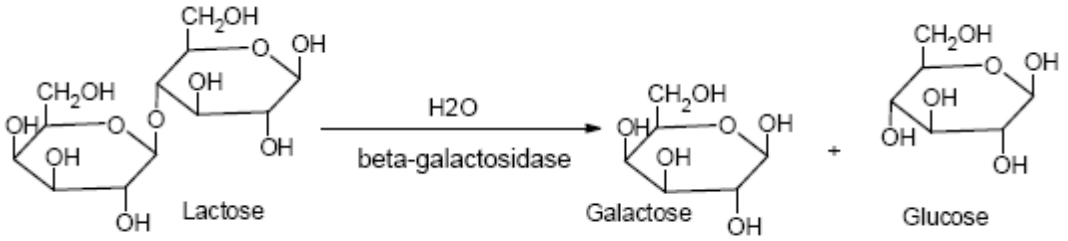

A.

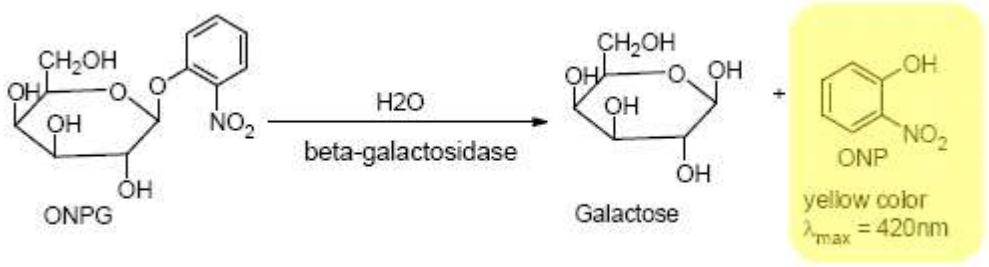

B.

Figure 3.7 A. Hydrolysis of lactose by β-galactosidase. The products are galactose and glucose. B. Hydrolysis of o-nitrophenyl-β-D-galactoside by β-galactosidase. The products are galactose and o-nitrophenol.

In order to maximize the difference between wt-AcrB and R780A-AcrB, two factors during cell culture were optimized. One of them is culture time after induction. AcrB is a large protein and it takes time for the cell to accumulate the fusion protein to a certain amount after induction. After the addition of 3 μM isopropyl β-D-1-thiogalactopyranoside (IPTG), the same volume of culture was taken out at different time point. And then Miller Assay was applied to measure the activity of β-galactosidase. As show in Figure 3.8A, the activity difference between wt-AcrB and R780A-AcrB was small for the first 3 h after induction. After about 6 h of induction, it can be obviously seen that activity of β-galactosidase for LexA-wt-AcrB was much lower than that of the mutant, indicating that the activity is suppressed due to LexA dimerization which is caused by oligomerization of wt-AcrB. At the same time, the mutant strain has higher activity of β-

galactosidase. This is because LexA domains have less chance to dimerize, when R780A-AcrB cannot form well-associated oligomer.

Another factor I optimized is concentration of IPTG. Different concentrations of IPTG were used to induce expression of fusion proteins, 0.5 μM, 1 μM, 5 μM, 10 μM, 50 μM, 100 μM, 500 μM and 1mM. As shown in Figure 3.8B, low concentrations of IPTG are needed to differentiate wt-AcrB and mutant. When IPTG is in the range of 0.5 μM~5 μM, there are bigger activity difference between the wild-type and mutant. When IPTG concentration is higher than 10 μM, enzyme activity for both strains are lower, and the difference between them become less obvious. This might be due to higher concentration of IPTG makes cell less healthy, which results in lower enzyme activity for both strains.

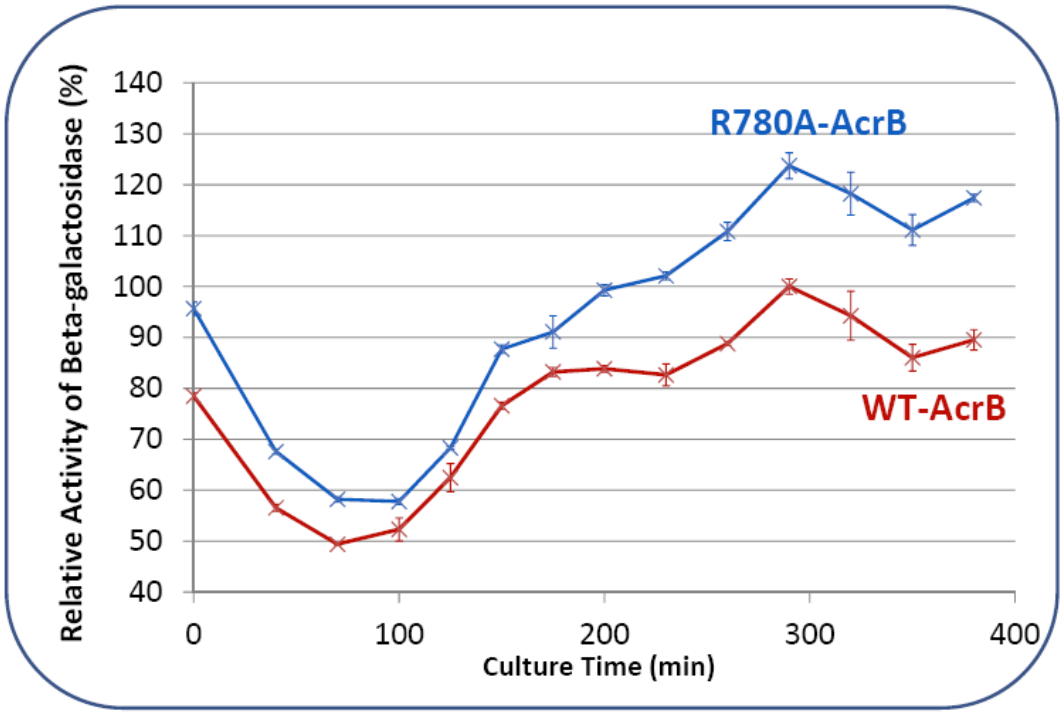

A.

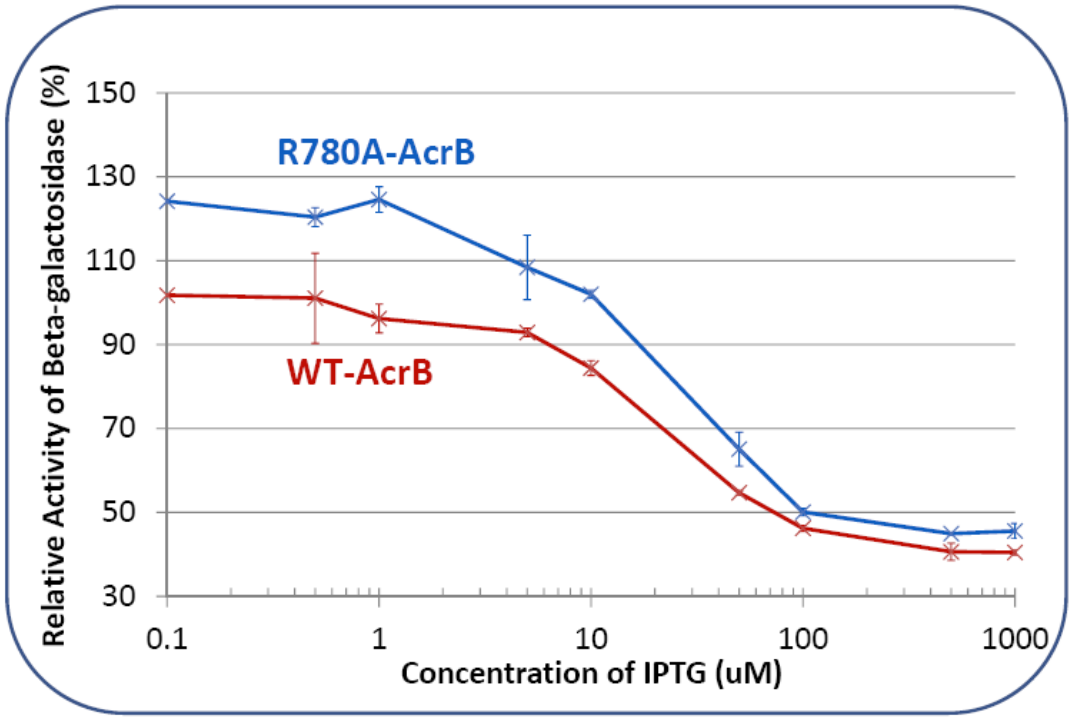

B.

Figure 3.8 Miller Assay result for strains SU101 expressing LexA-wt-AcrB (red) or LexA-R780A-AcrB (blue). Role of culture time when IPTG concentration is 3 μM (A) and IPTG

concentration when culture time is 5h (B) were studied. (Range of IPTG concentration: 0.1 μM, 0.5 μM, 1 μM, 5 μM, 10 μM, 50 μM, 100 μM, 500 μM, 1 mM)

3.4 Conclusions

GALLEX is a system that can be used to measure the oligomerization capacity of simple transmembrane helix. In this project, I modified the system to differentiate oligomerization status between wt-AcrB and mutant AcrB. By constructing a series of fusion proteins with different length linkers between LexA and AcrB, I found that when there is an 18aa linker fusing LexA and AcrB, oligomerization difference between the wild-type and mutant can be displayed by testing the activity of β-galactosidase. After culture condition optimization, it was found that wt strain has 25% lower enzyme activity compared with the mutant strain, when induced for 6 h by 1 μM IPTG. In published research, which applied GALLEX system to study oligomerization of GpA TM single helix, there is about 50% difference of enzyme activity between the wild-type and mutant.[52] In this study, GpA TM helix is very small, containing only 19 amino acids. For my project, AcrB is a big membrane protein which has 1049 residues for each monomer. I think the giant size of AcrB is the primary reason why the enzyme activity difference can only reach to 25%. Another possible reason for the smaller difference might be that AcrB is a trimer, while only dimer of LexA is needed to bind to promoter. Maybe trimerization of AcrB makes dimerization of LexA less efficient.

Chapter IV Life time measurement of a constitutively expressed multidrug efflux pump

4.1 Introduction

Proteins are a major component of all cells and play many essential roles as structural materials, building blocks, catalytic elements, transporters, channels, and signaling molecules. Life times of specific proteins are closely correlated with their stability, function, and the metabolic status of the cell. Half-lives of proteins in cells range from minutes to days and is usually monitored using pulse-chase experiments involving isotope labeling, in which cells are exposed to a specific isotope (H3, C14, or S35-Met) for a short period of time (pulse) before switched into a normal culture medium (chase).[196-199] The degradation of the isotopically labeled protein is then monitored over time. While the pulse-chase experiment has the advantage of being highly sensitive, convenient, and generally applicable to all proteins, the involvement of radioactive materials makes it a potential health hazard and undesirable for experiments that last for several days. A non-radioactive method, which replaced radio isotopic labeling with a non-natural amino acid azidohomoalanine (AHA) (Figure 4.1), has been developed and applied in many different researches.[200-201] Orphan lab has developed this approach to visualize newly synthesized proteins in environmental microbes *in situ*.[202] Schuman et al. have used this method to measure the life-time of TrkB, a neurotrophin receptor, and the presynaptic protein Bassoon.[203] Due to their structural similarity, AHA can be incorporated into protein sequences by methionyl-tRNA synthetase if methionine (Met) is not available. Subsequently, the AHA-containing protein can be detected after purification/immune-precipitation and labeling with probe molecules containing an alkyne group via the well-established click chemistry.[204] In this study, the half-life of multidrug efflux pump protein AcrB in *E. coli* was determined, using both the conventional S35-Met pulse-chase method and the non-radioactive AHA-labeling method. I found that the

lifetimes of AcrA and AcrB are extraordinarily long (six days), many times of the doubling time of *E. coli* cells.

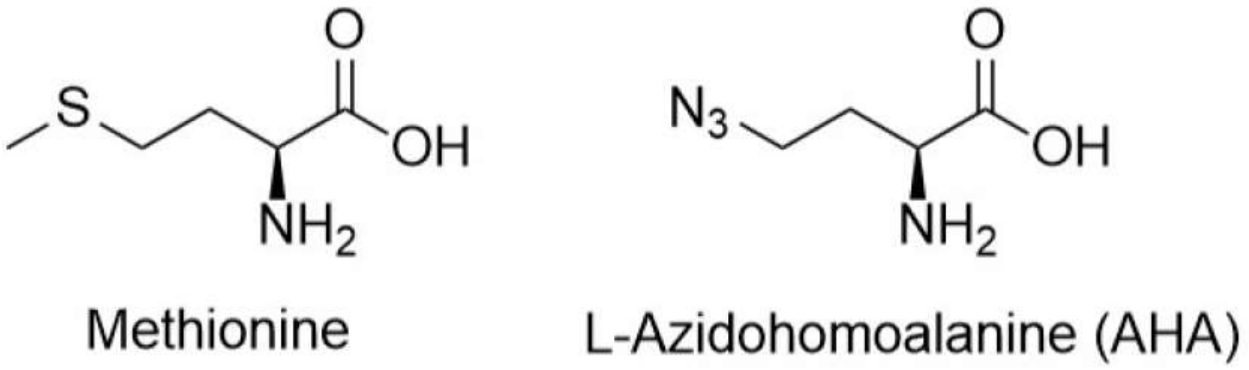

Figure 4.1 Structures of methionine and AHA.

4.2 Materials and Methods

4.2.1 Materials

Strain DL41 was obtained from the Coli Genetic Stock Center (Yale University). The custom polyclonal rabbit anti-AcrA antibody was obtained from GenScript (Piscataway, NJ).

4.2.2 Creation of gene knockout strains

Knockout strains DL41*ΔacrB* and DL41*ΔacrAB* were created using Quick & easy *E. coli* gene deletion kit (Gene Bridges GmbH, Heidelberg, Germany) following the manufacturer's protocol. The target genes in the knockout strains were replaced with a kanamycin resistance cassette. Colony PCR was applied to confirm that target genes have been replaced.

4.2.3 EtBr accumulation assay

The EtBr accumulation assay was performed as described in section 3.3.3.

4.2.4 Pulse chase experiment

E. coli cells containing respective plasmids were cultivated overnight at 37 ℃ in LB broth and diluted 50-fold into 6 mL LB broth on next day. When the OD reached 1.2, cells were harvested at 4,500 rpm for 10 min at room temperature, resuspended in 6 mL M9 medium, and then cultured at 37 ^{o}C with shaking overnight. Next morning cells were harvested and resuspended in 6 mL M9 medium with 19 amino acids (no methionine). S35-Met (1000 Ci/mmol) was added to final concentration 50 μCi/ml for 2 min, and then a 400-fold excess of non-radioactive Met (20 mM) was added. The cell culture was returned to the shaker, and aliquots of samples (1ml for each sample) were withdrawn at the indicated time, centrifuged and frozen. After all samples

were obtained, cells were resuspended in 200 µl buffer containing 20 mM sodium phosphate (pH 7.5), 0.2 M NaCl, 10% glycerol, 1 mM PMSF, and 0.4% lysozyme. Cells were lysed via freezing/thawing (F/T) cycles: cell suspension samples were incubated in ethanol/dry ice bath (-72^{o}C) for 3 min, then transferred to room temperature water bath for 5 min (20 ^{o}C). Between each F/T cycle, samples were vortexed for 1 min. The freezing/thawing/vortexing process was repeated for 6 times to make sure cells were lysed. The membrane fraction was collected by ultra-centrifugation (100,000×g, 1 hour) and then suspended in phosphate buffer containing 1% (w/v) DDM. Insoluble material was removed by centrifugation. The extracted protein in supernatant was purified using NTA superflow resin as previously described.[205] Protein was analyzed by SDS-PAGE, and radioisotope-labeled protein was visualized by Typhoon FLA 9500 laser scanner.

4.2.5 AHA incorporation and labeling

Plasmids pQE70-AcrB and pQE70-AcrB-Dloop were constructed in a previous study.[205] They were transformed into DL41*ΔacrB* or DL41*ΔacrAB* for protein expression under the basal condition without induction. *E. coli* were cultured overnight at 37 ℃ in LB broth. On the next day, overnight culture was diluted 250-fold into the M9 minimum medium, and cultured at 37 ^{o}C overnight. On the third day, the overnight culture was diluted 10-fold into fresh M9 medium containing 19 amino acids (40 µg/ml) and AHA (50 µg/ml). After the indicated incubation time, cells were harvested by centrifugation and either used directly for protein purification or frozen as indicated.

AcrB extraction and purification were conducted as described using NTA superflow resin except for the following modifications.[205] The cells were resuspended and lysed in 20 mM sodium phosphate (pH 7.5), 0.2 M NaCl, 0.03% DDM, and 1 mM PMSF, washed using the same buffer, and eluted using 10 mM sodium acetate, 100 mM NaCl, 3% SDS (pH 4.0). After elution, the pH of the fraction was adjusted back to pH 7.4 using an aliquot of 1 M phosphate buffer for the labeling reaction.

In AcrA lifetime experiment, cells were collected from 5 mL of culture and resuspended in a buffer containing 20 mM sodium phosphate (pH 7.5), 0.2 M NaCl, 10% glycerol, and 1 mM PMSF. After the cells were disrupted using sonication, the membrane fraction was collected by centrifugation and then solubilized in sodium phosphate buffer containing 1% Triton X-100 for 2 h. Protein extraction solution was incubated with anti-AcrA antibody (5 μl) at 4 ℃ in a rotator for 2 h. PMSF and protease inhibitor cocktail was added to inhibit protein degradation. Protein A beads were washed with sodium phosphate buffer and incubated with 5% BSA in sodium phosphate buffer in 4 ℃ for 2~4 h to decrease non-specific binding. After incubating the protein extraction solution with BSA saturated protein A beads at 4 ℃ for 1 h, beads were washed with 0.1% Tween-20 in sodium phosphate buffer for 4 times. Protein AcrA was eluted with 3% SDS sodium phosphate buffer (pH7.5) by incubation for 10 min at 70 ℃.

The click reaction was performed following a published protocol.[206] Purified AHA-containing protein was incubated with 200 μM Tris(benzyltriazolylmethyl) amine (TBTA), 500 μM ascorbic acid, 50 μM alkyne-biotin (PEG4 carboxamide-Propargyl Biotin), and 200 μM $CuSO_4$. The reaction was allowed to proceed overnight at room temperature and analyzed using anti-biotin Western blot.

4.3 Results and Discussion

4.3.1 The incorporation of AHA did not affect the activity of the AcrAB-TolC efflux system

While the incorporation of AHA into the sequence of proteins has been demonstrated in several cases, it is not always clear if the replacement of Met by AHA would affect the structure and function of the protein to be studied. We used a well-established EtBr efflux assay to investigate if the replacement of Met by AHA would affect the structure and function of the AcrAB-TolC system.[191] EtBr is actively transported by the AcrAB-TolC system. In the absence of AcrB, EtBr diffuses across the cell membrane into the bacteria, upon which its fluorescence increases drastically due to intercalation into nucleic acid. In the presence of active pumping, the outward efflux counter-acts the effect of the inward diffusion and EtBr is effectively removed from the cell. Therefore, the fluorescence does not increase as significantly.

We first created an *acrB* gene knockout strain of DL41 (DL41*ΔacrB*), and then transformed a plasmid encoding AcrB into the strain (DL41*ΔacrB*-pQE70-AcrB). As shown in Figure 4.1, DL41*ΔacrB* rapidly accumulated EtBr, while the wild-type DL41 did not. The introduction of pQE70-AcrB reduced the EtBr fluorescence of DL41*ΔacrB* to a level close to that of the parent strain, indicating that AcrB encoded in the plasmid is fully functional. Next, we used the *acrB* knockout strain to examine the effect of AHA incorporation on AcrB activity. In addition, since the incorporation of AHA is not protein-specific, it is necessary to confirm that the replacement of Met by AHA in general does not affect the growth and EtBr accumulation of the bacteria. DL41*ΔacrB* transformed with pQE70-AcrB were cultured in a minimum media supplemented with 19 essential amino acids plus Met or AHA, and their EtBr accumulation plots were collected (Figure 4.2). The fluorescence of DL41*ΔacrB*-pQE70-AcrB remained low in both Met-

and AHA-containing media, indicating that the activity of the efflux system was not affected by replacing Met in the proteins with AHA.

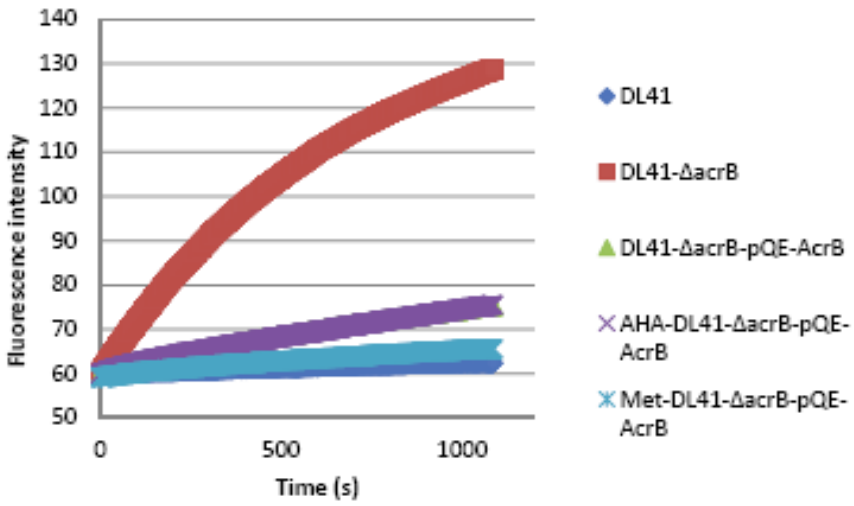

Figure 4.2 Real-time measurement of EtBr accumulation for strain DL41, DL41 *ΔacrB* and DL41*ΔacrB*-pQE-AcrB in different medium (green is LB medium, purple is AHA-containing medium, blue is Met-containing medium). Note: the green curve is overlapped with the purple one.

4.3.2 The life-time of AcrB is longer than 24 hours as measured using the S35-Met pulse-chase experiment

We first used the conventional S35-Met pulse-chase experiment to estimate the life time of AcrB. DL41*ΔacrB*-pQE70-AcrB was used in this study. The bacteria were cultured in the presence of 50 uCi/ml (1000 Ci/mmol) S35-Met for 2 min, and then a 400-fold excess of non-radioactive Met (20 mM) was added. The cell culture was returned to the shaker, and aliquots of samples were withdrawn at the indicated time and analyzed (Figure 4.3). The intensity of the

radioactively labeled AcrB did not decrease over 24 hours. To confirm that the observation was not due to signal saturation or other artifacts, we repeated the experiment multiple times and tested the samples with different dilutions. The same conclusion was reached at each time. The need for performing experiments with long incubation time lasting for several days prompted us to look into an alternative method that does not require the usage of radioactive compound.

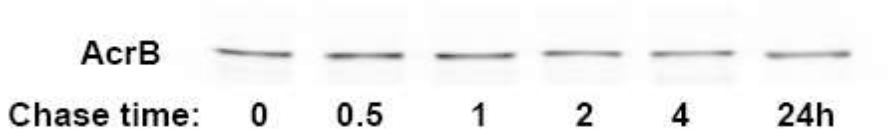

Figure 4.3 Degradation of S35-Met-AcrB determined by pulse-chase experiment.

4.3.3 Determination of the half-life of AcrB through the incorporation of AHA

The incorporation and labeling of AHA was developed as a non-radioactive method to trace proteins.[207] Its application has been demonstrated for several soluble proteins. To make the method useful for integral membrane proteins, we conducted extensive experiment to optimize the condition.

4.3.3.1 Optimization of labeling condition

To make AHA-containing proteins visible for detection, a labeling step has to be performed in which the click chemistry is used to attach a probe (a fluorescent dye or biotin) to the azido group in the side chain of AHA. A major challenge of applying the AHA-based tracing method to integral membrane proteins is the difficulty of reacting AHA with the alkyne probe. Our initial attempts of following the literature protocol for soluble proteins yielded very low level of labeling. In membrane proteins such as AcrB, the AHA side chains (originally Met side chains)

tend to be less accessible for reaction as compared to their counterparts in soluble proteins. We found that the following modifications are essential for the application of the method to AcrB.

First, the most important factor affecting the outcome of labeling is the unfolding of the target protein. We found that the protein needed to be fully unfolded to yield reproducible and high level of labeling. We experimented with unfolding AcrB using 8 M urea and 3% SDS before proceeding to the click reaction. Without the presence of denaturing reagent, no labeling could be observed. When 8 M urea was present, a weak labeling signal could be observed, indicating a small percentage of AHA became accessible to reaction. Decent labeling could only be achieved after the protein was completely unfolded using 3% (w/v) SDS before labeling.

Second, another important factor for reaction is the reducing reagent. In the click chemistry reaction the Cu (I) catalyst is prepared in situ by reducing a Cu (II) salt with a reducing agent. While many studies in literature reported using tris (2-carboxyethyl) phosphine (TECP) as the reducing reagent, we found ascorbic acid worked better in our experiment.[208]

In addition, we found that imidazole had an inhibitory effect on the click reaction. Our AcrB constructs contain histag at their N-termini for purification. When high concentration of imidazole was used for elution, the fractions could not be used directly in labeling. The presence of imidazole, even as low as 1 mM, significantly inhibited the labeling reaction. After imidazole was removed via dialysis, the reaction could occur. To simplify the labeling procedure, we eluted our protein using a change of pH as described in Materials and Method. The elution buffer was 10 mM sodium acetate (pH 4.0), 100 mM NaCl, 0.03% DDM. The reduction of pH leads to protonation of the histidine side chains in the histag, which effectively disrupted the interaction

with the Ni-NTA resin. Because labeling will be conducted under denaturing conditions, the potential effect of low pH on protein folding is not a concern for this application. After elution, the pH of the fraction was adjusted back to pH 7.5 using an aliquot of high concentration phosphate buffer for the labeling reaction.

4.3.3.2 The dilution effect

Due to the long life-time of AcrB, an unavoidable technical concern emerged: the dilution effect. When a parent bacterium divides into two daughter bacteria, the AHA-labeled proteins are also divided into the two daughter cells. As shown in Figure 4.4, the starting *E. coli* cell (1^{st} generation) is cultured in a media containing AHA but not Met. Assuming the cell has 8 molecules of AcrB, all containing AHA (Blue). The cell is then transferred into a media containing Met (but not AHA). After the cell doubles, the two daughter cells (2^{nd} generation) each still contains 8 molecules of AcrB, but only 4 molecules in each cell contains AHA. The other 4 molecules, which are newly synthesized in the absence of AHA, are not labeled. Accordingly, four and eight *E. coli* cells are produced in 3^{rd} and 4^{th} generations, respectively, with 25% or 12.5% of their AcrB molecules containing AHA. Therefore, to trace the disappearance of AHA-labeled AcrB, care has to be taken to collect all offspring from the same number of cells at each time point.

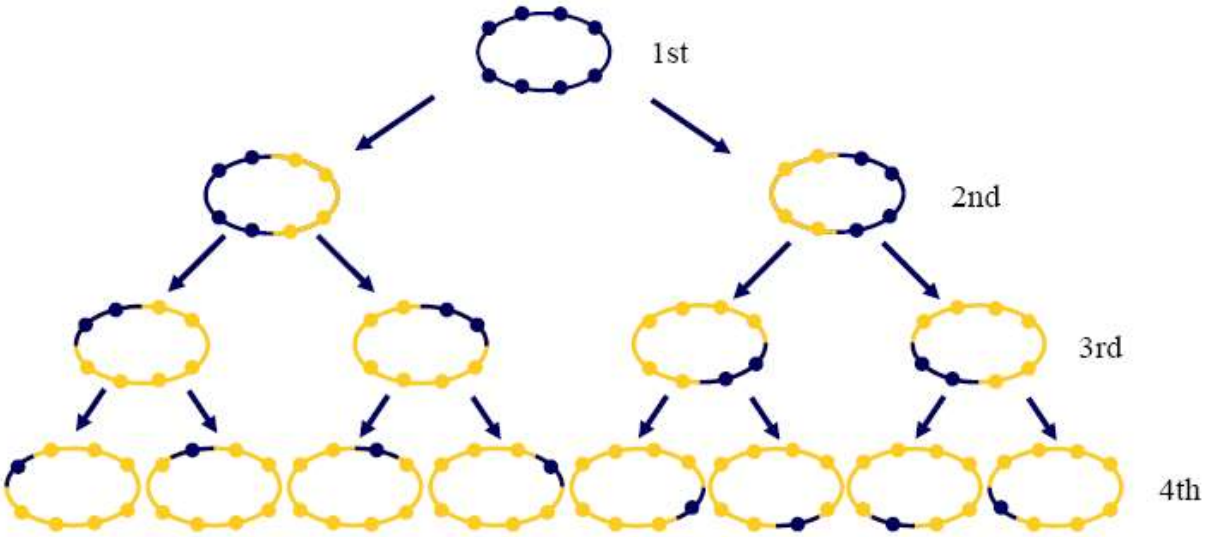

Figure 4.4 The dilution effect. Assume the starting *E. coli* cells (1st generation), which are cultured in AHA-media, contains 8 molecules of AHA-AcrB (Blue). After the cell is transferred into a media containing Met (but not AHA), the 2nd generation cells each still contains 8 molecules of AcrB, but only 4 of them contains AHA (blue). The other 4 newly synthesized AcrB molecules contain normal Met (yellow). Accordingly, the 3rd and 4th generation cells contains 25% or 12.5% AHA-AcrB (blue), respectively. Potential effect of degradation is not considered in this scheme.

Therefore, for this study, the proper sampling approach is to divide the AHA-containing *E. coli* cells into n+1 parts (for sampling of n days) (Figure 4.5). On day 0 (right before switching into a Met-media), one part is centrifuged to collect the cells and frozen. The rest of the samples are cultured to allow the *E. coli* cells to grow and divide. After one day, the second sample is centrifuged to collect the cells, and frozen. And so on until the n^{th} day. To keep the cells viable, all cultures were centrifuged each day and resuspended into fresh media. The number of cells kept on increasing each day until they reach saturation, so did the amount of AcrB purified from

the cell pellet. But since the amount of starting materials, the AHA-containing AcrB, was the same in each sample, the observed decrease of the intensity of the biotinylated AHA-AcrB band reflected the degradation of AcrB molecules produced during the incubation time in which AHA was present in the media.

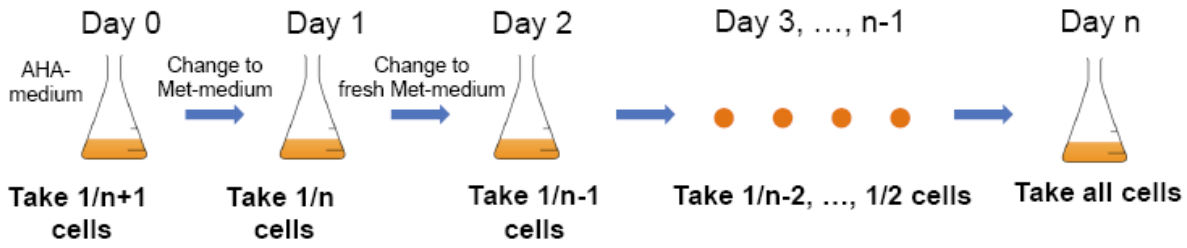

Figure 4.5 Sampling method used to detect lifetime of AcrB.

4.3.3.3 Determination of the lifetime of AcrB

To determine the lifetime of AcrB, we first cultured *E. coli* cells in the presence of AHA, and then chased using Met for seven days. To make the experiment practical, we kept the overall volume of the culture fixed at 10 mL. We acknowledge keeping the OD, or cell density, fixed over time would be a more desirable approach. However, we found that we cannot slow down the growth enough to keep the culture volume practical over the seven days experiment period. Another concern about the increase of volume is the drastic difference of cell mass, which would make it impossible to scale the purification and labeling protocols in a proper way to compare samples collected in successive days.

The analyses of AcrB samples extracted from cell pellets collected over seven days were shown in Figure 4.6. Figure 4.6A is the coomassie blue stain to reflect the overall level of AcrB, while Figure 4.6B is an image of the anti-biotin Western blot of the same set of samples. The band

intensities of the coomassie stained gel increased over time, as a result of an increase of the overall number of cells. Due to the limitation of volume, the overall number of *E. coli*, and thus the AcrB extracted from the sample, did not increase further once the cell culture reached saturation. The biotinylated AHA-AcrB band is clearly visible for the first 5 days of incubation, and becomes much smaller in day 6. Figure 4.6C shows the degradation process of S35-Met-AcrB by using pulse-chase method over longer chase time, which is 7 days. From the image, it can be seen that the bands intensity decrease gradually. On day 7, the radioactive signal can barely be detected, which is consistent with the result from AHA-incorporation method. We conclude that the life-time of AcrB in *E. coli* cells under our experimental condition was 5-6 days.

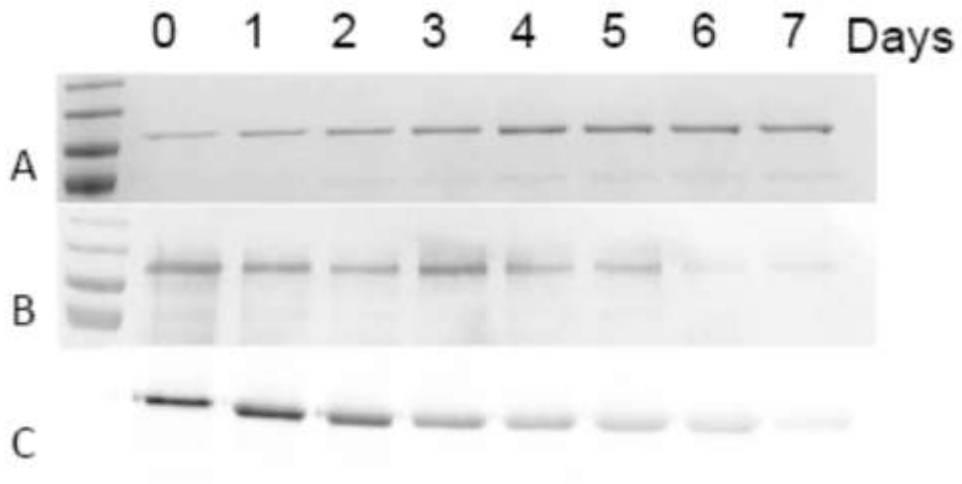

Figure 4.6 Tracing the disappearance of AcrB by using both AHA-incorporation method and S35-Met pulse-chase method. A. Commassie blue stain of purified AcrB from samples collected after the indicated time. B. Anti-biotin western blot of purified AcrB from samples collected after the indicated time. C. Degradation of [35S]-Met-AcrB determined by pulse-chase experiment. Note: Figure 4.5C was obtained by our group member Zhaoshuai and is included here for the completeness of the discussion.

4.3.3.4 Lifetime of a functionless AcrB mutant

AcrB is constitutively expressed. The level of AcrB in *E. coli* does not response drastically with the concentration of potential inducers in the environment. For example, Rosenberg et al. have shown that the presence of various cholates induced the production of AcrB by 1.1 to 1.7 folds.[209] Therefore, we speculate that the long lifetime of AcrB is not correlated with its function, since the production of the protein is not sensitive to the presence of substrate in the environment (and thus the need for active efflux). To examine if this is the case, we determined the lifetime of a functionless mutant, AcrB-Dloop.[205] In this mutant, residues 211 to 227, which are important for inter-subunit interaction, were deleted. We monitored the degradation of AHA-labeled AcrB-Dloop as described above, and found that it lasted for 4-5 days before the AHA signal disappeared (Figure 4.7). Compared with the lifetime result of the wild-type AcrB, functionless AcrB-Dloop doesn't have a significantly shorter lifetime, which indicates that active efflux is not a prerequisite for the long lifetime of the protein.

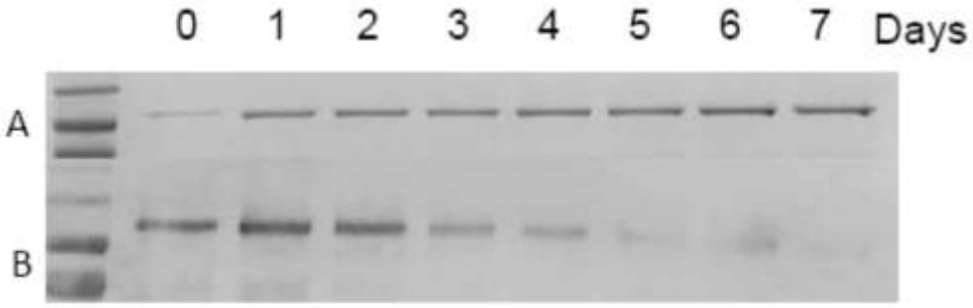

Figure 4.7 Tracing the disappearance of AHA-containing AcrB-Dloop via biotinylation. A. commassie blue stain. B. anti-biotin Western blot.

4.3.3.5 Effect of AcrA on AcrB stability

AcrA is a periplasmic protein partner of AcrB. Both proteins, as well as the outer membrane channel TolC, are critical for drug efflux. While it is generally accepted that TolC does not constantly forming a docking complex with AcrA and AcrB, it was less clear if AcrA and AcrB interact with each other in the absence of active efflux. If the presence of AcrA influences the lifetime of AcrB, then they are more likely to form a complex even without active efflux. To examine the effect of AcrA on AcrB lifetime, we created an *acrA* and *acrB* double knockout strain, DL41*ΔacrAB*, and then compared the lifetime of AcrB (Figure 4.8). We found that the absence of AcrA significantly reduced the lifetime of AcrB by 2 days. The AHA-AcrB signal disappeared after 3 days. This observation suggests that AcrA interacts with AcrB even in the absence of active efflux. And such interaction helps to stabilize the structure of AcrB in the cell membrane and increase its lifetime.

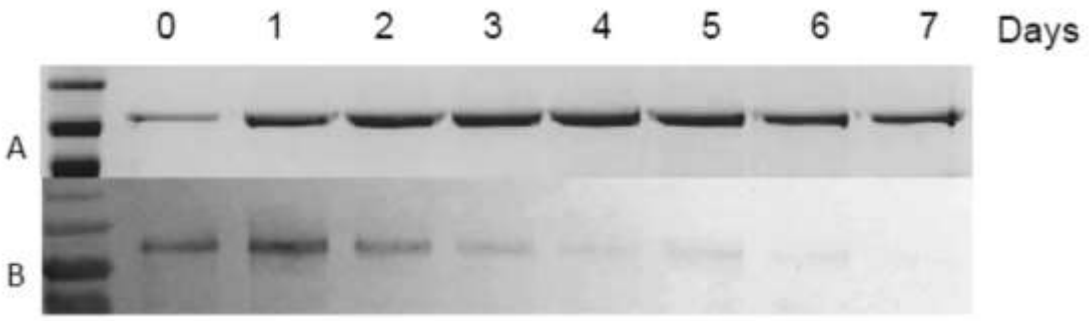

Figure 4.8 Tracing the disappearance of AHA-containing AcrB via biotinylation in the absence of AcrA. A. Commassie blue stain. B. Anti-biotin Western blot.

4.3.3.6 Lifetime of AcrA

The gene expressing AcrA and AcrB are clustered, with the starting codon of *acrB* only 23 bases downstream of the stop codon of *acrA*. Therefore, they are likely to share the same mRNA

during protein production. Since the functions of AcrA and AcrB depend closely on each other, we speculate that the lifetime of AcrA is likely to be comparable to that of AcrB. Using the same method, we determined the lifetime of AcrA. We found that AHA-AcrA also lasted for 5-6 days in *E. coli* cells under the same experimental condition, consistent with our expectation (Figure 4.9).

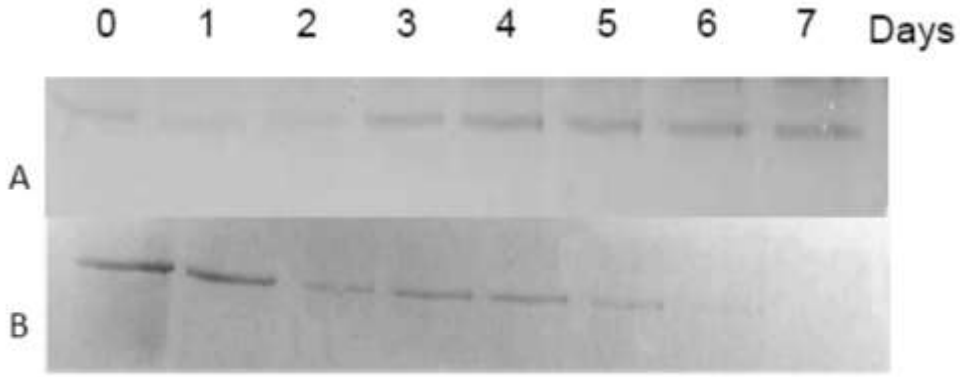

Figure 4.9 Tracing the disappearance of AHA-containing AcrA via biotinylation. A. Commassie blue stain. B. Anti-biotin Western blot.

4.4 Conclusions

In summary, we found that the life time of AcrA and AcrB were several days in *E. coli* cells. We have to point out that the metabolic condition of the cells must have an impact on the life time of proteins in the cells. In our experiment, we had to fix the volume of the culture to make it experimentally practical to compare samples collected over seven days. Therefore, for samples of later dates the cell density in the culture was constantly in the state of saturation, and we changed the cells into fresh media every day to keep the cells viable. Despite of this limitation, we were able to obtain interesting information about the lifetime of an important efflux transporter in *E. coli*. We found that the longevity of AcrB does not correlate with active efflux, but depend on the presence of its protein partner AcrA. The lifetime of AcrA is comparable to that of AcrB, which is reasonable as AcrA and AcrB are likely co-translated and their cellular functions are correlated.

The average lifetimes of proteins in different organisms have been the focus of several studies. Belle et al. measured the half-life of 3,751 proteins in the yeast proteome and found the distribution of half-lives to be approximately log-normal, with a mean and median half-life of ~43 min.[210] Systematic studies of mammalian cell lines cultured in vitro reveal that the average half-life of proteins ranges from hours to days, while the degradation rates of different protein families seemed to be conserved between mouse and human.[211, 212] Similar studies on *E. coli* were performed several decades ago. The half-life for bacterial proteins has been reported to be ~20 h.[213-216] In a more recent study, Larrabee et al. monitored the turnover of ~250 soluble proteins in *E. coli* growing at the log phase and found that the majority of them were not degraded to any appreciable extent in 70 min.[198] These studies indicate that although the doubling time and protein synthesis rate of bacteria cells are many folds faster than that of the

eukaryotic cells, the protein degradation rate in general is not significantly faster. Different proteins in the same cell could have drastically different rate of degradation. AcrA and AcrB are undoubtedly among the longer lived ones. This is consistent with their preventative protection role in the cell. It is intriguing to ask if membrane proteins tend to have longer life time compared to soluble proteins. On the one hand, the biogenesis of membrane proteins consumes more energy as the nascent polypeptide chain needs to be targeted and inserted into the proper membrane. On the other hand, the degradation of membrane proteins required the removal of the highly hydrophobic transmembrane segments from the membrane. The answer to this question requires the analysis of the lifetime of more membrane proteins, which had been hindered by the intrinsic difficulty to extract and characterize these highly hydrophobic targets.

Chapter V The ssra-tag facilitated digestion of an integral membrane protein

5.1 Introduction

In bacteria, the major players in protein degradation are ATP-dependent proteases, including HslUV, ClpAP, ClpXP, Lon, FtsH, and their homologs.[217-220] These proteases utilize their ATPase functions to facilitate the unfolding and translocation of substrate proteins. Among them, ClpAP and ClpXP are complexes of two proteins, an unfoldase ClpX/ClpA, and a peptidase ClpP.[221-223] By itself ClpP can degrade small peptide substrates, but to degrade larger proteins it needs to form a complex with an ATPase, such as ClpA or ClpX, which dissociates stable protein complexes and unfolds proteins at the expense of ATP hydrolysis (Figure 5.1A). One role of the ClpXP and ClpAP complexes is to degrade proteins bearing the ssrA-tag. In bacteria, the ssrA-tagging system is evolved to get rid of incompletely synthesized proteins which result from stalled synthesis of the ribosome.[224-226] They are tagged for destruction by the co-translational addition of an 11-residue peptide (AANDENYALAA) by an amazing molecule tm-RNA (Figure 5.1B).[227, 228] This ssrA mechanism effectively degrades nonsense proteins and releases/recycles ribosomes.[72, 229] While the degradation of ssrA-tagged soluble proteins has been well studied, similar process of membrane proteins has not been investigated. Here we report that the introduction of the ssrA-tag lead to the complete degradation of a large integral membrane protein AcrB.

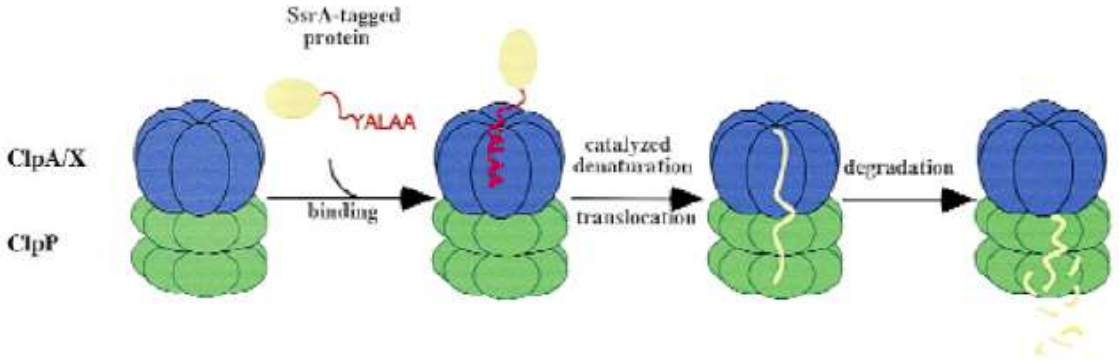

A.

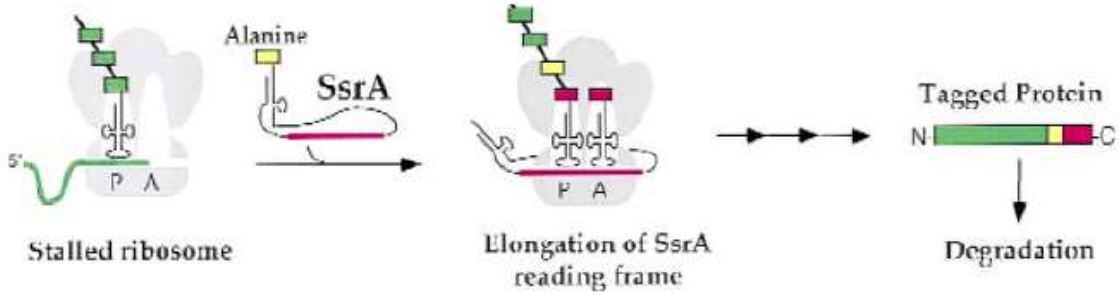

B.

Figure 5.1 A. degradation process of ssra-tagged protein by ClpA/X-ClpP system. B. Addition of ssra-tag to translation stalled protein. Reprinted by permission from Macmillan Publishers Ltd: [Nature structural and molecular biology] (The SsrA-SmpB system for protein tagging, directed degradation and ribosome rescue), copyright (2000).

5.2 Materials and Methods

5.2.1 Creation of gene knockout strains

Strains DL41, BW25113 and its single gene knockout strains were obtained from the Coli Genetic Stock Center (Yale University). Gene knockout strains DL41*ΔacrBΔclpX*, DL41*ΔacrBΔclpA*, DL41*ΔacrBΔclpP*, and DL41*ΔacrBΔsspB* were created using Quick & Easy E. coli gene deletion kit (Gene Bridges GmbH, Heidelberg, Germany) following the manufacturer's protocol. The target genes in the knockout strains were replaced with a kanamycin resistance cassette. Colony PCR was used to confirm that target genes had been replaced.

5.2.2 Construction of plasmids

The gene encoding AcrB was amplified by PCR from *E. coli* genomic DNA and then digested with SphI and BamHI. A stop codon was added after the last *acrB* codon. The fragment was inserted into an expression vector pQE70 between the restriction sites SphI and BglII to create plasmid pQE-AcrB. For pQE-AcrB-His_6, the stop codon was not included. The *acrB* gene was inserted in frame to the vector-derived C-terminal histag. To create pQE-AcrB-ssrA and pQE-AcrB-His_6-ssrA, pQE-AcrB or pQE-AcrB-His_6 was used as the template, respectively. The oligonucleotide encoding the ssrA-tag was inserted after the last *acrB* codon using one-step PCR following the method described in literature.[190]

Plasmids were also constructed to express ClpP and ClpX with a His_6 tag. Plasmid pQE70-His_6-ClpP was obtained from Addgene. The gene encoding ClpX was inserted into the vector pET28a

in frame between the restriction enzyme cutting sites NdeI and XhoI to create pET28a-His_6-ClpX.

5.2.3 Analysis of AcrB amount by Western blot

The indicated plasmid was transformed into the corresponding strains. To examine AcrB expression under the basal condition, 3 mL of *E. coli* cells were cultured overnight and collected via centrifugation. The cell pellet was sonicated in a lysis buffer (50 mM Na-Pi pH 7.5, 100 mM NaCl). Next, the SDS-loading dye was directly added into the lysate and the samples were resolved using SDS-PAGE, followed by Western blot using an anti-AcrB antibody raised against a peptide sequence corresponding to residues 1032 to 1045 of AcrB (AcrB-CT-antibody) or against purified full length AcrB (AcrB-FL-antibody).[230]

5.2.4 S35-Met pulse-chase experiment

The pulse-chase experiment was performed as described in section 4.2.4.

5.2.5 Protein expression and purification

To avoid potential contamination from genomic AcrB, pQE-AcrB-His_6 and pQE-AcrB-His_6-ssrA were transformed into DL41*ΔacrBΔClpX* for expression. A single colony from a freshly transformed plate was used to inoculate 3 mL LB media supplemented with ampicillin and kanamycin and cultured overnight. The overnight culture was used to inoculate 600 mL of fresh LB media supplemented with ampicillin and kanamycin. The culture was incubated with shaking at 37 ℃ overnight. Cells were harvested the next morning by centrifuge. Protein was purified

following the procedure described in section 2.2.2. After elution, the samples were dialyzed against a dialysis buffer (0.03% DDM, 30 mM Tris, 0.5 M NaCl, pH 7.9) overnight at 4 ^{o}C to remove imidazole.

5.2.6 CD spectroscopy

CD was performed using a JASCO J-810 spectrometer with 1 nm bandwidth. The instrumentation principle of circular dichroism spectrometer is illustrated in the following diagram.

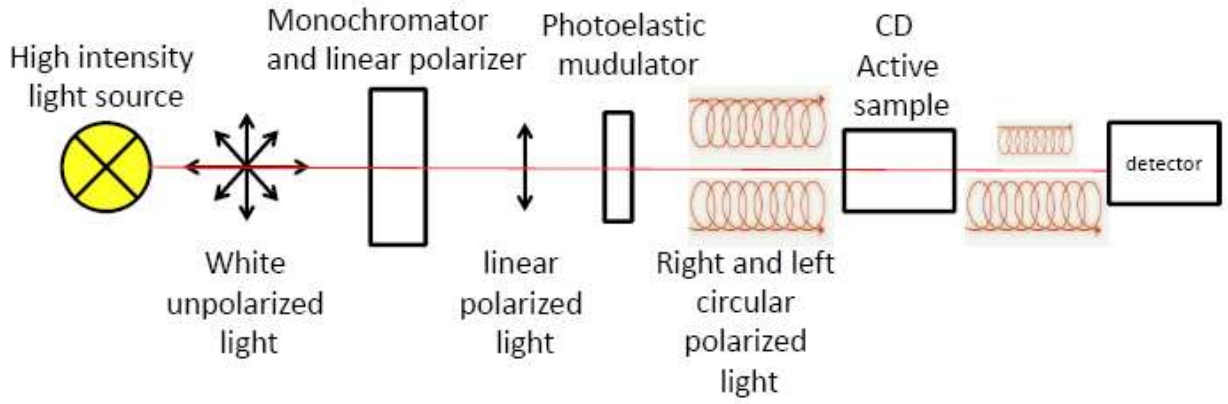

Figure 5.2 Instrumentation of circular dichroism spectrometer. (Note: this figure was drawn by referring to instrumentation principle at website http://chemwiki.ucdavis.edu/Core/Physical_Chemistry/Spectroscopy/Electronic_Spectroscopy/Circular_Dichroism)

Circular dichroism is an absorption spectroscopy method which detects the absorption difference of left and right circularly polarized light by chiral molecules, such as proteins and small organic molecules. As the instrumentation diagram shows in figure 5.2, light is firstly linearly polarized after passing through a linear polarizer, and then divided into right and left circular polarized

light by photoelastic mudulator. Chiral samples have different absorption of left and right circular polarized light and this difference can provide secondary structural information for protein samples. Protein samples were dialyzed overnight into a low salt buffer (10 mM sodium-phosphate, 50 mM NaCl, 0.03% DDM, pH 7.5) before the CD measurement. Blank scans were collected using the exterior dialysis buffer. For far-UV CD spectra, samples in 1 mm path length cuvette were scanned in the wavelength range of 260–190 nm. All spectra were corrected for blanks. Protein concentrations were determined using the Bradford assay.

5.2.7 *In vivo* digestion test

To detect the degradation of AcrB-His_6-ssrA in cell upon the induction of ClpX, DL41*ΔacrBΔclpX* (kanamycin (kan) resistance) was co-transformed with two compatible plasmids: pQE70-AcrB-His_6-ssrA (ampicillin (amp) resistance) and pBAD33-ClpX (chloramphenicol (cam) resistance). The strain was cultured overnight in LB-kan/amp/cam, and diluted 100-fold into fresh LB-kan/amp/cam media the next morning. The cells were cultured at 30 ^{o}C with shaking (250 rpm) until the OD_{600} reached 0.4, and then collected by centrifugation at 4,500 rpm for 10 min. The cell pellet was resuspended into fresh LB-kan/amp/cam and split into three portions: one portion was left on ice (the "no additional growth" control). Arabinose (0.1% w/v) was added into the second portion. The second and third portions were cultured for an additional 2 hours at 28 ^{o}C with shaking (250 rpm). Next, all three samples were centrifuged, and the cell pellets were treated as described in section 5.2.3 and subjected to anti-AcrB Western blot analysis to measure the amount of AcrB-ssra.

5.2.8 *In vitro* digestion assay

Digestion of detergent solubilized AcrB was performed according to the published protocol.[231] Briefly, AcrB-His_6-ssrA was expressed and purified from DL41*ΔacrBΔclpX*. After elution, the sample was dialyzed to remove the high concentration of imidazole. Expression and purification of His_6-ClpX and His_6-ClpP were conducted following published protocols.[72] The activity of purified His_6-ClpX, His_6-ClpP, and the assay buffer system was confirmed using purified GFP-ssrA as the substrate. For AcrB-His_6-ssrA digestion, AcrB-His_6-ssrA, ClpX and ClpP were added at the specified molar ratio in the assay buffer including the ATP regeneration system (25 mM HEPES-KOH, pH7.6, 200 mM KCl, 10 mM $MgCl_2$, 10% glycerol, 2 mM DTT, 5 mM ATP, 16 mM creatine phosphate, and 0.032 mg/mL creatine kinase) supplemented with 0.03% DDM. A control sample was also set up which was identical except that no ATP was present. After incubated overnight, the level of AcrB-His_6-ssrA in the presence of ATP was determined using anti-AcrB Western blot.

5.3 Results and Discussion

5.3.1 The ssrA tag does not change the secondary structure of AcrB

To demonstrate that the addition of the ssrA tag did not affect the membrane integration and folding of AcrB, we compared the circular dichroism (CD) spectra of purified AcrB-His_6 and AcrB-His_6-ssrA (Figure 5.3). AcrB-His_6-ssrA was purified from membrane vesicles, indicating that the membrane integration was not compromised by the C-terminal tag. This is consistent with our expectation as the membrane integration of inner membrane proteins is co-translational. For a large protein such as AcrB, the membrane insertion should be close to complete before the C-terminal ssrA-tag emerges from the exit tunnel of the ribosome. The CD spectra of detergent-

solubilized AcrB-His_6 and AcrB-His_6-ssrA superimposed well onto each other, indicating the presence of the tag did not affect the overall folding of the protein.

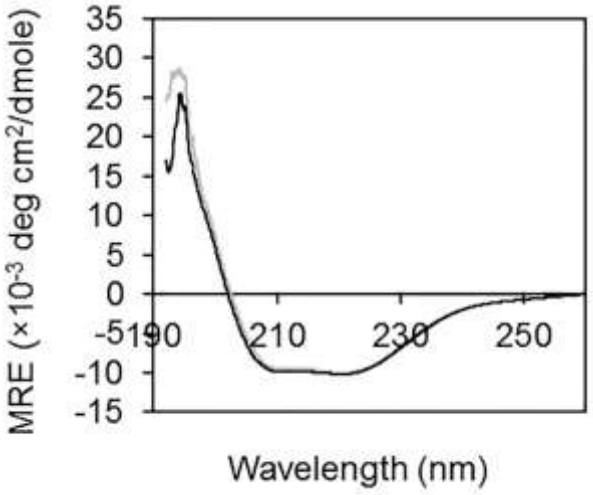

Figure 5.3 CD Spectra of AcrB-His_6 (black) and AcrB-His_6-ssrA (grey).

5.3.2 AcrB-ssra can be digested at a much faster rate than the wild-type AcrB

AcrB can be purified and easily crystallized, suggesting that its structure is intrinsically stable. However, the introduction of the oligonucleotide encoding the ssrA-tag into the *acrB* gene right before its stop codon rendered the protein no longer detectable in the cell lysate. We transformed plasmid pQE-AcrB or pQE-AcrB-ssrA into BW25113*ΔacrB* and examined protein expression under the basal condition. As shown in Figure 5.4, wild-type AcrB expressed well and yielded a clear band on the blot (lane 1). However, after we added the ssrA tag to the protein, its expression was completely abolished (lanes 2). Earlier studies show that the last five residues YALAA of the ssrA tag is the critical factor, which also promotes degradation although at a lower efficiency.[74] To confirm that the degradation was actually caused by the tag, we also constructed AcrB with the truncated ssrA tag (AcrB-5aa ssrA). As expected, the expression level

of the protein was much lower than that of the wild-type AcrB, but is still clearly observable (Figure 5.4, lane 3). For the rest of the study, by AcrB-ssrA we indicate AcrB bearing the 11-residue ssrA tag at the C-terminus. Since the AcrB-CT antibody recognizes a specific peptide sequence close to the C-terminus of the protein, we have also repeated the experiment using an anti-AcrB antibody raised against the full length AcrB (AcrB-FL antibody).

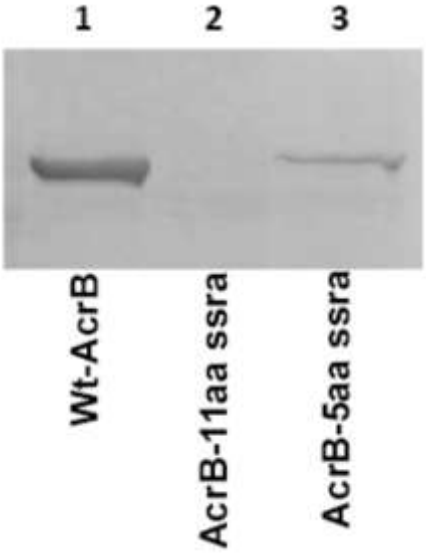

Figure 5.4 Anti-AcrB Western blot analyses of membrane extracts obtained from DL41-*ΔacrB* strain containing plasmids encoded wt-AcrB, AcrB-11aa ssra, AcrB-5aa ssra.

To confirm that the lack of AcrB-ssrA is a result of degradation, not a defect in translation, we conducted the S35-Met pulse chase experiment (Figure 5.5). A His_6 tag was inserted at the C-terminus of AcrB, right before the ssrA tag. DL41*ΔacrB* transformed with plasmids pQE-AcrB-His_6 or pQE-AcrB-His_6-ssrA was cultured in the presence of S35-Met for 2 min, and then chased using a large excess of cold Met. As discussed above, AcrB-His_6 was very stable and the intensity did not significantly decrease over the 24 hours of this experiment. In the case of AcrB-His_6-ssrA, a clear band could be seen at time 0, indicating normal expression, but the band

intensity of AcrB-His_6-ssrA dropped to the background level within ~15 min, indicating fast degradation.

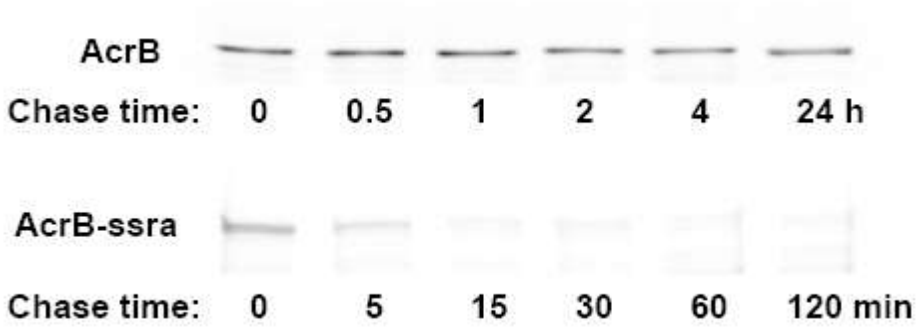

Figure 5.5 Degradation of S35-Met-AcrB-His_6 and S35-Met-AcrB-His_6-ssra determined by the pulse-chase experiment. Note the difference in the unit of the time.

5.3.3 Degradation of AcrB-ssra is mediated by ClpXP/SspB system

To investigate if the degradation is mediated by the ClpAP and/or ClpXP, we obtained single gene knockout strains lacking each gene from the Yale Coli Genetic Stock Center, and transformed plasmid encoding AcrB-ssrA to examine the level of degradation (Figure 5.6). We examined the effect of knocking out five single genes, including *clpA*, *clpX*, *clpP*, *sspB*, *prc*. Among them, ClpA is similar to ClpX and also functions with ClpP.[224] SspB is a known chaperone that enhances the degradation of ssrA-tagged substrate by increasing the binding affinity and lowering the K_M.[232-235] Of the 11 residues in the ssrA tag, only the terminal AA-COOH is directly involved in ClpX binding. Several residues upper stream in the tag (AANEDNY) mediate binding to SspB, which aids in the delivery of ssrA-tagged protein to ClpXP.[235] Prc is a periplasmic protease (also known as Tsp) that degrades protein substrates in a

carboxy-terminal-specific manner and is known to degrade ssrA tagged proteins that are exported to the periplasm.[225]

Plasmid pQE-AcrB-ssrA was transformed into the indicated strains, and the cellular AcrB-ssrA level was determined using anti-AcrB Western blot with the AcrB-CT-antibody. We found that residual AcrB-ssrA could be detected in three strains: *ΔclpX*, *ΔclpP* and *ΔsspB* (Figure 5.6 A, B). Among them, *ΔclpX* contains the highest level of residual AcrB-ssrA. And because the strains still contain the genomic AcrB, a protein band at a slightly smaller molecular weight could be observed in all samples (the extra amino acids in the tag slowed down the migration of the protein in the gel). The presence of these two bands further confirmed that the production (or more likely, degradation) of the wild-type AcrB was not affected in the knockout strains so the degradation is ssrA-tag specific. In the parent strain (lanes 6 and 7), the transformation with the plasmid did not lead to a detectable AcrB-ssrA band. The same was observed in the *ΔclpA* or *Δprc* strains, suggesting that ClpA and Prc are not involved.

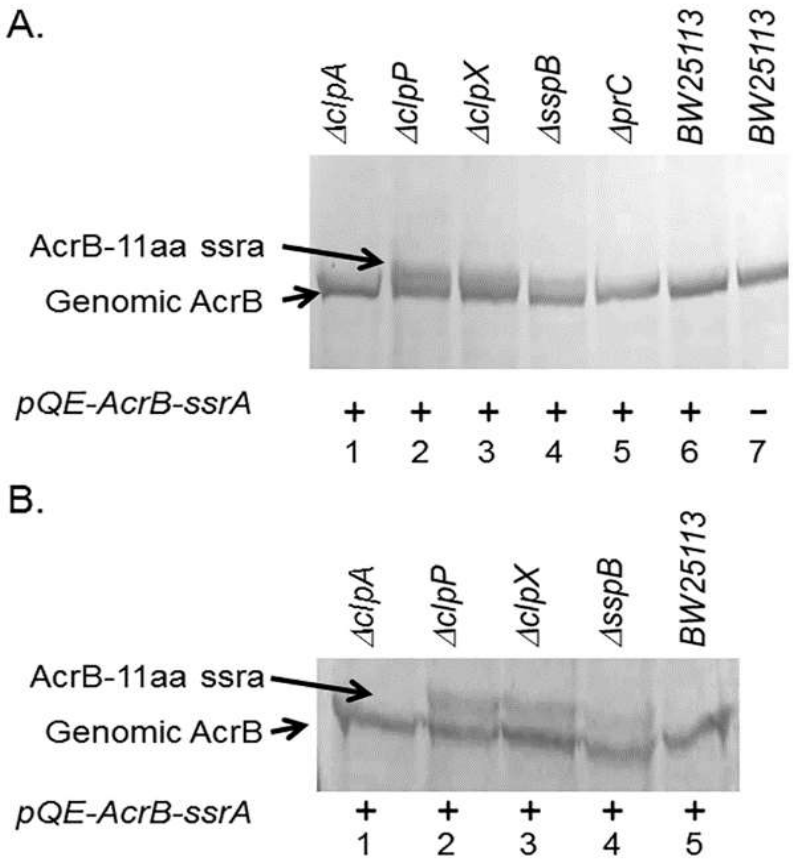

Figure 5.6 Anti-AcrB Western blot analyses of membrane vesicles. A. Single gene knockout strains of BW25113 missing the indicated gene expressing AcrB-ssrA from a plasmid. Result was analyzed using 8% SDS-PAGE. The last two lanes are the parent strain with or without the plasmid, respectively. B. Same as in A, but analyzed on a 6% gel to better separate the genomic AcrB and AcrB-ssrA.

5.3.4 ClpXP is not the only protease system that degrades AcrB-ssra

To determine the level of degradation, we first created double knockout strains to further eliminate the genomic *acrB* gene, and then transformed plasmids pQE-AcrB or pQE-AcrB-ssrA into each strain for comparison (Figure 5.7). Assuming the transcription and translation was not

affected by the last a few nucleotides/amino acids making up the ssrA tag, the difference in the detected protein level should reveal information about the level of degradation. We found that the degradation level in *ΔclpX* is approximately 60-70%. In *ΔclpP* and *ΔsspB*, the degradation level reached 80-90%. These results indicate that 1) ClpXP and SspB are involved in the degradation of AcrB-ssrA; 2) there are likely other proteins involves in the degradation as well.

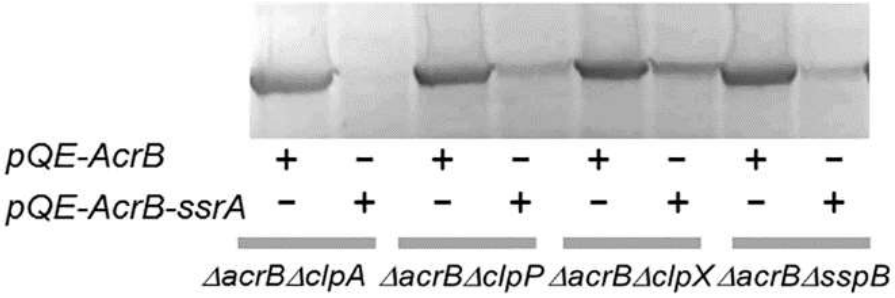

Figure 5.7 Expression of AcrB or AcrB-ssrA in the indicated double knockout strain.

5.3.5 *In vivo* digestion of AcrB-ssra

Two plasmids pQE70-AcrB-ssra and pBAD33-ClpX were co-transformed into strain DL41-*ΔacrB-ΔclpX*. The reason to choose pBAD33 as a vector to express ClpX is that pBAD33 is a tightly controlled plasmid, and the expression of ClpX can be switched on in the presence of L-arabinose. The *DL41ΔacrBΔclpX* strain containing only one plasmid pQE-AcrB-His_6-ssrA was also treated similarly and used as a control. When pBAD-ClpX was co-transformed with pQE-AcrB-His_6-ssrA, the induction of ClpX expression led to a significant drop of AcrB level, which was not observed in the control strain lacking pBAD-ClpX. Samples 2 and 3 have similar AcrB levels. This result indicates that the induced expression of ClpX accelerated the degradation of AcrB-His_6-ssrA, including the portion that was synthesized before the time of the induction.

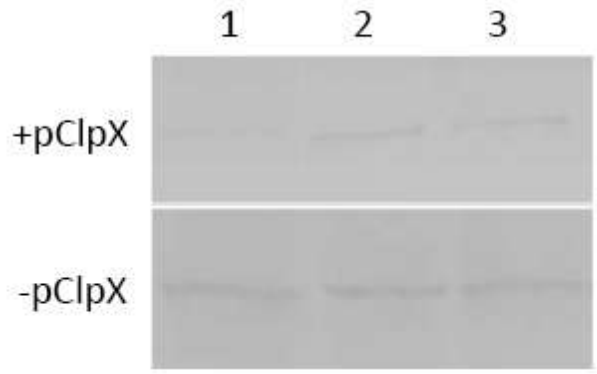

Figure 5.8 Anti-AcrB Western blot analysis of whole cell lysate prepared from DL41-*ΔacrB-ΔclpX* transformed with pQE-AcrB-His_6-ssrA and pBAD-ClpX (pClpX) (top) or pQE-AcrB-His_6-ssrA alone (bottom). AcrB-His_6-ssrA was expressed at the basal level without induction, and then the cell culture was divided equally into three samples: arabinose was added into the first sample to induce the expression of ClpX (lane 1). Sample 1 and sample 2 (lane 2) were incubated for an additional 2 hours at 28 ^{o}C, while sample 3 (lane 3) was left on ice.

5.3.6 *In vitro* digestion of AcrB-ssra by ClpXP system

The ultimate test of the degradation of AcrB-ssrA by ClpXP is to purify each component and conduct the degradation assay in a test tube. Since AcrB-ssrA is completely degraded in wild-type *E. coli*, we expressed and purified it in *DL41ΔacrBΔclpX*. A His_6 tag was inserted between the last amino acid of AcrB and the ssrA tag to facilitate purification. As described above, the addition of his-tag did not affect the degradation of the protein. The expression and purification of AcrB-his_6-ssrA were performed as described for AcrB-His_6.[170, 171] After elution, the sample was dialyzed to remove the high concentration of imidazole. Plasmids were also constructed to express ClpP and ClpX with N-terminal His_6 tag. Expression and purification of His_6-ClpX and His_6-ClpP were conducted following published protocols.[72] In our preliminary test, we set up

two reactions, one contains AcrB-His_6-ssrA, ClpX, ClpP at a molar ratio of AcrB-His_6-ssrA: $(ClpX)_6$: $(ClpP)_{14}$ = 1:15:50 in the assay buffer including the ATP regeneration system supplemented with 0.03% DDM. The negative control was identical except that no ATP was present. After incubated overnight at 30 ^oC, the level of AcrB-His_6-ssrA in the presence of ATP was determined using anti-AcrB Western blot to be approximately 30~40% of the control sample. The level of degradation could not be improved by the addition of more ClpXP or the increase of digestion time, indicating that under the current experimental condition the efficiency of the protease is quite low. To better quantify the rate of digestion, a better in vitro assay is clearly necessary.

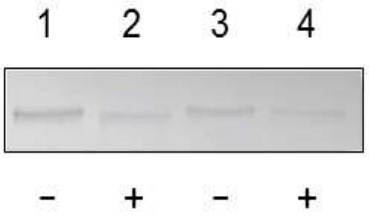

Figure 5.9 Anti-AcrB Western blot analysis of degradation of detergent solubilized AcrB-His_6-ssrA *in vitro*. Lanes 1 and 2 contain 0.2 μg AcrB-His_6-ssrA, and lanes 3 and 4 contain 0.1 μg AcrB-His_6-ssrA. Lanes 2 and 4 also contains ClpX and ClpP at the molar ratio of AcrB : $ClpX_6$: $ClpP_{14}$=1:15:50.

5.3.7 Length of C-terminus of AcrB affects efficiency of digestion by ClpXP

C-terminus of AcrB (from R1031 to H1049) has uncoiled structure and is not inserted into the membrane (Figure 5.10). We assume that if ClpXP system can digest AcrB-ssra that has properly inserted into the membrane, the C-terminus length of AcrB should influence its digestion

efficiency. If AcrB-ssra is digested while being translated, there should be no difference for the degradation of all AcrB-ssra with different C-terminal lengths.

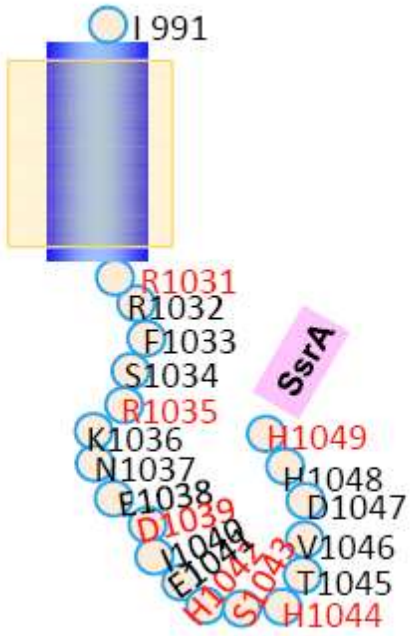

Figure 5.10 Amino acid sequence of AcrB C-terminus. Orange rectangle represents inner membrane of *E. coli* cell. The blue rectangle means the last transmembrane domain of AcrB, which starts from I991 and ends at R1031. The last residues in different truncated AcrB-ssra are labeled in red.

A series of ssra-tagged AcrB with shortened C-terminus length were constructed: 1031, 1035, 1039, 1042, 1043, 1044, 1049-AcrB-ssra. The number indicates the last amino acid before histag and ssra-tag. An anti-AcrB Western blot showed that expression levels of these truncated proteins without the ssrA-tag are similar as that of the wild-type AcrB. By adding the ssrA-tag, more and more AcrB-ssrA can be detected when the C-terminus becomes shorter (Figure 5.11A). 1049-AcrB-ssra is completely degraded, while ~90% of 1031-AcrB-ssra remained. For 1039-

AcrB-ssra, about 50% of it can be digested (Figure 5.11B). This result suggests that ClpXP-SspB complex may need to interact with a fragment of a certain length that is exposed to the cytoplasm to initiate digestion of AcrB-ssra.

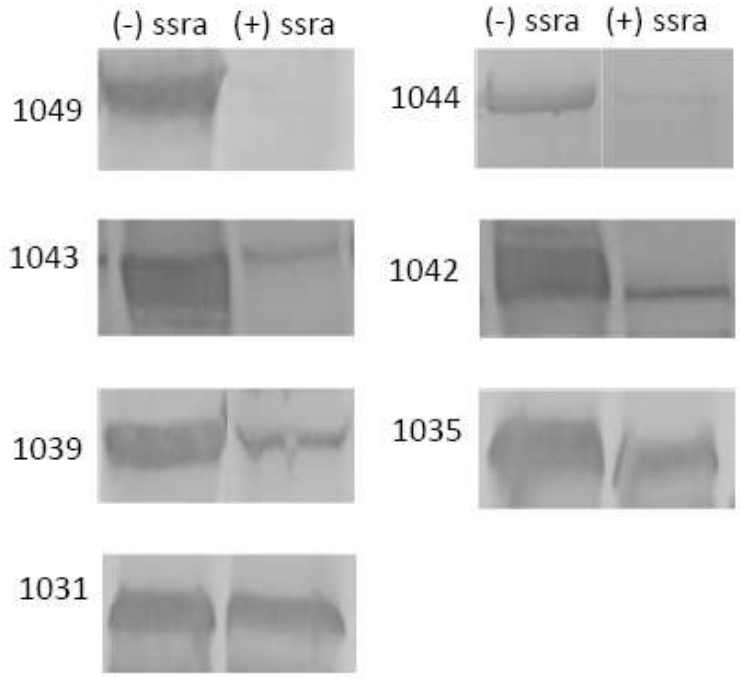

A.

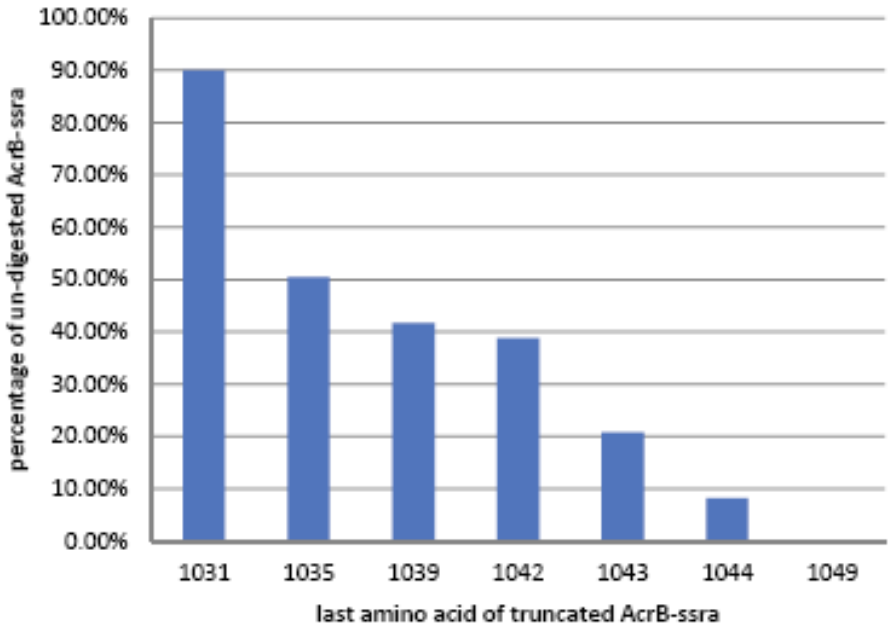

B.

Figure 5.11 A. Expression level of different truncated AcrB [(-)ssra] and corresponding AcrB-ssra [(+)ssra] analyzed by anti-AcrB Western blot. B. Percentage of truncated AcrB-ssra (1031-1049) that cannot be digested.

5.4 Conclusions

In summary, we discovered that the introduction of an extra 11 amino acid residues, the ssrA-tag, at the C-terminus of this large 1049-residue and highly stable integral membrane protein leads to its complete degradation. It was found that ClpX, ClpP, and SspB are involved in the degradation of ssrA-tagged AcrB in cells. At the same time, there should be other proteases that participating degradation of AcrB-ssra. *In vivo* test showed that AcrB-ssra that has been properly inserted into membrane can be digested by ClpXP. AcrB-ssra with different C-terminus lengths have various degradation efficiency. This test also confirmed that the well folded and inserted AcrB-ssra can be digested by ClpXP complex. An *in vitro* test showed that ClpXP could degrade detergent-solubilized AcrB-ssrA using purified proteins. The addition of the tag did not have a detectable effect of the overall secondary structure composition of the protein. These results lead to an exciting new question: how is an integral membrane protein efficiently degraded by a soluble protease complex in the cell? The required dislodging of the transmembrane helices of the protein substrate and even more strikingly, the long hydrophilic loop, through the cell membrane is extra challenge for the system to concur. Many more studies are clearly required to elucidate this interesting and fundamentally important question.

REFERENCES

1. Goodsell, D. S., Olson, A. J. (2000) Structural symmetry and protein function. Annu. Rev. Biophys. Biomol. Struct. 29, 105–53.
2. Gabizon, R., Friedler, A. (2014) Allosteric modulation of protein oligomerization: an emerging approach to drug design. Front Chem. 2, 9.
3. Ali, M. H., Imperiali, B. (2005) Protein oligomerization: how and why. Bioorg Med Chem. 13, 5013-20.
4. Kumar, S., Tsai, C. J., Nussinov, R. (2000) Factors enhancing protein thermostability. Protein Eng. 13,179-91.
5. Hashimoto, K., Panchenko, A. R. (2010) Mechanisms of protein oligomerization, the critical role of insertions and deletions in maintaining different oligomeric states. Proc Natl Acad Sci U S A. 107, 20352-7.
6. Salminen, T., Teplyakov, A., Kankare, J., Cooperman, B. S., Lahti R, Goldman A. (1996) An unusual route to thermostability disclosed by the comparison of Thermus thermophilus and Escherichia coli inorganic pyrophosphatases. Protein Sci. 5, 1014-25.
7. Miller S, Lesk AM, Janin J, Chothia C. (1987) The accessible surface area and stability of oligomeric proteins. Nature. 328, 834-6.
8. Walden, H., Bell, G. S., Russell, R. J., Siebers, B., Hensel, R. and Taylor, G. L. (2001) Tiny TIM: A Small, Tetrameric, Hyperthermostable Triosephosphate Isomerase. J. Mol. Biol., 306, 745-757.
9. Dunn, M. F. (2005) Zinc–ligand interactions modulate assembly and stability of the insulin hexamer–a review. BioMetals, 18, 295-303.

10. Dong, C., Beis, K., Nesper, J., Brunkan-LaMontagne, A. L., Clarke, B. R., Whitfield, C., Naismith, J. H. (2006) Wza the translocon for *E. coli* capsular polysaccharides defines a new class of membrane protein. Nature, 444, 226-229.

11. Selwood, T., Jaffe, E. K. (2012) Dynamic dissociating homo-oligomers and the control of protein function. Arch Biochem Biophys. 519, 131-43.

12. Carlier, M. F., Pantaloni, D. (1978) Slow association-dissociation equilibrium of NADP-linked isocitrate dehydrogenase from beef liver in relation to catalytic activity. Eur J Biochem. 89, 511-6.

13. Shashidharamurthy, R., Koteiche, H. A., Dong, J., McHaourab, H. S. (2005) Mechanism of chaperone function in small heat shock proteins: dissociation of the HSP27 oligomer is required for recognition and binding of destabilized T4 lysozyme. J Biol Chem. 280, 5281-9.

14. Shallom, D., Golan, G., Shoham, G., Shoham, Y. (2004) Effect of dimer dissociation on activity and thermostability of the α-glucuronidase from *Geobacillus stearothermophilus*: dissecting the different oligomeric forms of family 67 glycoside hydrolases. J Bacteriol. 186, 6928-37.

15. Streicher, S. L., Tyler, B. (1981) Regulation of glutamine synthetase activity by adenylylation in the Gram-positive bacterium *Streptomyces cattleya*. Proc Natl Acad Sci U S A. 78, 229-33.

16. Eisenberg, D., Gill, H. S., Pfluegl, G. M., Rotstein, S. H. (2000) Structure-function relationships of glutamine synthetases. Biochim Biophys Acta. 1477, 122-45.

17. Gill, H. S., Eisenberg, D. (2001) The crystal structure of phosphinothricin in the active site of glutamine synthetase illuminates the mechanism of enzymatic inhibition. Biochemistry 40, 1903-1912.

18. Meng, G., St Geme, J. W. 3rd, Waksman, G. (2008) Repetitive architecture of the Haemophilus influenzae Hia trimeric autotransporter. J Mol Biol. 384, 824-36.

19. Cotter, S. E., Surana, N. K., St Geme, J.W. 3rd. (2005) Trimeric autotransporters: a distinct subfamily of autotransporter proteins. Trends Microbiol. 13, 199-205.

20. Changeux, J. P., Edelstein, S. J. (1998) Allosteric receptors after 30 years. Neuron. 21, 959-80.

21. Helmstaedt, K., Krappmann, S., Braus, G. H. (2001) Allosteric regulation of catalytic activity: Escherichia coli aspartate transcarbamoylase versus yeast chorismate mutase. Microbiol Mol Biol Rev. 65, 404-21.

22. Mitternacht, S. and Berezovsky, I. N. (2011) Binding Leverage as a Molecular Basis for Allosteric Regulation. PLoS Computational Biology, 7, e1002148.

23. Saroff, H. A. (1972) Action of Hemoglobin. Cooperative and Bohr Effects. The Journal of Physical Chemistry, 76, 1597-1607.

24. Traut, T. W. (1994) Dissociation of enzyme oligomers: a mechanism for allosteric regulation. Crit Rev Biochem Mol Biol. 29, 125-63.

25. Gabizon, R., Friedler, A. (2014) Allosteric modulation of protein oligomerization: an emerging approach to drug design. Front Chem. 2, 9.

26. Thoden, J. B., Miran, S. G., Phillips, J. C., Howard, A. J., Raushel, F. M., Holden, H. M. (1998) Carbamoyl phosphate synthetase: caught in the act of glutamine hydrolysis. Biochemistry. 37, 8825-31.

27. Kim, J., Raushel, F. M. (2001) Allosteric control of the oligomerization of carbamoyl phosphate synthetase from *Escherichia coli*. Biochemistry. 40, 11030-6.

28. Kanno, D. M., Levitus, M. (2014) Protein oligomerization equilibria and kinetics investigated by fluorescence correlation spectroscopy: a mathematical treatment. J Phys Chem B. 118, 12404-15.

29. Sergeev, M., Godin, A. G., Kao, L., Abuladze, N., Wiseman, P. W., Kurtz, I. (2012) Determination of membrane protein transporter oligomerization in native tissue using spatial fluorescence intensity fluctuation analysis. PLoS One. 7, e36215.

30. Rajagopalan, S., Huang, F., Fersht, A. R. (2011) Single-Molecule Characterization of Oligomerization Kinetics and Equilibria of the Tumor Suppressor P53. Nucleic Acids Res. 39, 2294−2303.

31. Schlepckow, K., Schwalbe, H. (2013) Molecular mechanism of prion protein oligomerization at atomic resolution. Angew Chem Int Ed Engl. 52, 10002-5.

32. Ulbrich, M. H., Isacoff, E. Y. (2007) Subunit counting in membrane-bound proteins. Nat Methods. 4, 319-21.

33. Heuberger, E. H., Veenhoff, L. M., Duurkens, R. H., Friesen, R. H., Poolman, B. (2002) Oligomeric state of membrane transport proteins analyzed with blue native electrophoresis and analytical ultracentrifugation. J Mol Biol. 317, 591-600.

34. Fleming, K. G., Ackerman, A. L. and Engelman, D. M. (1997) The Effect of Point Mutations on the Free Energy of Transmembrane a-Helix Dimerization. J. Mol. Biol., 272, 266-275.

35. Loura, L. M., Prieto, M. (2011) FRET in Membrane Biophysics: An Overview. Front Physiol. 2, 82.

36. James, J. R., Oliveira, M. I., Carmo, A. M., Iaboni, A., Davis, S. J. (2006) A rigorous experimental framework for detecting protein oligomerization using bioluminescence resonance energy transfer. Nat Methods. 3, 1001-6.

37. Comps-Agrar, L., Maurel, D., Rondard, P., Pin, J. P., Trinquet, E., Prézeau, L. (2011) Cell-surface protein-protein interaction analysis with time-resolved FRET and snap-tag technologies: application to G protein-coupled receptor oligomerization. Methods Mol Biol. 756, 201-14.

38. Yeow, E. K. & Clayton, A. H. (2007) Enumeration of Oligomerization States of Membrane Proteins in Living Cells by Homo-FRET Spectroscopy and Microscopy: Theory and Application. Biophys J. 92, 3098–3104.

39. Blouin, S., Craggs, T. D., Lafontaine, D. A., Penedo, J. C. (2009) Functional studies of DNA-protein interactions using FRET techniques. Methods Mol Biol. 543, 475-502.

40. Kajihara, D., Abe, R., Iijima, I., Komiyama, C., Sisido, M., Hohsaka, T. (2006) FRET analysis of protein conformational change through position-specific incorporation of fluorescent amino acids. Nat Methods. 3, 923-9.

41. You, M., Li, E., Wimley, W. C., Hristova, K. (2005) Förster resonance energy transfer in liposomes: Measurements of transmembrane helix dimerization in the native bilayer environment. Analytical Biochemistry, 340, 154-164.

42. Adair, B. D. and Engelman, D. M. (1994) Glycophorin A Helical Transmembrane Domains Dimerize in Phospholipid Bilayers: A Resonance Energy Transfer Study. Biochemistry, 33, 5539-5544.

43. Mischke, R., Kleemann, R., Brunner, H., Bernhagen, J. (1998) Cross-linking and mutational analysis of the oligomerization state of the cytokine macrophage migration inhibitory factor (MIF). FEBS Lett. 427, 85-90.

44. Dombkowski, A. A., Sultana, K. Z., Craig, D. B. (2014) Protein disulfide engineering. FEBS Lett. 588, 206-12.

45. Zeng, F. Y., Hopp, A., Soldner, A., Wess, J. (1999) Use of a disulfide cross-linking strategy to study muscarinic receptor structure and mechanisms of activation. J Biol Chem. 274, 16629-46.

46. Cristian, L., Lear, J. D. and DeGrado, W. F. (2003) Determination of membrane protein stability via thermodynamic coupling of folding to thiol–disulfide interchange. Protein Science, 12, 1732-1740.

47. Carpenter, T., Bond, P. J., Khalid, S., Sansom, M. S. (2008) Self-assembly of a simple membrane protein: coarse-grained molecular dynamics simulations of the influenza M2 channel. Biophys J. 95, 3790-801.

48. Cristian, L., Lear, J. D. and DeGrado, W. F. (2003) Use of thiol-disulfide equilibria to measure the energetics of assembly of transmembrane helices in phospholipid bilayers. Proc. Natl. Acad. Sci. USA., 100, 14772-14777.

49. Stanley, A. M., Chuawong, P., Hendrickson, T. L. and Fleming, K. G. (2006) Energetics of Outer Membrane Phospholipase A (OMPLA) Dimerization. J. Mol. Biol., 358, 120-131.

50. Luo, S. Z., Mo, X., Afshar-Kharghan, V., Srinivasan, S., Lo ́pez, J. A. and Li, R. (2007) Glycoprotein Ibα forms disulfide bonds with 2 glycoprotein Ibα subunits in the resting platelet. Blood, 15, 603-609.

51. Russ, W. P. and Engelman, D. M. (1999) TOXCAT: A measure of transmembrane helix association in a biological membrane. Proc. Natl. Acad. Sci. USA., 96, 863-868.

52. Schneider, D. and Engelman, D. M. (2003) GALLEX, a Measurement of Heterologous Association of Transmembrane Helices in a Biological Membrane. J. Biol. Chem., 278, 3105-3111.

53. Morgan, S. J., Felek, S., Gadwal, S., Koropatkin, N. M., Perry, J. W., Bryson, A. B., Krukonis, E. S. (2011) The two faces of ToxR: activator of ompU, co-regulator of toxT in Vibrio cholerae. Mol Microbiol. 81, 113-28.

54. Russ, W. P. and Engelman, D. M. (2000) The GxxxG Motif: A Framework for Transmembrane Helix-Helix Association. J. Mol. Biol., 296, 911-919.

55. Hengge, R., Bukau, B. (2003) Proteolysis in prokaryotes: protein quality control and regulatory principles. Mol Microbiol. 49, 1451-62.

56. Hoskins, J. R., Yanagihara, K., Mizuuchi, K., Wickner, S. (2002) ClpAP and ClpXP degrade proteins with tags located in the interior of the primary sequence. Proc Natl Acad Sci U S A. 99, 11037-42

57. Pan, Q., Losick, R. (2003) Unique degradation signal for ClpCP in Bacillus subtilis. J Bacteriol. 185, 5275-8.

58. Ogura, T., Wilkinson, A. J. (2001) AAA+ superfamily ATPases: common structure--diverse function. Genes Cells. 6, 575-97.

59. Ortega, J., Lee, H. S., Maurizi, M. R., Steven, A. C. (2004) ClpA and ClpX ATPases bind simultaneously to opposite ends of ClpP peptidase to form active hybrid complexes. J Struct Biol. 146, 217-26.

60. Wang, F., Mei, Z., Qi, Y., Yan, C., Hu, Q., Wang, J., Shi, Y. (2011) Structure and mechanism of the hexameric MecA-ClpC molecular machine. Nature. 471, 331-5.

61. Gottesman, S. (2003) Proteolysis in bacterial regulatory circuits. Annu Rev Cell Dev Biol. 19, 565-87.

62. Duman, R. E., Löwe, J. (2010) Crystal structures of Bacillus subtilis Lon protease. J Mol Biol. 401, 653-70.

63. Cha, S. S., An, Y. J., Lee, C. R., Lee, H. S., Kim, Y. G., Kim, S. J., Kwon, K. K., De Donatis, G. M., Lee, J. H., Maurizi, M. R., Kang, S. G. (2010) Crystal structure of Lon protease: molecular architecture of gated entry to a sequestered degradation chamber. EMBO J. 29, 3520-30.

64. Krzywda, S., Brzozowski, A. M., Verma, C., Karata, K., Ogura, T., Wilkinson, A. J. (2002) The crystal structure of the AAA domain of the ATP-dependent protease FtsH of *Escherichia coli* at 1.5 A resolution. Structure. 10, 1073-83.

65. Tomoyasu, T., Gamer, J., Bukau, B., Kanemori, M., Mori, H., Rutman, A. J., Oppenheim, A. B., Yura, T., Yamanaka, K., Niki, H., et al. (1995) *Escherichia coli* FtsH is a membrane-bound, ATP-dependent protease which degrades the heat-shock transcription factor sigma 32. EMBO J. 14, 2551-60.

66. Alba, B. M., Leeds, J. A., Onufryk, C., Lu, C. Z., and Gross, C. A. (2002) DegS and YaeL participate sequentially in the cleavage of RseA to activate the sE-dependent extracytoplasmic stress response. Genes Dev. 16, 2156– 2168.

67. Kobiler, O., Koby, S., Teff, D., Court, D., Oppenheim, A. B. (2002) The phage lambda CII transcriptional activator carries a C-terminal domain signaling for rapid proteolysis. Proc Natl Acad Sci U S A. 99, 14964-9.

68. Akiyama, Y., Ito, K. (2003) Reconstitution of membrane proteolysis by FtsH. J Biol Chem. 278, 18146-53.

69. Yamada-Inagawa, T., Okuno, T., Karata, K., Yamanaka, K., Ogura, T. (2003) Conserved pore residues in the AAA protease FtsH are important for proteolysis and its coupling to ATP hydrolysis. J Biol Chem. 278, 50182-7.

70. Krojer, T., Garrido-Franco, M., Huber, R., Ehrmann, M., Clausen, T. (2002) Crystal structure of DegP (HtrA) reveals a new protease-chaperone machine. Nature. 416, 455-9.

71. Krojer, T., Sawa, J., Schäfer, E., Saibil, H. R., Ehrmann, M., Clausen, T. (2008) Structural basis for the regulated protease and chaperone function of DegP. Nature. 453, 885-90

72. Farrell, C. M., Grossman, A. D., Sauer, R. T. (2005) Cytoplasmic degradation of ssrA-tagged proteins. Mol Microbiol. 57, 1750-61.

73. Flynn, J. M., Levchenko, I., Seidel, M., Wickner, S.H., Sauer, R. T., Baker, T. A. (2001) Overlapping recognition determinants within the ssrA degradation tag allow modulation of proteolysis. Proc Natl Acad Sci U S A. 98, 10584-9.

74. Karzai, A. W., Roche, E. D., Sauer, R. T. The SsrA-SmpB system for protein tagging, directed degradation and ribosome rescue. Nat Struct Biol. 7, 449-55.

75. Konovalova, A., Søgaard-Andersen, L., Kroos, L. (2014) Regulated proteolysis in bacterial development. FEMS Microbiol Rev. 38, 493-522.

76. Ye, Y., Fortini, M. E. (2000) Proteolysis and developmental signal transduction. Semin Cell Dev Biol. 11, 211-21.

77. Barchinger, S. E., Ades, S. E. (2013) Regulated proteolysis: control of the *Escherichia coli* σ(E)-dependent cell envelope stress response. Subcell Biochem. 66, 129-60.

78. Dalbey, R. E., Wang, P., van Dijl, J. M. (2012) Membrane proteases in the bacterial protein secretion and quality control pathway. Microbiol Mol Biol Rev. 76, 311-30.

79. Krüger, E., Hecker, M. (1998) The first gene of the Bacillus subtilis clpC operon, ctsR, encodes a negative regulator of its own operon and other class III heat shock genes. J Bacteriol. 180, 6681-8.

80. Fuhrmann, J., Schmidt, A., Spiess, S., Lehner, A., Turgay, K., Mechtler, K., Charpentier, E., Clausen, T. (2009) McsB is a protein arginine kinase that phosphorylates and inhibits the heat-shock regulator CtsR. Science. 324, 1323-7.

81. Elsholz, A. K., Michalik, S., Zühlke, D., Hecker, M., Gerth, U. (2010) CtsR, the Gram-positive master regulator of protein quality control, feels the heat. EMBO J. 29, 3621-9.

82. Varshavsky, A. (1996) The N-end rule: functions, mysteries, uses. Proc Natl Acad Sci U S A. 93, 12142-9.

83. Tasaki, T., Sriram, S. M., Park, K. S., Kwon, Y. T. (2012) The N-end rule pathway. Annu Rev Biochem. 81, 261-89.

84. Tobias, J. W., Shrader, T. E., Rocap, G., Varshavsky, A. (1991) The N-end rule in bacteria. Science. 254, 1374-7.

85. Bartel, B., Wünning, I., Varshavsky, A. (1990) The recognition component of the N-end rule pathway. EMBO J. 9, 3179-89.

86. Abramochkin, G., Shrader, T. E. (1995) The leucyl/phenylalanyl-tRNA-protein transferase. Overexpression and characterization of substrate recognition, domain structure, and secondary structure. J Biol Chem. 270, 20621-8.

87. Erbse, A., Schmidt, R., Bornemann, T., Schneider-Mergener, J., Mogk, A., Zahn, R., Dougan, D. A., Bukau, B. (2006) ClpS is an essential component of the N-end rule pathway in *Escherichia coli*. Nature. 439, 753-6.

88. Xiao, Q., Zhang, F., Nacev, B. A., Liu, J. O., Pei, D. (2010) Protein N-terminal processing: substrate specificity of *Escherichia coli* and human methionine aminopeptidases. Biochemistry. 49, 5588-99.

89. Mitrophanov, A. Y., Groisman, E. A. (2008) Signal integration in bacterial two-component regulatory systems. Genes Dev. 22, 2601-11

90. Hengge-Aronis, R. (2002) Signal transduction and regulatory mechanisms involved in control of the sigma(S) (RpoS) subunit of RNA polymerase. Microbiol Mol Biol Rev. 66, 373-95,

91. Battesti, A., Gottesman, S. (2013) Roles of adaptor proteins in regulation of bacterial proteolysis. Curr Opin Microbiol. 16, 140-7.

92. Li, T., Weaver, C. L., Lin, J., Duran, E. C., Miller, J. M., Lucius, A. L. (2015) Escherichia coli ClpB is a non-processive polypeptide translocase. Biochem J. 470, 39-52.

93. Hsueh, Y. H., Cozy, L. M., Sham, L. T., Calvo, R. A., Gutu, A. D., Winkler, M. E., Kearns, D. B. (2011) DegU-phosphate activates expression of the anti-sigma factor FlgM in Bacillus subtilis. Mol Microbiol. 81,1092-108.

94. Moens, S., Vanderleyden, J. (1996) Functions of bacterial flagella. Crit Rev Microbiol. 22, 67-100.

95. Hsueh, Y. H., Cozy, L. M., Sham, L. T., Calvo, R. A., Gutu, A. D., Winkler, M. E., Kearns, D. B. (2011) DegU-phosphate activates expression of the anti-σ factor FlgM in Bacillus subtilis. Mol Microbiol. 81, 1092-108.

96. Ogura, M., Tsukahara, K. (2010) Autoregulation of the Bacillus subtilis response regulator gene degU is coupled with the proteolysis of DegU-P by ClpCP. Mol Microbiol. 75, 1244-59.

97. Hinz, A. J., Larson, D. E., Smith, C. S., Brun, Y. V. (2003) The *Caulobacter crescentus* polar organelle development protein PodJ is differentially localized and is required for polar targeting of the PleC development regulator. Mol Microbiol. 47, 929-41.

98. Chen, J. C., Viollier, P. H., Shapiro, L. (2005) A membrane metalloprotease participates in the sequential degradation of a *Caulobacter* polarity determinant. Mol Microbiol. 55, 1085-103.

99. Treuner-Lange, A., Søgaard-Andersen, L. (2014) Regulation of cell polarity in bacteria. J Cell Biol. 206, 7-17.

100. Jenal, U. (2009) The role of proteolysis in the *Caulobacter crescentus* cell cycle and development. Res Microbiol. 160, 687-95.

101. Chen, J. C., Hottes, A. K., McAdams, H. H., McGrath, P. T., Viollier, P. H., Shapiro, L. (2006) Cytokinesis signals truncation of the PodJ polarity factor by a cell cycle-regulated protease. EMBO J. 25, 377-86.

102. Chen, J. C., Viollier, P. H., Shapiro, L. (2005) A membrane metalloprotease participates in the sequential degradation of a Caulobacter polarity determinant. Mol Microbiol. 55, 1085-103.

103. Curtis, P. D., Quardokus, E. M., Lawler, M. L., Guo, X., Klein, D., Chen, J. C., Arnold, R. J., Brun, Y. V. (2012) The scaffolding and signalling functions of a localization factor impact polar development. Mol Microbiol. 84, 712-35.

104. Hawkey, P. M. (1998) The origins and molecular basis of antibiotic resistance. BMJ. 317, 657–660.

105. Davies, J. and Davies, D. (2010) Origins and Evolution of Antibiotic Resistance. Microbiol Mol Biol Rev. 74, 417–433.

106. Lupo, A., Coyne, S. and Berendonk, T. U. (2012) Origin and Evolution of Antibiotic Resistance: The Common Mechanisms of Emergence and Spread in Water Bodies. Front Microbiol. 3, 18.

107. Nikaido, H. (2009) Multidrug resistance in bacteria. Annu Rev Biochem. 78, 119-46.

108. Chambers, H. F., Deleo, F. R. (2009) Waves of resistance: *Staphylococcus aureus* in the antibiotic era. Nat Rev Microbiol. 7, 629-41.

109. Spellberg, B., Guidos, R., Gilbert, D., Bradley, J., Boucher, H. W., Scheld, W. M., Bartlett, J. G., Edwards, J. Jr. Infectious Diseases Society of America. (2008) The epidemic of antibiotic-resistant infections: a call to action for the medical community from the Infectious Diseases Society of America. Clin Infect Dis. 46, 155-64.

110. Shah, A. (2013) Tackling the crisis of antibiotic resistance. South Asian J Cancer. 2, 3–4.

111. Roca, I., Akova, M., Baquero, F., Carlet, J., Cavaleri, M., Coenen, S., Cohen, J. et al. (2015) The global threat of antimicrobial resistance: science for intervention. New Microbes New Infect. 6, 22-9.

112. Alekshun, M. N., Levy, S. B. (2007) Molecular mechanisms of antibacterial multidrug resistance. Cell. 128, 1037-50.

113. Blair, J. M., Webber, M. A., Baylay, A. J., Ogbolu, D. O., Piddock, L.J. (2015) Molecular mechanisms of antibiotic resistance. Nat Rev Microbiol. 13, 42-51.

114. Wright, G. D. (2005) Bacterial resistance to antibiotics: enzymatic degradation and modification. Adv Drug Deliv Rev. 57, 1451-70.

115. Moore, I. F., Hughes, D. W., Wright, G. D. (2005) Tigecycline is modified by the flavin-dependent monooxygenase TetX. Biochemistry. 44, 11829-35.

116. Lambert, P. A. (2005) Bacterial resistance to antibiotics: modified target sites. Adv Drug Deliv Rev. 57, 1471-85.

117. Ishihara, S., Bitner, J. J., Farley, G. H., Gillock, E. T. (2013) Vancomycin-resistant Gram-positive cocci isolated from the saliva of wild songbirds. Curr Microbiol. 66, 337-43.

118. Allen, N. E., Hobbs, Jr, J. N. and Nicas, T. I. (1996) Inhibition of peptidoglycan biosynthesis in vancomycin-susceptible and -resistant bacteria by a semisynthetic glycopeptide antibiotic. Antimicrob Agents Chemother. 40, 2356–2362.

119. Courvalin, P. (2006) Vancomycin resistance in Gram-positive cocci. Clin Infect Dis. 42, Suppl 1:S25-34.

120. Poole, K. (2007) Efflux pumps as antimicrobial resistance mechanisms. Ann Med. 39, 162-76.

121. Webber, M. A., Piddock, L. J. (2003) The importance of efflux pumps in bacterial antibiotic resistance. J Antimicrob Chemother. 51, 9-11.

122. Kumar, S. and Varela, M. F. (2012) Biochemistry of Bacterial Multidrug Efflux Pumps. Int J Mol Sci., 13, 4484–4495.

123. Sun, J., Deng, Z., Yan, A. (2014) Bacterial multidrug efflux pumps: mechanisms, physiology and pharmacological exploitations. Biochem Biophys Res Commun. 453, 254-67.

124. Sato, T., Yokota, S., Okubo, T., Ishihara, K., Ueno, H., Muramatsu, Y., Fujii, N., Tamura, Y. (2013) Contribution of the AcrAB-TolC efflux pump to high-level fluoroquinolone resistance in *Escherichia coli* isolated from dogs and humans. J Vet Med Sci. 75, 407-14.

125. Andersen, J. L., He, G. X., Kakarla, P., KC, R., Kumar S., et al. (2015) Multidrug efflux pumps from *Enterobacteriaceae*, *Vibrio cholerae* and *Staphylococcus aureus* bacterial food pathogens. Int J Environ Res Public Health. 12, 1487-547.

126. Xu, Z., Yan, A. (2015) Multidrug Efflux Systems in Microaerobic and Anaerobic Bacteria. Antibiotics (Basel). 4, 379-96.

127. Li, X. and Nikaido, H. (2009) Efflux-Mediated Drug Resistance in Bacteria: an Update. Drugs. 69, 1555–1623.

128. Piddock, L. J. (2006) Clinically Relevant Chromosomally Encoded Multidrug Resistance Efflux Pumps in Bacteria. Clin Microbiol Rev. 19, 382–402.

129. Van Bambeke, F., Balzi, E., Tulkens, P. M. (2000) Antibiotic efflux pumps. Biochem Pharmacol. 60, 457-70.

130. Nikaido, H., Takatsuka, Y. (2009) Mechanisms of RND multidrug efflux pumps. Biochim Biophys Acta. 1794, 769-81.

131. Anes, J., McCusker, M. P., Fanning, S., Martins, M. (2015) The ins and outs of RND efflux pumps in Escherichia coli. Front Microbiol. 6, 587.

132. Daury, L., Orange, F., Taveau, J. C., Verchère, A., Monlezun, L. et al. (2016) Tripartite assembly of RND multidrug efflux pumps. Nat Commun. 7, 10731.

133. Tikhonova, E B., Zgurskaya, H. I. (2004) AcrA, AcrB, and TolC of *Escherichia coli* Form a Stable Intermembrane Multidrug Efflux Complex. J Biol Chem. 279, 32116-24.

134. Srikumar, R., Tsang, E., Poole, K. (1999) Contribution of the MexAB-OprM multidrug efflux system to the β-lactam resistance of penicillin-binding protein and β-lactamase-derepressed mutants of *Pseudomonas aeruginosa*. J Antimicrob Chemother. 44, 537-40.

135. Piddock, L. J. (2006) Multidrug-resistance efflux pumps - not just for resistance. Nat Rev Microbiol. 4, 629-36.

136. Law, C. J., Maloney, P. C., Wang, D. N. (2008) Ins and outs of major facilitator superfamily antiporters. Annu Rev Microbiol. 62, 289-305.

137. Reddy, V. S., Shlykov, M. A., Castillo, R., Sun, E. I., Saier, M. H. Jr. (2012) The major facilitator superfamily (MFS) revisited. FEBS J. 279, 2022-35.

138. Yan, N. (2013) Structural advances for the major facilitator superfamily (MFS) transporters. Trends Biochem Sci. 38, 151-9.

139. Abramson, J., Smirnova, I., Kasho, V., Verner, G., Iwata, S., Kaback, H. R. (2003) The lactose permease of *Escherichia coli*: overall structure, the sugar-binding site and the alternating access model for transport. FEBS Lett. 555, 96-101.

140. Wisedchaisri, G., Park, M. S., Iadanza, M. G., Zheng, H., Gonen, T. (2014) Proton-coupled sugar transport in the prototypical major facilitator superfamily protein XylE. Nat Commun. 5, 4521.

141. Yan, N. (2015) Structural Biology of the Major Facilitator Superfamily Transporters. Annu Rev Biophys. 44, 257-83.

142. Davidson, A. L., Chen, J. (2004) ATP-binding cassette transporters in bacteria. Annu Rev Biochem. 73, 241-68.

143. Locher, K. P. (2009) Structure and mechanism of ATP-binding cassette transporters. Philos Trans R Soc Lond B Biol Sci. 364, 239-45.

144. Davidson, A. L., Dassa, E., Orelle, C., Chen, J. (2008) Structure, function, and evolution of bacterial ATP-binding cassette systems. Microbiol Mol Biol Rev. 72, 317-64.

145. Krewulak, K. D., Vogel, H. J. (2008) Structural biology of bacterial iron uptake. Biochim Biophys Acta. 1778, 1781-804.

146. Poulsen, B. E., Cunningham, F., Lee, K. K., Deber, C. M. (2011) Modulation of substrate efflux in bacterial small multidrug resistance proteins by mutations at the dimer interface. J Bacteriol. 193, 5929-35.

147. Bay, D. C., Rommens, K. L., Turner, R. J. (2008) Small multidrug resistance proteins: a multidrug transporter family that continues to grow. Biochim Biophys Acta. 1778, 1814-38.

148. Chen, Y. J., Pornillos, O., Lieu, S., Ma, C., Chen, A. P., Chang, G. (2007) X-ray structure of EmrE supports dual topology model. Proc Natl Acad Sci U S A. 104, 18999-9004.

149. Lehner, I., Basting, D., Meyer, B., Haase, W., Manolikas, T. et al. (2008) The key residue for substrate transport (Glu14) in the EmrE dimer is asymmetric. J Biol Chem. 283, 3281-8.

150. McAleese, F., Petersen, P., Ruzin, A., Dunman, P. M., Murphy, E., Projan, S. J., Bradford, P. A. (2005) A novel MATE family efflux pump contributes to the reduced susceptibility of laboratory-derived *Staphylococcus aureus* mutants to tigecycline. Antimicrob Agents Chemother. 49, 1865-71.

151. Morita, Y., Kodama, K., Shiota, S., Mine, T., Kataoka, A., Mizushima, T., Tsuchiya, T. (1998) NorM, a putative multidrug efflux protein, of Vibrio parahaemolyticus and its homolog in Escherichia coli. Antimicrob Agents Chemother. 42, 1778-82.

152. Omote, H., Hiasa, M., Matsumoto, T., Otsuka, M., Moriyama, Y. (2006) The MATE proteins as fundamental transporters of metabolic and xenobiotic organic cations. Trends Pharmacol Sci. 27, 587-93.

153. He, X., Szewczyk, P., Karyakin, A., Evin, M., Hong, W. X., Zhang, Q., Chang, G. (2010) Structure of a cation-bound multidrug and toxic compound extrusion transporter. Nature. 467, 991-4.

154. Merritt, M. E. and Donaldson, J. R. (2009) Effect of bile salts on the DNA and membrane integrity of enteric bacteria. Journal of Medical Microbiology, 58, 1533-1541.

155. Nikaido, H. (2003) Molecular basis of bacterial outer membrane permeability revisited. Microbiol Mol Biol Rev. 67, 593-656.

156. Thanassi, D. G., Cheng, L. W., Nikaido, H. (1997) Active Efflux of Bile Salts by *Escherichia coli.* J. Bacteriol., 179, 2512-2518.

157. Yu, E. W., Aires, J. R. and Nikaido, H. (2003) AcrB Multidrug Efflux Pump of Escherichia coli: Composite Substrate-Binding Cavity of Exceptional Flexibility Generates Its Extremely Wide Substrate Specificity. J. Bacteriol., 185, 5657-5664.

158. Tikhonova, E. B. and Zgurskaya, H. I. (2004) AcrA, AcrB, and TolC of Escherichia coli Form a Stable Intermembrane Multidrug Efflux Complex. J. Biol. Chem., 279, 32116-32124.

159. Alvarez-Ortega, C., Olivares, J., Mart ńez, J. L. (2013) RND multidrug efflux pumps: what are they good for? Front Microbiol. 4, 7.

160. Murakami, S., Nakashima, R., Yamashita, E., Yamaguchi, A. (2002) Crystal structure of bacterial multidrug efflux transporter AcrB. Nature, 419, 587-593.

161. Murakami, S., Nakashima, R., Yamashita, E., Matsumoto, T. & Yamaguchi, A. (2006) Crystal structures of a multidrug transporter reveal a functionally rotating mechanism. Nature, 443, 173-179.

162. Seeger, M. A., Schiefner, A., Eicher, T., Verrey, F., Diederichs, K., Pos, K. M. (2006) Structural Asymmetry of AcrB Trimer Suggests a Peristaltic Pump Mechanism. Science, 331, 1295-1298.

163. Cull, M. G. and Schatz, P. J. (2000) Biotinylation of Proteins *in Vivo* and *in Vitro* Using Small Peptide Tags. Methods in Enzymology, 326, 430-440.

164. Chapman-Smith, A. and Cronan Jr., J. E. (1999) The enzymatic biotinylation of proteins: a post-translational modification of exceptional specificity. Trends in Biochemical Sciences, 24, 359-363.

165. Beckett, D., Kovaleva, E. and Schatz, P. J. (1999) A minimal peptide substrate in biotin holoenzyme synthetase-catalyzed biotinylation. Protein Sci., 8, 921-929.

166. Clarke, O. B., Gulbis, J. M. (2012) Oligomerization at the membrane: potassium channel structure and function. Adv Exp Med Biol. 747, 122-36.

167. Kilic, S., Bachmann, A. L., Bryan, L. C. & Fierz, B. (2015) Multivalency governs HP1 association dynamics with the silent chromatin state. *Nat. Commun.*, 6, 7313.

168. Fatmi, M. Q. & Chang, C. A. (2010) The Role of Oligomerization and Cooperative Regulation in Protein Function: The Case of Tryptophan Synthase. *PLoS Comput Biol.* 6(11): e1000994.

169. Levy, E. D., Pereira-Leal, J. B., Chothia, C., Teichmann, S. A. (2006) 3D Complex: A Structural Classification of Protein Complexes. PLoS Computational Biology, 2, 1395-1406.

170. Lu, W., Zhong, M., Wei, Y. (2011) Folding of AcrB Subunit Precedes Trimerization. *J Mol Biol.* 411, 264-74.

171. Lu, W., Zhong, M. & Wei, Y. (2011). A reporter platform for the monitoring of in vivo conformational changes in AcrB. Protein Pept. Lett. 18, 863–871.

172. Takatsuka, Y. & Nikaido, H. (2009). Covalently linked trimer of the AcrB multidrug efflux pump provides support for the functional rotating mechanism. J. Bacteriol. 191, 1729–1737.

173. Green, N. M. (1965) A spectrophotometric assay for avidin and biotin based on binding of dyes by avidin. Biochem. J., 94, 23c–24c.

174. Green, N. M. (1970) Spectrophotometric determination of avidin and biotin. *Methods in Enzymology*, 18, 418.

175. Palade, G. E. (1955) A small particulate component of the cytoplasm. J. Biophys. Biochem. Cytol., 1, 59-68.

176. Ladant, D., Karimova, G. (2000) Genetic systems for analyzing protein–protein interactions in bacteria. Research in Microbiology. 151, 711–720

177. Daines, D. A. & Silver, R. P. (2000) Evidence for Multimerization of Neu Proteins Involved in Polysialic Acid Synthesis in *Escherichia coli* K1 Using Improved LexA-Based Vectors. J. Bacteriol. 182, 5267-5270.

178. Fernández De Henestrosa, A.R., Ogi, T., Aoyagi, S., Chafin, D., Hayes, J.J., Ohmori, H., Woodgate, R. (2000) Identification of additional genes belonging to the LexA regulon in *Escherichia coli*. Mol Microbiol. 35, 1560-72.

179. Brent, R., Ptashne, M. (1981) Mechanism of action of the lexA gene product. Proc Natl Acad Sci U S A. 78, 4204-8.

180. Kim, B., Little, J. W. (1992) Dimerization of a specific DNA-binding protein on the DNA. Science, 255, 203-206.

181. Schnarr, M., Pouyet, J., Granger-Schnarr, M., Daune, M. (1985) Large-scale purification, oligomerization equilibria, and specific interaction of the LexA repressor of *Escherichia coli*. Biochemistry 24, 2812-2818.

182. Schnarr, M., Granger-Schnarr, M., Hurstel, S., Pouyet, J. (1988) The carboxy-terminal domain of the LexA repressor oligomerises essentially as the entire protein. FEBS Lett 234, 56-60.

183. Porte, D., Oertel-Buchheit, P., Granger-Schnarr, M., Schnarr, M. (1995). Fos Leucine Zipper Variants with Increased Association Capacity. J Biol Chem., 270, 22721-22730.

184. Juers, D. H., Matthews, B. W. & Huber, R. E. (2012) *LacZ* β-galactosidase: Structure and function of an enzyme of historical and molecular biological importance. Protein Sci. 21, 1792–1807.

185. Luo, Y., Pfuetzner, R. A., Mosimann, S., Paetzel, M., Frey, E. A., Cherney, M., Kim, B., Little, J. W. and Strynadka, N.C.J. (2001) Crystal Structure of LexA: A Conformational Switch for Regulation of Self-Cleavage. Cell, 106, 585-594.

186. Dmitrova,, M., Youn ès-Cauet, G., Oertel-Buchheit, P., Porte, D., Schnarr, M., Granger-Schnarr, M. (1998) A new LexA-based genetic system for monitoring and analyzing protein heterodimerization in Escherichia coli. Mol Gen Genet. 257, 205-12.

187. Schneider, D., Engelman, D. M. (2004).Involvement of Transmembrane Domain Interactions in Signal Transduction by alpha/beta Integrins. J Biol Chem., 279, 9840-9846.

188. Escher, C., Cymer, F., Schneider, D. (2009). Two GxxxG-Like Motifs Facilitate Promiscuous Interactions of the Human ErbB Transmembrane Domains. J. Mol. Biol., 389, 10-16.

189. King, G. and Dixon, A. M. (2010). Evidence for role of transmembrane helix–helix interactions in the assembly of the Class II major histocompatibility complex. Mol. BioSyst., 6, 1650-1661.

190. Li, C., Wen, A., Shen, B., Lu, J., Huang, Y., Chang, Y. (2011) FastCloning: a highly simplified, purification-free, sequence- and ligation-independent PCR cloning method. BMC Biotechnol. 11, doi: 10.1186/1472-6750-11-92.

191. Li, X. Z., Poole, K., Nikaido, H. (2003) Contributions of MexAB-OprM and an EmrE Homolog to Intrinsic Resistance of Pseudomonas aeruginosa to Aminoglycosides and Dyes. Antimicrobial Agents and Chemotherapy, 47, 27–33.

192. MacConkey, A. (1905) Lactose-fermenting bacteria in feces. J. Hyg. 5, 333-378.

193. Zhang, X., Bremer, H. (1995) Control of the *Escherichia coli* rrnB P1 promoter strength by ppGpp. J Biol Chem. 12, 11181-9.

194. Lepecq, J. B., Paoletti, C. (1967) A fluorescent complex between ethidium bromide and nucleic acids: Physical—Chemical characterization. Journal of Molecular Biology. 27, 87-106.

195. Yu, L., Lu, W., Ye, C., Wang, Z., Zhong, M., Chai, Q., Sheetz, M., Wei, Y. (2013) Role of a conserved residue R780 in Escherichia coli multidrug transporter AcrB. Biochemistry. 52, 6790-6.

196. Dice, J. F. (1987) Molecular determinants of protein half-lives in eukaryotic cells. FASEB J. 1, 349-57.

197. Gottesman, S., Gottesman, M., Shaw, J. E., Pearson, M. L. (1981) Protein degradation in *E. coli*: The ion mutation and bacteriophage Lambda N and cll protein stability. Cell. 24, 225-33.

198. Larrabee, K. L., Phillips, J. O., Williams, G. J. & Larrabee, A. R. (1980) The relative rates of protein synthesis and degradation in a growing culture of *Escherichia coli*. J Biol Chem. 255, 4125-30.

199. Bogsch, E. G., Sargent, F., Stanley, N. R., Berks, B. C., Robinson, C., Palmer, T. (1998) An essential component of a novel bacterial protein export system with homologues in plastids and mitochondria. J Biol Chem. 273, 18003-6.

200. Martell, J., Weerapana, E. (2014) Applications of copper-catalyzed click chemistry in activity-based protein profiling. Molecules. 19, 1378-93.

201. Avti, P. K., Maysinger, D., Kakkar, A. (2013) Alkyne-azide "click" chemistry in designing nanocarriers for applications in biology. Molecules. 18, 9531-49.

202. Hatzenpichler, R., Scheller, S., Tavormina, P. L., Babin, B. M., Tirrell, D. A., Orphan, V. J. (2014) In situ visualization of newly synthesized proteins in environmental microbes using amino acid tagging and click chemistry. Environ Microbiol. 16, 2568-90.

203. tom Dieck, S., Kochen, L., Hanus, C., Heumüller, M., Bartnik, I., Nassim-Assir, B., Merk, K., Mosler, T., Garg, S., Bunse, S., Tirrell, D. A., Schuman, E. M. (2015) Direct visualization of newly synthesized target proteins in situ. Nature methods. 12, 411-4.

204. Link, A. J., Tirrell, D. A. (2003) Cell surface labeling of Escherichia coli via copper(I)-catalyzed [3+2] cycloaddition. J Am Chem Soc. 125, 11164-5.

205. Lu, W., Zhong, M., Chai, Q., Wang, Z., Yu, L., Wei, Y. (2014) Functional relevance of AcrB Trimerization in pump assembly and substrate binding. PLoS One. 9, e89143.

206. Link, A. J., Vink, M. K., Tirrell, D. A. (2004) Presentation and Detection of Azide Functionality in Bacterial Cell Surface Proteins. J. AM. CHEM. SOC. 126, 10598-10602.

207. Hinz, F. I., Dieterich, D. C., Tirrell, D. A., Schuman, E. M. (2012) Noncanonical amino acid labeling *in vivo* to visualize and affinity purify newly synthesized proteins in larval zebrafish. ACS Chem. Neurosci. 3, 40–9.

208. Rostovtsev, V. V., Green, L. G., Fokin, V. V., Sharpless, K. B. (2002) A stepwise huisgen cycloaddition process: copper(I)-catalyzed regioselective "ligation" of azides and terminal alkynes. Angew Chem Int Ed Engl. 41, 2596-9.

209. Rosenberg, E. Y., Bertenthal, D., Nilles, M. L., Bertrand, K. P., Nikaido, H. (2003) Bile salts and fatty acids induce the expression of Escherichia coli AcrAB multidrug efflux pump through their interaction with Rob regulatory protein. Molecular Microbiology. 48, 1609–19.

210. Belle, A., Tanay, A., Bitincka, L., Shamir, R., O'Shea, E. K. (2006) Quantification of protein half-lives in the budding yeast proteome. Proc Natl Acad Sci U S A. 103, 13004-9.

211. Cambridge, S. B., Gnad, F., Nguyen, C., Bermejo, J. L., Krüger, M., Mann, M. (2011) Systems-wide proteomic analysis in mammalian cells reveals conserved, functional protein turnover. J Proteome Res. 10, 5275-84.

212. Yen, H. C., Xu, Q., Chou, D. M., Zhao, Z., Elledge, S. J. (2008) Global protein stability profiling in mammalian cells. Science. 322, 918-23.

213. Willetts, N. S. (1967) Intracellular protein breakdown in non-growing cells of Escherichia coli. Biochem J. 103, 453-61.

214. Koch, A. L., Levy, H. R. (1955) Protein turnover in growing cultures of Escherichia coli. J Biol Chem. 217, 947-57.

215. Luscombe, M., Phelps, C. F. (1967) The composition and physicochemical properties of bovine nasal-septa protein-polysaccharide complex. Biochem J. 102, 110-9.

216. Borek, E., Ponticorvo, L., & Rittenberg, D. (1958) Protein turnover in micro-organisms. Proc Natl Acad Sci U S A. 44, 369–374.

217. Gottesman, S. (1996) Proteases and their targets in *Escherichia coli*, Annu. Rev. Genet. 30, 465-506.

218. Fougan, D. A., Mogk, A., and Bukau, B. (2002) Protein folding and degradation in bacterial: To degrade or not to degrade? That is the question, CMLS Cell Mol. Life Sci. 59, 1607-1616.

219. Hanson, P. I., and Whiteheart, S. W. (2005) AAA+ proteins: have engine, will work, Nat. Rev. Mol. Cell Biol. 6, 519–529.

220. Sauer, R. T., and Baker, T. A. (2011) AAA+ proteases: ATP-fueled machines of protein destruction, Annu. Rev. Biochem. 80, 587-612.

221. Baker, T. A., and Sauer, R. T. (2012) ClpXP, an ATP-powered unfolding and proten-degradation machine, Biochim. Biophys. Acta 1823, 15-28.

222. Levchenko, I., Luo, L., and Baker, T. A. (1995) Disassembly of the Mu transposase tetramer by the ClpX chaperone, Genes Dev. 9, 2399–2408.

223. Kruklitis, R., Welty, D. J., and Nakai, H. (1996) ClpX protein of Escherichia coli activates bacteriophage Mu transposase in the strand transfer complex for initiation of Mu DNA synthesis, EMBO J. 15, 935–944.

224. Gottesman, S., Roche, E., Zhou, Y. N., and Sauer, R. T. (1998) The ClpXP and ClpAP proteases degrade proteins with C-terminal peptide tails added by the SsrA tagging system. Genes Dev. 12, 1338–1347.

225. Keiler, K. C., Waller, P. R. H., and Sauer, R. T. (1996) Role of a peptide-tagging system in degradation of proteins translated from damaged mRNA, Science. 271, 990–993.

226. Moore, S. E., and Sauer, R. T. (2007) The tmRNA system for translational surveillance and ribosome rescue, Annu. Rev. Biochem. 76, 101–124.

227. Moore, S. D., and Sauer, R. T. (2005) Ribosome rescue: tmRNA tagging activity and capacity in *Escherichia coli*, Mol. Micro. 58, 456–466.

228. Karzai, A. W., Roche, E. D., and Sauer, R. T. (2000) The SsrA−SmpB system for protein tagging, directed degradation and ribosome rescue, Nat. Struc. Biol. 7, 449 – 455.

229. Lies, M., and Maurizi, M. R. (2008) Turnover of endogenous SsrA-tagged proteins mediated by ATP-dependent proteases in Escherichia coli, J. Biol. Chem. 283, 22918–22929.

230. Zgurskaya, H. I., and Nikaido, H. (1999) Bypassing the periplasm: Reconstitution of the AcrAB multidrug efflux pump of Escherichia coli, Proc. Natl. Acad. Sci. USA. 96, 7190–7195.

231. Wah, D. A., Levchenko, I., Rieckhof, G. E., Bolon, D. N., Baker, T. A. and Sauer, R. T. (2003) Flexible Linkers Leash the Substrate Binding Domain of SspB to a Peptide Module that Stabilizes Delivery Complexes with the AAA+ ClpXP Protease, Molecular Cell 12, 355–363.

232. Levchenko, I., Seidel, M., Sauer, R. T., and Baker, T. A. (2000) A specificity-enhancing factor for the ClpXP degradation machine, Science 289, 2354–2356.

233. Flynn, J. F., Levchenko, I., Sauer, R. T., and Baker, T. A. (2004) Modulating substrate choice: the SspB adaptor delivers a regulator of the extracytoplasmic-stress response to the AAA+ protease ClpXP for degradation, Genes Dev. 18, 2292–2301.

234. McGinness, K. E., Baker, T. A., and Sauer, R. T. (2006) Engineering controllable protein degradation, Mol. Cell. 22, 701–707.

235. Bolon, D. N., Grant, R. A., Baker, T. A., and Sauer, R. T. (2004) Nucleotide-dependent substrate handoff from the SspB adaptor to the AAA+ ClpXP protease, Mol. Cell. 16, 343–350.

Vita

Personal information

Name	Qian Chai
Place of Birth	China
Nationality	China

Education

2006-2009	M. S. in Medicinal Chemistry	Shanghai Institute of Material Medica, Shanghai, China
2002-2006	B. S. in Pharmacy	Sichuan University, Chengdu, China

Awards and Honors

- Nov. 2014, 1st place in Centennial Kentucky Academy of Science Meeting Graduate Student Research Competition (Physiology and Biochemistry Section)
- Academic year 2014~2015, University of Kentucky RCTF fellowship.
- Academic year 2013~2014, University of Kentucky RCTF fellowship.
- Apr. 2013, Honorable Mention in 39th annual Naff symposium poster session.

Publications

- **Qian Chai**, Zhaoshuai Wang, Stacy R. Webb, Rebecca E. Dutch, Yinan Wei*. The ssrA-

tag facilitated digestion of an integral membrane protein. *Biochemistry*. **2016**, 55, 2301-4.

- **Qian Chai**, Stacy Webb, Rebecca Dutch, Yinan Wei*. Lifetime measurement of a constitutively expressed multidrug efflux pump. Submitted.
- Zhaoshuai Wang, Meng Zhong, **Qian Chai**, Yinan Wei. Repressive mutations restore function-loss caused by the disruption of trimerization in Escherichia coli multidrug transporter AcrB. *Front Microbiol*. **2015**, 6, 4.
- **Qian Chai**, Brent Ferrell, Meng Zhong, Xinyi Zhang, Cui Ye, Yinan Wei*. Diverse sequences are functional at the C-terminus of the E. coli periplasmic chaperone SurA. *PEDS*. **2014**, 27, 111-116.
- Cui Ye, Zhaoshuai Wang, Meng Zhong, **Qian Chai**, Yinan Wei. Correlation between AcrB trimer association affinity and efflux activity. *Biochemistry*. **2014**, 53, 3738-46.
- Wei Lu, Meng Zhong, **Qian Chai**, Zhaoshuai Wang, Linliang Yu, Yinan Wei. Functional relevance of AcrB Trimerization in pump assembly and substrate binding. *PLoS One*. **2014**, 9, e89143.
- Cui Ye, **Qian Chai**, Meng Zhong, Yinan Wei*. Effect of crowding by Ficolls on OmpA and OmpT refolding and membrane insertion. *Protein Sci.* **2013**, 22, 239-245.
- Linliang Yu, Wei Lu, Zhaoshuai Wang, Meng Zhong, **Qian Chai**, Michael Sheetz, Yinan Wei. Role of a conserved residue R780 in Escherichia coli multidrug transporter AcrB. *Biochemistry*. **2013**, 52, 6790-6.
- Meng Zhong, Brent Ferrel, Wei Lu, **Qian Chai**, Yinan Wei. Insights into the function and structural flexibility of the periplasmic molecular chaperone SurA. *J Bacteriol*. **2013**, 195, 1061-7.
- **Qian Chai**, Wei Lu, Meng Zhong, Linliang Yu, Jun Fang, Tong Wang, Huilin Li,

Haining Zhu, Yinan Wei*. Assembling of AcrB trimer in cell membrane. *J Mol Biol.* **2012**, 423, 123-134.

- **Qian Chai**, Qiang Shen, Lanping Ma, Xin Wang, Tao Meng, Jingya Li, Jia Li, Jingkang Shen*. Discovery and Structure-activity Relationships of Tetrahydro-3H cyclopenta[c]quinolines Scaffold-based Potential PTP1B Inhibitors. *Chemical Journal of Chinese Universities* **2011**, 32, 306-315.
- Tianyu Liu, Hailei Cui, **Qian Chai**, Jun Long, Bangjing Li, Yong Wu, Lisheng Ding, Yingchun Chen. Organocatalytic asymmetric Friedel-Crafts alkylation/cascade reactions of naphthols and nitroolefins. *Chem Commun*. **2007**, 14, 2228-30.
- Tianyu Liu, Rui Li, **Qian Chai**, Jun Long, Bangjing Li, Yong Wu, Lisheng Ding and Yingchun Chen*. Enantioselective Michael Addition of α-Substituted Cyanoacetates to Vinyl Ketones Catalyzed by Bifunctional Organocatalysts. *Chem. Eur. J.* **2007**, 13, 319 – 327.

Presentations

- Gordon Research Conferences: Membrane Protein Folding, 2015, Waltham, MA. Poster presentation.
- 100th Annual Meeting of the Kentucky Academy of Science, 2014, Lexington, KY. Oral presentation.
- Frontiers in Structural Biology of Membrane Proteins Symposium, 2013, Birmingham, AL. Poster presentation.